

**Using Field Assessment and Numerical Modelling Tools to  
Optimize a Water Abstraction System in the Shashane Sand  
River Aquifer (Zimbabwe)**

**Ahmed Walid Moulahoum**

Thesis to obtain the Master of Science Degree in  
**Environmental Engineering**

**Supervisors:**

Dr. Tibor Stigter (IHE-Delft)  
Prof. Luís Filipe Tavares Ribeiro  
MSc. Mieke Hulshof (Acacia Water B.V.)

**Examination Committee**

Chairperson: Prof. Ramiro Joaquim De Jesus Neves  
Supervisor: Prof. Luís Filipe Tavares Ribeiro  
Members of the Committee: Marta Faneca (Deltares)

**September 2018**

# Using Field Assessment and Numerical Modelling Tools to Optimize a Water Abstraction System in the Shashane Sand River Aquifer (Zimbabwe)

Master of Science Thesis  
by  
**Ahmed Walid Moulahoum**

Supervisor  
**Prof. Michael McClain**

Mentors  
**Dr. Tibor Stigter**  
**MSc. Mieke Hulshof**

Examination committee  
**Michael McClain (IHE-Delft)**  
**Tibor Stigter (IHE-Delft)**  
**Mieke Hulshof (Acacia Water)**  
**Marta Faneca (Deltares)**

This thesis is submitted in partial fulfilment of the requirements for the academic degree of

**Master of Science in Water Science and Engineering**  
UNESCO-IHE Institute for Water Education, Delft, the Netherlands

**Master of Science in Environmental Engineering**  
Instituto Superior Técnico, Universidade de Lisboa, Portugal

**Master of Science in Hydro Science and Engineering**  
Technische Universität Dresden, Germany

MSc research host institution  
IHE-Delft, Delft, the Netherlands

**August 2018**

## DECLARAÇÃO

Eu Ahmed Walid Moulahoum, aluno do Instituto Superior Técnico n.º 427274  
autor da dissertação para obtenção do Grau de Mestre em Engenharia do Ambiente,  
com o título Using Field Assessment and Numerical Modelling Tools to Optimize a  
Water Abstraction System in the Shashane Sand River Aquifer (Zimbabwe)

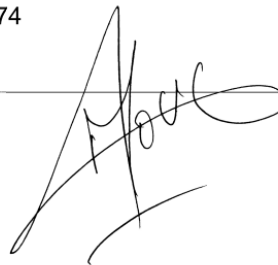
concedo ao Instituto Superior Técnico uma licença perpétua, mas não exclusiva, para utilizar esta dissertação para fins de ensino ou investigação e autorizo-o a inseri-la, bem como ao seu resumo alargado, em formato pdf, na sua página da internet, com endereço [www.tecnico.ulisboa.pt](http://www.tecnico.ulisboa.pt) de modo a permitir a sua divulgação junto de todos os que acedam àquela página, e, com o mesmo propósito de divulgação, a responder favoravelmente aos pedidos de instituições de ensino ou de investigação e Centros de Documentação ou Bibliotecas, remetendo-lhes aqueles mesmos ficheiros em formato pdf, mas fazendo uma expressa menção, seja na sua página na internet seja quando da remessa atrás referida, à obrigação de quem assim aceda àquela minha dissertação e respectivo resumo alargado em salvaguardar os meus direitos de autor sobre estes documentos, que me são conferidos pelo Código do Direito de Autor e dos Direitos Conexos.

Lisboa, a 12 de Setembro de 201 8

O aluno n.º 427274

Ahmed Walid Moulahoum

(nome)



# Acknowledgments

I am extremely grateful for both my mentors Dr. Tibor Stigter and Mieke Hulshof for being very patient, supportive and most importantly encouraging from our first Skype call until the night before the submission of this work. Mieke, you inspire me for you are a true example of what a hardworking, smart and successful environmental expert should be. Tibor, your support since my admission to the Masters was always comforting. During the thesis I appreciate your guidance, your constructive feedback filled with positive energy and empathy which shows what an experienced pedagogue you are. Your passion for the aquifers shines and it influences all those around you.

Special thanks go to Prof. Michael McClain for his orientation and research wisdom right when it was needed.

I thank Prof. Pieter Van der Zaag and all the A4labs team for giving me the opportunity to do my research and add value to the A4labs project.

I genuinely thank Dr. Stephen Hussey for his support and guidance during the fieldwork. I thank Eng. Bongani Mpofo for his support during the field planning. And all the helpful and joyful team at Dabane. Your warm hearts and beautiful smiles will remain a lasting memory. I hope we will cross paths again

I sincerely thank the A4labs partners at the NUST University in Zimbabwe for helping me to successfully perform the geophysics assessment. I particularly thank Dr. Annatoria Chinyama making sure that everything goes to plan. I thank Ms. Sakhile Ndlovu and Mr. Mervyn Gumbo for supporting me in the field but also for the analysis and interpretations of the results.

I thank the people of Acacia Water and more particularly Arjen Oord and Daniela Benedicto van Dalen for the exciting guiding discussions we had about modelling.

Thanks to all my professors at IST Lisboa and TU Dresden. In particular, I thank Luis Ribeiro and Teresa Melo for being there for us and guiding us since the first day in this Master program.

Thanks to all the GroundwatCH students for being good colleagues, friends and a big and happy international family.

Among all, this achievement wouldn't have been possible if not for the enormous support, encouragement and patience during these very difficult times, of my blessed family. I thank my mother and father for staying so strong for having me far away from them. I love you and miss you every day more than the other. I thank my brother for always being there for me. I thank my best friend Aghiles for the laughs that dissipate any stress. I am also enormously grateful to Luciana for keeping me sane when the world around me seemed to crumble. I am very lucky to have all of you.

# Resumo

Na perspectiva de encontrar recursos hídricos alternativos para as comunidades rurais poderem garantir não só as suas necessidades atuais como também um futuro aumento da produção agrícola, uma porção do Rio Sashane, no sul do Zimbabué, foi considerada como caso de estudo para caracterização de aquíferos aluviais arenosos e análise do potencial de sustentar tais esquemas de desenvolvimento. Para atingir o objetivo do presente estudo foi combinada uma análise in-situ com modelação.

De forma a determinar as propriedades hidráulicas que definem a geometria, o armazenamento e a capacidade de escoamento do aquífero foram realizadas uma análise granulométrica do solo em conjunto com in-situ slug-tests e uma avaliação geofísica. Os registos de descarga bem como dos dados do nível do lençol freático foram utilizados para fornecer uma análise dinâmica da frequência de recarga e de potenciais perdas de água do sistema. Os resultados foram utilizados para construir um modelo numérico transiente tridimensional de águas subterrâneas a fim de compreender o fluxo de águas subterrâneas e a variação natural de armazenamento. Adicionalmente, o modelo foi utilizado para estimar a recarga do sistema bem como avaliar o impacto das captações intensificadas no armazenamento e nos diferentes componentes hidrológicos do aquífero.

O aquífero apresenta uma capacidade útil de armazenamento de 0.35 Mm<sup>3</sup> para o troço de 5.6 Km estudado e que é naturalmente reduzida para metade devido à evaporação. Quando as captações são aumentadas menos água é evaporada. O sistema tem o potencial para fornecer 800 m<sup>3</sup>/dia, sem falhas, o que suporta irrigar uma potencial área de 3.5 ha/km. Apesar do aumento das captações, a recarga na estação húmida quente é, na maioria dos casos, assegurada pelo escoamento superficial, com exceção dos anos de seca que ocorrem uma vez a cada 20 anos. O aumento das captações resultou num incremento da recarga que resulta, até certo ponto, na diminuição do escoamento superficial no ano seguinte, o que afeta os utilizadores a jusante, incluindo ecossistemas dependentes, requerendo mais estudos.

O aquífero em estudo pode apoiar planos de desenvolvimento socioeconómicos substanciais pois, como demonstrado, se associado a boas práticas de gestão, pode resultar numa melhoria considerável dos meios de subsistência. A utilização do modelo pode ser estendida para testar diferentes alternativas de desenvolvimento e como uma instrumento para justificação de futuras decisões de desenvolvimento.

**Palavras-chave:** Rios de areia, modelação, MODFLOW, transitório, aquífero aluvial

# Abstract

In the perspective of finding alternative water resources for rural communities to support current needs and future increased crop production, a portion of the Shashane River in the southern part of Zimbabwe is considered as a case study to characterize sand river alluvial aquifers and analyse the potential in sustaining such development schemes. Field assessment was coupled with modelling to achieve the objective of this research.

Soil gradation analysis in combination with in-situ slug tests and geophysical assessment were performed to determine the hydraulic properties that define the geometry, storage and flow capacity of the aquifer. Discharge records as well as groundwater level data were used to provide a dynamic analysis on the recharge frequency and the potential water losses from the system. The findings were used to build a 3D transient numerical groundwater model in order to understand the groundwater flow and the natural variation of the storage. In addition, the model was used to estimate the recharge of the system as well as assess the impact of intensified abstractions on the storage and on the different hydrologic components of the aquifer.

The aquifer has an available storage capacity of 0.35 Mm<sup>3</sup> per the studied stretch of 5.6km. Such capacity is depleted naturally to its half due to evaporation. Less water is evaporated when abstractions are increased. The system has the potential to fulfil a total demand of 800 m<sup>3</sup>/day without failure which can irrigate a potential area of 3.5 ha per km. Despite the increased abstractions, the recharge in the following wet season is almost certainly ensured by surface flow except for some dry years that occur once every 20 years. The increased abstractions lead to an increase in recharge which reduces runoff in the following year to a certain extent and thus affect other users downstream, including dependent ecosystems, which requires further studies.

The aquifer studied can support substantial socio-economic development plans as it was shown that if coupled with good management practices, it can lead to considerable livelihood improvement. The use of the model can be extended to test different development alternatives and serves as a tool to justify future development decisions.

**Key words:** Sand rivers, modelling, MODFLOW, transient, alluvial aquifer

# Table of Contents

<b>Acknowledgments</b>	<b>4</b>
<b>Resumo</b>	<b>5</b>
<b>Abstract</b>	<b>6</b>
<b>List of Figures</b>	<b>9</b>
<b>List of Tables</b>	<b>11</b>
<b>Abbreviations</b>	<b>12</b>
<b>Introduction</b>	<b>13</b>
1.1. Background information	13
1.2. Problem statement	15
1.3. Hypothesis	15
1.4. Research objectives	16
<b>Literature Review</b>	<b>17</b>
2.1. Formation of sand rivers	17
2.2. Dynamics of sand rivers	18
2.3. Quality of water in sand rivers	19
2.4. Use of sand rivers and abstraction techniques	19
<b>Study Area</b>	<b>21</b>
3.1. Location and topography	21
3.2. Climate	22
3.3. Geology and soils	22
3.4. Hydrology and hydrogeology	23
3.5. Socio-economic situation	24
3.6. Tshelanyemba study site	24
<b>Research Methodology</b>	<b>26</b>
4.1. Research design	28
4.2. Research techniques	29
4.2.1. Climatic data collection	29
4.2.2. Total station survey	31
4.2.3. Probing	31
4.2.4. Geo-electrical surveys	32
4.2.5. Aquifer properties	34
4.2.6. Groundwater levels	35
4.3. Groundwater model	37
4.3.1. Conceptual model	38
4.3.2. Simplified tank model	39

4.3.3. Numerical groundwater model	40
4.3.4. Scenario development	45
<b>Results and Discussion</b>	<b>47</b>
5.1. Characterization of aquifer parameters	47
5.1.1. Texture and permeability	47
5.1.2. Average slope and hydraulic gradient	49
5.1.3. Depth and thickness	49
Geophysical assessment	49
5.1.4. Probing	53
5.1.5. Groundwater storage capacity	54
5.2. Dynamic analysis	56
5.2.1. Groundwater level dynamics	56
5.2.2. Groundwater flow	59
5.2.3. Surface water dynamics	60
5.2.4. Dry spells and dry season	62
5.3. Abstraction potential	64
5.3.1. Simplified tank model	64
5.3.2. Numerical groundwater model	66
5.3.3. Scenarios simulation	71
5.4. General discussion	77
<b>Conclusions and Recommendations</b>	<b>84</b>
6.1. Conclusions	84
6.2. Recommendations:	86
<b>References</b>	<b>87</b>
<b>Appendix</b>	<b>91</b>
Appendix A Sediment analysis	91
Appendix B Slug tests	92
Appendix C Probing and Geophysics	92
Appendix D Hydrological data	95
Appendix E Groundwater model	98
Appendix F Sensitivity Analysis	100



# List of Figures

Figure 1-1: Percentage of population using an unimproved drinking water source (WHO, 2016) .....	13
Figure 2-1: Process of erosion of low organic matter soils due to rainfall (Hussey, 2005).....	17
Figure 3-1: Location and topography map of the study .....	21
Figure 3-2: (a) water level at a depth of 20 cm from the sand level and (b) Shashani sand river in dry surface conditions .....	23
Figure 3-3: Land tenure patterns in Zimbabwe pre-1980 (Whitlow 1985).....	24
Figure 3-4: Location of the study site .....	25
Figure 3-5: (a) Joma pump used to pump water to (b) collection tank in the nutrition garden ..	25
Figure 4-1: Phases of research .....	28
Figure 4-2: Framework of research methodology.....	29
Figure 4-3: Location of the discharge gauges.....	30
Figure 4-4: Probed cross-sections .....	31
Figure 4-5: Location of geophysical profiles.....	33
Figure 4-6: Location of sediment samples .....	34
Figure 4-7: Piezometers installed at location 3. Pb3A manual measurements and Pb3B for diver measurements.....	36
Figure 4-8: Illustration of estimation of daily ET based on groundwater fluctuation using the Hays method. (Fahle & Dietrich, 2014) .....	37
Figure 4-9: Illustration of the importance of positioning the abstraction wells.....	45
Figure 5-1: Grain size distribution of the sediment sampled in the study area.....	47
Figure 5-2: (a) Example of size grain distribution at different depths in the study area.(b) gravels encountered during drilling at 2 m depth .....	48
Figure 5-3: Geophysical longitudinal profiles. (a) ERT1: electrical resistivity (b) ERT2: Formation Factor (c) ERT2: electrical resistivity .....	51
Figure 5-4: Interpretation of VES in the middle of the riverbed.....	51
Figure 5-5: Interpreted subsurface model .....	52
Figure 5-6: Profile of the bank along a gully.....	52
Figure 5-7: Deep water level in a tributary .....	53
Figure 5-8: Probed cross section elevation and physical resistance profile.....	54
Figure 5-9: Developed 3D model of the riverbed in the Tshelanyemba study area.....	56
Figure 5-10 : Relative water level drop for diver Pb3B and Pb6B compared to simulated water level drop caused by evapotranspiration.....	57
Figure 5-11 : Logger groundwater level reading and daily max-mean water level ratios for the recorded period from 2012 to 2018 .....	58
Figure 5-12: Flow duration curve for the daily discharge (m <sup>3</sup> /s) measured between October 1973 and February 2001 for the discharge gauging stations at the upstream of the	

Antelope dam, the Antelope spillway and the outlet of the Shashane catchment (confluence with Shashe).....	61
Figure 5-13: Duration and frequency of the dry spells, and yearly runoff from HY1974 to HY2000. Number (1 to 10) are indicative of the order of occurrence of the dry spell .....	63
Figure 5-14: Duration of the dry season between HY1974 and HY2000 in the Shashane sub- catchment .....	63
Figure 5-15: Storage variation using the simplified water balance for 16 years of available data .....	65
Figure 5-16: Performance of the calibrated model heads in comparison to the measured heads .....	66
Figure 5-17: Summary of the sensitivity analysis results .....	68
Figure 5-18: Calculated recharge for the Tshelanyemba study site. Volume are reported on the y axis and the labels in mm .....	69
Figure 5-19: Calculated monthly recharge flux to the study area .....	70
Figure 5-20: Comparison of annual recharge of the alluvial riverbed and annual runoff for the catchment .....	71
Figure 5-21: Percentage of meeting the daily demand for an average hydrological year .....	72
Figure 5-22: Variation of storage for an average hydrological year for the different scenarios. 000 m <sup>3</sup> .....	72
Figure 5-23: Percentage of meeting the total demand in the dry season (263 days) .....	73
Figure 5-24: Total annual evaporation in comparison to the abstracted volumes as a function of a specified daily demand .....	74
Figure 5-25: Percentage of meeting demand for Strategies 2, 3 and 4.....	74
Figure 5-26: Annual recharge for scenarios with pumping and without pumping, compared to annual runoff .....	75
Figure 5-27: outcropping rock at the riverbank .....	79
Figure 5-28: Roots penetrating the sand deposits .....	79
Figure 5-29: longitudinal cross section of a portion of the modelled riverbed illustrating the effect of the subsurface obstacles on the water level variation locally.....	82
Figure 6-1: Precipitation data at the installed weather station .....	Error! Bookmark not defined.

# List of Tables

<b>Table 1: Groundwater development potential of formations occurring in south-western Zimbabwe .....</b>	<b>23</b>
<b>Table 2: Model grid and time discretization parameters .....</b>	<b>41</b>
<b>Table 3: Parameter variation for the sensitivity analysis .....</b>	<b>45</b>
<b>Table 4: Summary of spatial strategies and abstraction rate scenarios .....</b>	<b>46</b>
<b>Table 5: Comparison of available volume per area of river channel in three different areas .....</b>	<b>55</b>
<b>Table 6: Summary of the parameters used for the calibration .....</b>	<b>66</b>
<b>Table 7: Potential irrigated area for an average dry season for the 5.6 km studied stretch .....</b>	<b>75</b>

# Abbreviations

WL:	Water level
ERT:	Electrical Resistivity Tomography
VES:	Vertical Electrical Sounding
IP:	Induced Polarization
NGO:	Non-Governmental Organization
GMWL:	Global Meteoric Water Line
LMWL:	Local Meteoric Water Line
WMO:	World Meteorological Organization
WHO:	World Health Organization
ET:	Evapotranspiration
PET:	Potential Evapotranspiration
NUST:	National University of Science and Technology
UZ:	University of Zimbabwe
FAO:	Food and Agriculture Organization
ARC2:	African Rainfall Climatology from the Famine Early Warning System
MODIS:	Moderate Resolution Imaging Spectroradiometer
ZINWA:	Zimbabwe National Water Authority
GDP:	Gross domestic product
GW:	Groundwater
DEM:	Digital Elevation Model
EC:	Electrical Conductivity
USCS:	Unified Soil Classification System
HY:	Hydrologic Year

# Introduction

## 1.1. Background information

### What’s wrong with (semi-arid and arid) Africa?

Water is a resource that is mistakenly considered to be both renewable and infinite putting it under the threat of excessive and unsustainable use. Its uneven availability creates zones of high and scarce abundance. While wet areas rigorously thrive in the abundance of this resource in the advancement of a healthy quality of life, dry areas struggle with the management of this scarce resource to promote development and socio-economic prosperity. According to WHO, a total of 663 million people in the world do not have access to improved sources of drinking water in 2015 (WHO 2016), of which the majority lives in Africa (**Figure 1-1**)

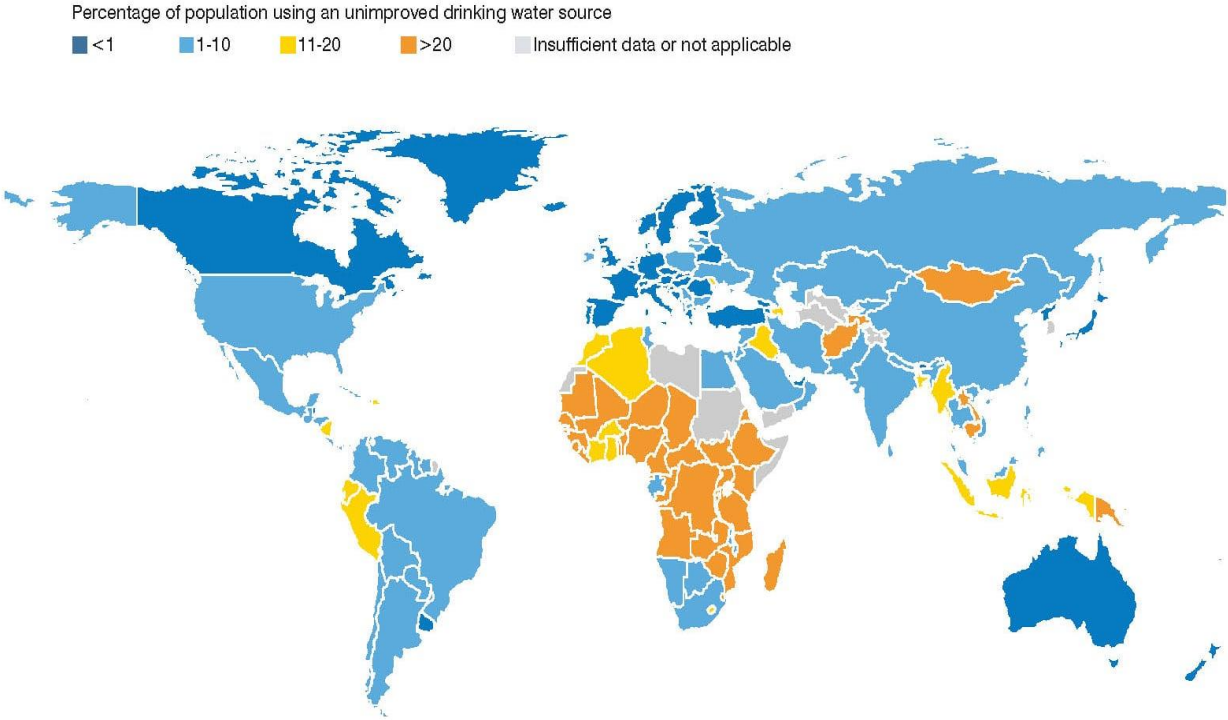


Figure 1-1: Percentage of population using an unimproved drinking water source (WHO, 2016)

The situation in rural sub-Saharan Africa is more critical. According to WHO (2016) “only 16% of people there had access to drinking water through a household connection”. The availability of water resources ready for clean drinking water supply to the entire population of Africa is limited for reasons ranging from erratic unpredictable rainfall conditions, increased pollution of surface waters and high costs for fresh water infrastructure related investments. The lack of quality control and a very low level of education of the people increase the challenge. Semi-arid to arid regions in particular are characterized by unpredictable intense but short rainfalls that are met by high potential evapotranspiration demand leading to a pronounced interannual persisting droughts (Hussey, 2007). This water scarcity leads to marginalization and loss to socio-economic development of semi-arid to arid regions where smallholders cannot afford the losses induced by constant unreliable water supply (A4labs, 2016). For all of the above, reliability in water supply is of paramount importance to ensure development.

### **What is the solution?**

Given the limited amount of surface water, tapping into groundwater might be regarded as the best available solution to provide quick and clean water for the rural sub-Saharan population (Awuah, Nyarko, Owusu, & Osei-Bonsu, 2009). Groundwater comes with the benefit of being inertly protected from bacterial contamination due to its purifying potential, but also its long occurrence in underground aquifers buffers the drought effects linked to the unavailability of rainfall during the dry periods of the year. However, accessing this resource might be difficult due to high investment and operation costs, low yield of the aquifers and also risks of bacterial contamination by septic tanks. As an example, the weathered crystalline rocks which underlain the majority of the tropical Africa can function as an aquifer although the reported yields are low and the abstraction would be economically expensive (Mansell & Hussey, 2005). Sand beds of the ephemeral rivers have been reported to present an alternative easily accessible resource for groundwater exploitation that could compensate the unavailability of surface water.

### **Can Sand Rivers save Africa?**

The prevailing types of rivers in semi-arid and arid regions of southern Africa are sand-filled rivers formed as a consequence of the erosion of the surrounding steep bare land (Hussey, 2007). These rivers are ephemeral as a consequence to the erratic climate and, with exception of the largest systems, only flow as a direct response to rainfall. Despite that the surface of the riverbed is dry for most of the year, there is constant flow within its sandy formation (Mpala et al. 2016) which ensures provision of continuous, cheap and easily accessible clean water. For instance, Herbert (1998) reported that sand rivers in Botswana are able to cover the demand of almost one third of the population whereas Lasage et al. (2008) state that in Kitui, Kenya, more than 100,000 people have access to an increased water availability after using storage enhancement methods in sand river aquifers which resulted in a 60% rise in the average farmer’s income due to higher yields. In Zimbabwe, NGOs are increasingly using sand rivers to provide water to stressed communities (Mpala et al. 2016). The issue with sand rivers is that

very little research work has been done to quantify the availability of this resource and to understand the dynamics of the factors that control its replenishment.

### **Where is A4Labs in all this?**

A4labs is a development project coordinated by IHE Delft in cooperation with Acacia Water (Private Sector) and in Zimbabwe with Dabane trust (NGO) and the local universities (NUST and UZ). The project, also active in Mozambique and Ethiopia, aims to co-develop, test, share and compare with farmers and partners methodologies to create a reliable and sustainable source of water for agriculture in semi-arid to arid regions of Sub-Saharan Africa, using water underlying dry river beds and upscale these methodologies for use at river basin scale while maintaining sustainable abstraction limits and minimising negative social and ecological consequences. The project will study alternative ways in which water from alluvial aquifers can best be accessed and used for productive purposes and thus for socio-economic development (<http://a4labs.un-ihe.org/a4labs>).

## **1.2. Problem statement**

Water scarcity decreases the potential for development in semi-arid to arid regions in the sub-Saharan Africa. Particularly in rural areas, communities lack access to water during the dry season which prevents any perspectives of agricultural development. The Shashane catchment in Southern Zimbabwe is an illustrative example of such situation. The catchment is characterized by ephemeral river systems overlain by erratic rainfall patterns that make the water availability unreliable, resulting in a low agricultural productivity. Groundwater is usually the alternative source, but the rocky geology of the region makes extractions of this resource expensive and the quality not always suitable.

The sand river systems are characterized by perennial groundwater flow that constitute a potential and reliable water resource during the dry season. The Shashane sandy river bed in particular contains significant amounts of water. However, there is a limited understanding of the groundwater dynamics, the volumes of water stored and the sustainable abstraction rates. Hence, it is uncertain how much water is available to intensify crop production practices along the river.

## **1.3. Hypothesis**

*Groundwater from the riverbed alluvial aquifer can be used to support small scale irrigation schemes up to full depletion of its storage in the dry season, without significantly affecting river discharge in the subsequent wet season.*

## 1.4. Research objectives

The main objective of the study is to assess the spatial distribution and temporal variation of groundwater recharge, flow and storage in the Shashane “Sand River”, as well as its interactions with surface water flow, and optimize the location and abstraction volumes of water abstraction systems in the sand river.

To attain the main objective, specific research targets are developed focusing on characterization of the hydrogeology of the aquifer, surface and groundwater interactions, and finally the water consumption impact on the storage of the alluvial aquifer.

The specific objectives of the research are:

- To further characterize the hydrogeology of the sand river aquifer, with an emphasis on the sediment depth and the subsurface layer in order to locate potential locations for abstraction.
- To analyse the dynamics of the aquifer and the interaction of surface and groundwater and their impact on the storage of the aquifer
- To assess the impact of increased pumping on the storage of the aquifer and the potential area that the system can irrigate.



## CHAPTER 2

# Literature Review

### 2.1. Formation of sand rivers

Sand rivers, commonly known as luggas in East Africa and wadis in North Africa and the Middle East (Nissen-Petersen, 2006; Mpalla et al., 2016) are ephemeral sands formed generally by coarse-grained material which settles in the riverbeds (Mpalla et al., 2016). Their occurrence is caused by the extreme rainfall and temperature conditions (Davies, 1994). Erratic and low rainfall in combination with high temperatures results in low presence of soil matter which will lead to more compacted soils reducing the infiltration capacity and increasing the flow conditions. These conditions also mean that the soils are not fully developed, exposed and easily eroded and transported through runoff to the streams and eventually the river beds (Hussey, 2007) (**Figure 2-1**).

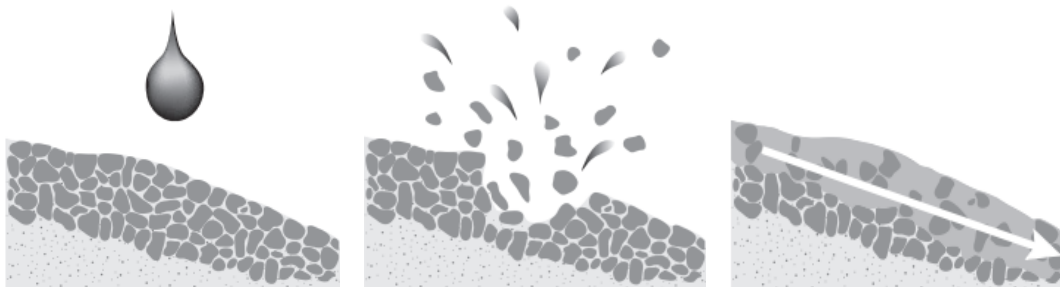


*Figure 2-1: Process of erosion of low organic matter soils due to rainfall (Hussey, 2005).*

The distribution of these rivers is conditioned by the river gradient, geometry of channels, and flow velocities (Moyce et. al, 2006). The riverbed mainly contains rocks and boulders while the finer sediments are carried further away and deposited downstream (Mansell & Hussey 2005; Hussey 2007). They are formed mainly due to either an increase of sediment supply, or a loss in the stream power which reduces the stream transportation capacity. The increase of the sediment supply is cause mainly by an acceleration of erosion mechanisms, whereas the loss of stream transportation capacity occurs generally due to a flattening of the channel gradient or an increase in the channel width (Richards, 1982). The dimensions of the aquifer are defined by the extent and thickness of the alluvial deposits in the channel and under the bounding river plains (Maspovo, 2008). Widths are in the order of tens to a few hundreds of meters, whereas depths do not exceed a few tens of meters. Thicknesses of the riverbeds of sand rivers vary for instance in Zimbabwe from 3 meters in Shashane catchment (Mansell and Hussey

2005) to 20 meters in the geologically enhanced aquifers of the upper Mzingwane catchment where slopes are gentle and therefore favour sediment accumulation (Moyce et al. 2006). In the Mara basin in Kenya, the vertical extent of the sand rivers was below 2 m which is shallow and full of discontinuities due to the bedrock irregularities (Wekesa, 2017). Geophysical surveys revealed that the thickness of the riverbed aquifer in the Northern Limpopo in Mozambique, vary between 10 to 15 m which is expected for a catchment of such a scale even if the riverbeds are less developed in the upstream parts (Abi, 2018).

Hydraulic conductivity of the sand rivers have been estimated between 40 to 200 m/day, whereas yields reach up to 5200  $m^3/day$  in the Mzingwane catchment (Moyce et al. 2006). Blok (2017) and Hussey (2005) used in-situ methods and found that the hydraulic conductivities of the sand aquifer in the Shashane river to be 48 m/day and 100 m/day respectively for the vertical and horizontal conductivities. Wekesa (2017) on the other hand, estimated lower hydraulic conductivities varying between 20 to 70 m/day. Total water storage for these sand aquifers may vary between 10 to 50 % of the total sand volume (Mansell & Hussey 2005) depending on the porosity of the sand. Sediments in the alluvial aquifer channels are typically clear and washed sands with excellent hydraulic properties (R. Owen & Dahlin, 2005). Finally, reported specific yield values vary between 15 to 20% (Mansell & Hussey, 2005; Moyce et. al, 2006). All in all, the characteristics abovementioned in addition to the reduced evaporation losses and the filtering capacity make sand river aquifers a high potential resource for water supply and irrigation.

## 2.2. Dynamics of sand rivers

Recharge of the sand rivers shallow aquifers is ensured by the river flow as an immediate response to rainfall. Due to the high vertical permeability, no flow in the river occurs until the sediments are saturated early in the wet season. Recharge can also occur with upstream dam releases during dry season such as the case with the Zhove dam in the Mzingwane catchment (Moyce et al. 2006) or the Antelope dam in the Shashani catchment.

Losses are due to evaporation from both the surface of the river channel and riparian vegetation, vertical and lateral seepage and direct well abstractions (Mansell & Hussey 2005). Evaporation losses from the river channel are dependent on the depth of the water below the surface of the sand in addition to the matric forces as a function of the sand properties (Moyce et al. 2006; Mansell & Hussey 2005). At the surface, evaporation losses are high and decrease in depth to reach an extinction depth of one meter (Moyce et al. 2006; Hellwig 1973; Wipplinger 1958). Wipplinger (1958) even suggests that as an effect of direct evaporation, the top 90 cm of groundwater is typically lost within the first 120 days at the end of the rainy season when inflows into the aquifer cease, but this loss rate depends mainly on the temperature, and radiation which vary in space and time. Water losses are greatest closer to the riverbed, and evaporation rates decrease as the levels declines suggesting that wide and shallow aquifers suffer more losses as compared to deep and narrow alluvial aquifers of the same volume

(Maspovo, 2008). Riparian vegetation with long roots often tap water if the alluvial aquifer which is connected to the river banks, and lead to significant losses through transpiration (Owen, 2000).

Seepage is a function of the geology. In cases of deep-weathered terrains or the presence of faults, seepage rates can be substantial (Love et al. 2011). Young crystalline rocks on the other hand, provide an impermeable bedrock and therefore seepage from the aquifer is negligible. No data is usually available for seepage from direct measurements and it is often combined with total losses (Mansell & Hussey, 2005). Many authors include the downstream groundwater movement through the sediments with the losses. However, these are typically insignificant as groundwater movement is slow and conditioned by the overwhelming effect of the gentle slopes, as well as the downstream losses are replenished by water from the upstream section of the river (Owen, 2000). The dynamics of the aquifer in dry and wet seasons condition the retention time of the water within the river channel and therefore the availability of water for exploitation (Hussey, 2007).

### **2.3. Quality of water in sand rivers**

The quality of water abstracted from sand rivers is generally considered high. It can be used to supply water for households and directly for irrigation purposes and livestock (Hussey 2007). Regular recharge and flushing by floods and dam releases allow the water to remain fresh and of good quality (Moyce et. al, 2006). The relatively rapid flow in comparison to deep bed groundwater aquifers, prevents salts accumulation (Wekesa, 2017), at the exception near storage enhanced structures where groundwater continuously discharges through evaporation and salinization increases (Carballo, 2018). Adding to that, water flow in the riverbed mimics a large scale slow-sand filtration system where water in the aquifer with all its impurities is put in contact with the surface of the sediments and contaminants, especially bacteria and viruses, attach to form a biological film (Huisman, 1974). However, the process of filtration cannot be expected to purify the water entirely and the challenge is raised especially where there is excessive contamination of the sediment such as by heavy loadings of livestock fouling (Hussey 2007; Svubure et al. 2011).

### **2.4. Use of sand rivers and abstraction techniques**

Water retained in dryland sand rivers has been used for centuries as an accepted practice (Hussey 2007). This water is typically used for water supply to rural communities and for meeting water requirements of some cases in southern Africa (Hussey, 2007; Hamer, 2008). Due to the challenges raised by the ephemeral state of the rivers, smallholder farmers are necessarily relying on the perennial groundwater in the riverbeds. Storage capacity of a sand river varies depending on its gradient, width of the channel, the depth of the sediment, in addition to the permeability and porosity of the soil (Mpalla & Hussey, 2016). Love et al. (2011) highlights that in the Lower Mzingwane current water usage from alluvial aquifers can be more than tripled to large scale irrigation schemes. Moyce et. al (2006) indicate that alluvial aquifers are more pronounced where slopes are gentler such as in the lower stretch of the

Mzingwane where water storage volumes can reach up to 7 Mm<sup>3</sup>, and thus supporting irrigation schemes reaching up to 700 ha. Hamer et al. (2008) on the other hand, estimated that the potential water supply in the Mnyabazi catchment in northern Limpopo reaches 3162 m<sup>3</sup> in a wet year and dries out after 5.7–8.7 months. However, the catchment was deemed to be too small to create a significant water storage and a sand dam could increase the capacity of storage.

Abstraction techniques vary depending on the development and accessibility of the area. Dwellers use scoop holes which are deepened as the water level drops in the dry season (Hussey 2007). The holes are seasonal and they tend to collapse or flood, therefore they are not sustainable. The traditional methods evolved to systems with screens to avoid abstraction of turbid water as well as added pumps to increase the abstracted volumes. Methods like infiltration galleries, caissons and sand wells are used to allow for easy abstractions. These low cost manual abstraction systems are easily applicable considering the low head difference between the alluvial aquifer and the fields on the riverbanks (Mansell & Hussey 2005), however installation is more difficult and relatively costly as drilling increases in difficulty depending on the nature of the riverbank (Hussey 2007).

## CHAPTER 3

# Study Area

### 3.1. Location and topography

The area considered for this study is located in the Matabeleland South Province in the southwestern part of Zimbabwe. It corresponds to the catchment of the Shashane river which flows south as a major tributary to the Shashe river, all part of the Limpopo catchment. The 206 km long river is used both for commercial use in its upstream part where it is dammed at two locations (Shashani dam and Gualameta/Antelope Dam), and for communal use in the remaining part where the study site is located (Mpala et al. 2016).

The topography of the region is similar to the relatively undulating terrain of the Northern area of the Limpopo basin. The elevation in the catchment varies from 1400 m in the upstream reach to 750 m in the downstream reach. The upstream is characterized by visible mountain ranges and incised deep gorges through the hills (**Figure 3-1**). The river uniformly slopes downstream to reach the broad flat-bottomed valleys (Ashton et al. 2001).

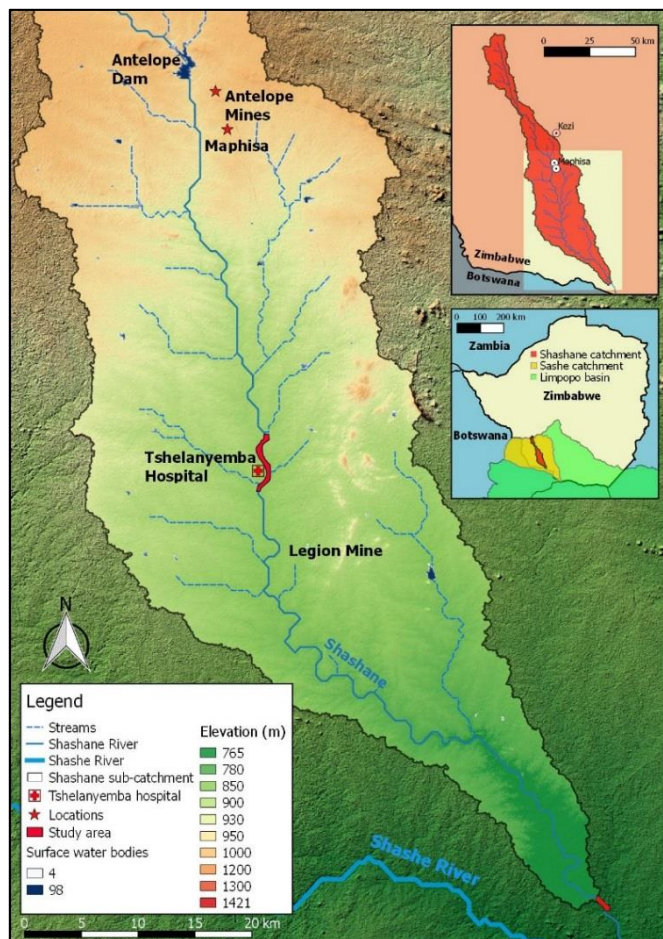


Figure 3-1: Location and topography map of the study

## 3.2. Climate

The study area is defined by a dry subtropical climate with precipitation value averaging 450 mm/year making it one of the driest areas in the region (Mansell and Hussey 2005). The area experiences one rainy season per year extending from November to March (Mpala et al. 2016). The occurrence of rain is erratic and characterized by intense and isolated rainstorms of 100 mm/h of intensity followed by long dry spells (Mpala et al. 2016; Mansell and Hussey 2005). Potential evapotranspiration attains values of 2000 mm/year as described by the FAO's drought assessment report of the Limpopo river basin. Actual evapotranspiration rates are limited by the lack of the water and therefore never reach the values of potential evapotranspiration. Mansell and Hussey (2005) state that the climatic setting of region generates a deficit in water availability and therefore the rain-fed agriculture in the southern part of Zimbabwe is very limited.

Climatic data is scarce in the region and only few stations measuring rainfall were reported. The longest record of rainfall was available at the Bulawayo weather station extending from 1978 to 2014. However, the stations do not represent the exact values in the study area but only depict the trends and the magnitudes. We rely therefore in this study on ARC2 and MODIS products or project weather station for precipitation and evapotranspiration respectively (**Appendix E**). These values are modelled and therefore contain already a degree of error. Previous work lead to the installation of a meteorological station which allows for accurate measurements of the climatic components in the study region although the length of the series is short and not representative of the interannual variations.

## 3.3. Geology and soils

The bedrock of the region is formed by granite gneiss rock with the presence of localized highly elevated greenstone belt formations (Ashton et al. 2001). The very low primary porosity of the granite leads that most of the aquifers in the south of Zimbabwe are associated with secondary porosity formed by the intersection between fractures and faults (Chinoda et al. 2009) which provide very low yields. Fluvial deposits on the other hand, consisting primarily of gravels and sands cover the river beds and feature cheap and easy access to good quality water (Chinoda et al. 2009).

The Shashani catchment is covered by Very shallow to moderately shallow sandy loams, formed from gneisses in its upstream part with localized occurrence of Moderately shallow, coarse-grained sands, derived from the granites. The remaining area is covered by internally draining shallow, clay soils with high sodium content and containing in the midlevel very shallow (30 cm) clays, formed from the Greenstone Belts. (FAO 2004; Ashton et al. 2001). The soils are shallow and poorly developed ranging from 30 cm to 150 cm, leading to a fast infiltration of the rainfall from the surface to the underlying bedrock (see **Appendix A**).

### 3.4. Hydrology and hydrogeology

The Shashane catchment drain to a 206 km long river that flow north to south-east with a meandering course near the flattening reach in the south. The tributaries with the main stream form a parallel drainage with high slopes upstream and gentler slopes downstream. The river is ephemeral and react mainly to rainfall or to the discharges of the Gulameta dam. Values of 33 mm/year were reported by Love et. al (2010) for the mean annual unit runoff. There are three discharge stations located at the Gulameta spillway, the Antelope mines and the downstream at the confluence with the Shashe River. As the river is ephemeral, it appears dry most of the time of the year however there is perennial groundwater flow in the dry river bed.

On the other hand, the groundwater resources in the region are strictly dominated by the geology. As described before, the south-western area of Zimbabwe is largely underlain by granites and gneisses of various ages which have a very low primary porosity. The potential of groundwater occurrence varies depending on the depth and spatial extent of second porosity (**Table 1**). Water tables are shallow and the boreholes yield from 10 to 100 m<sup>3</sup>/day which is capable of supporting villager water supply for domestic purposes (Interconsult A/S, 1985). Another very important groundwater resources is found in the alluvial deposits which cover about 0.7% of the country (ZINWA, 2008) (**Figure 3-2**). For instance, yields in these formations range between 40 to 5200 m<sup>3</sup>/day in the neighbouring Mzingwane catchment (Moyce et al. 2006). These groundwater resources are expected to support large scale irrigation



Figure 3-2: (a) water level at a depth of 20 cm from the sand level and (b) Shashani sand river in dry surface conditions (ZINWA, 2008).

Table 1: Groundwater development potential of formations occurring in south-western Zimbabwe

Lithology	Groundwater Development Potential	Water Table Depth (m)	Borehole Yield ( $m^3 day^{-1}$ )
Gneiss and young intrusive granite on post African and Pliocene Surface	Low	< 10	10 – 50
Alluvial deposits	High	Variable	100 - 5000
Metavolcanics (Greenstones)	Low to moderate	< 20	10 – 250

Source: Interconsult A/S 1984

### 3.5. Socio-economic situation

Zimbabwe's economy is unstable and volatile which results from the corruption and disastrous economic policies that increased the poverty level to 72% of the population (World Bank, 2017). Its economy highly relies on agriculture as this one accounts for 12% of its GDP in 2015 (World Bank). The many years of careful investment led to a sound commercial sector however, this result is disproportionate within the country due to the difference in land locations and ownership. The agricultural sector is segregated into commercial and peasant farming. The

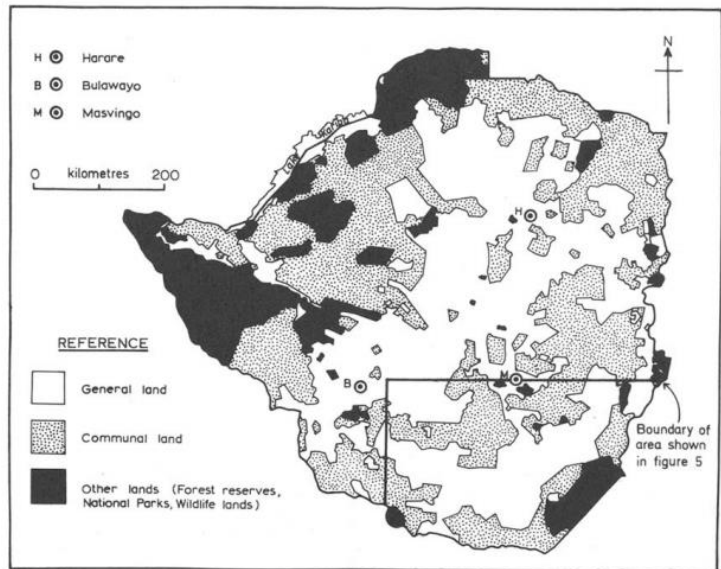


Figure 3-3: Land tenure patterns in Zimbabwe pre-1980 (Whitlow 1985)

The agricultural sector is segregated into commercial and peasant farming. The commercial farming sector operates on higher rainfall areas exceeding 100 000 hectares whereas peasant farms are distributed in marginalized rural areas and cultivated on fragmented units of no more than a few hectares (Whitlow 1985) (Figure 3-3). The study region is located within the communal land areas with smallholder farming and livestock being the main activity (A4labs, 2016). The region suffers from insufficient and irregular availability of water which reduce the production and increase the difficulty for development of these arid to semi-arid regions. NGOs are highly present in these regions and contribute significantly to the small-scale water supply and agricultural development strategies.

### 3.6. Tshelanyemba study site

The Antelope reservoir creates a physical obstacle that separates the catchment into two separate parts. The area downstream of the Antelope dam is considered the draining area contributing to runoff production in the Shashane River. Discharge observed at the outlet of the catchment is assumed to be the sole production of the catchment drainage system since the artificial releases from the dams are much smaller in magnitude and would probably never reach the outlet of the catchment. Along this area, the Shashane River stretches over a total of 102 km starting from the Antelope dam to the outlet of the catchment. The study area is located at 35 km downstream of the dam and continues for 5.6 km. The depth of the riverbed varies significantly depending on the local variation of the underlying bedrock. Despite these local variations of the bedrock, its general slope could be assumed similar to the slope of the surface of the riverbed.



The research site is located nearby the Tshelanyemba village (**Figure 3-4**). The villagers rely on an old borehole that was built by the water authority. The main consumptions come from the nutrition gardens which were designed by Dabane trust in the 90s and use solar pumps for abstraction, the local hospital and the high school of which the location of abstraction is unknown. Surveys conducted in 2017 revealed that the total consumption of the nutrition gardens amount to 1m<sup>3</sup>/week which is negligible in comparison to the storage capacity of the aquifer.

Pumping methods vary from rower pumps to submersible pumps powered by solar panels (**Figure 3-5**). Rower pumps are still the most reliable method and they are connected to the river bed through the bank and do not require any intensive maintenance. “Solar pumps” on the other hand remain dysfunctional especially if they are within the main channel and are flooded frequently. This recurrent flooding and the sediments movement disconnect the pipes and therefore pumping is not possible anymore. This technique makes the farmer retreat to manual pumping more often as the maintenance is only possible during the dry season and requires expertise only Dabane can provide.

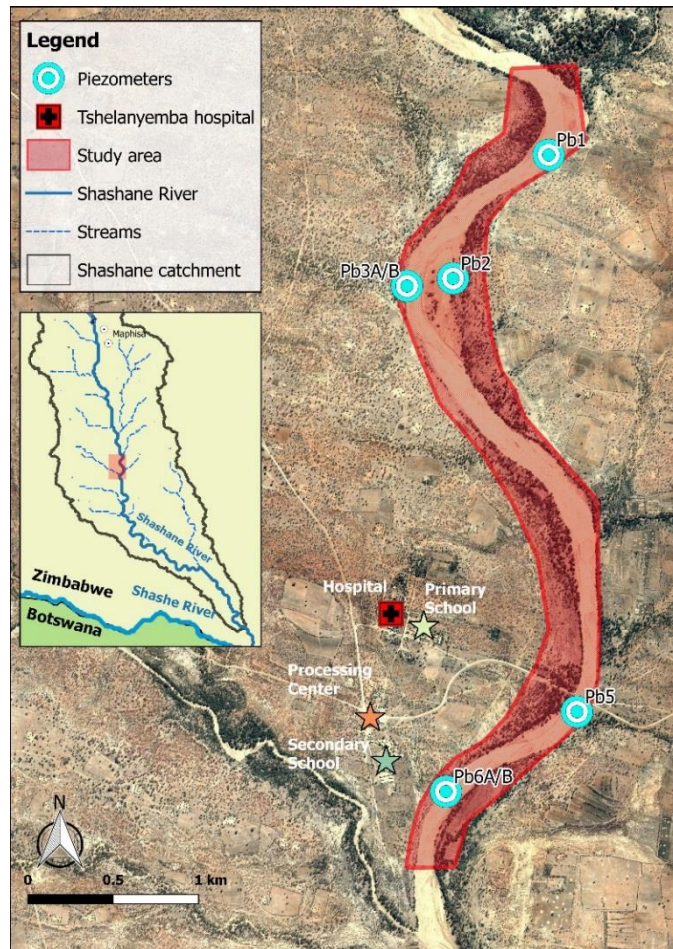


Figure 3-4: Location of the study site

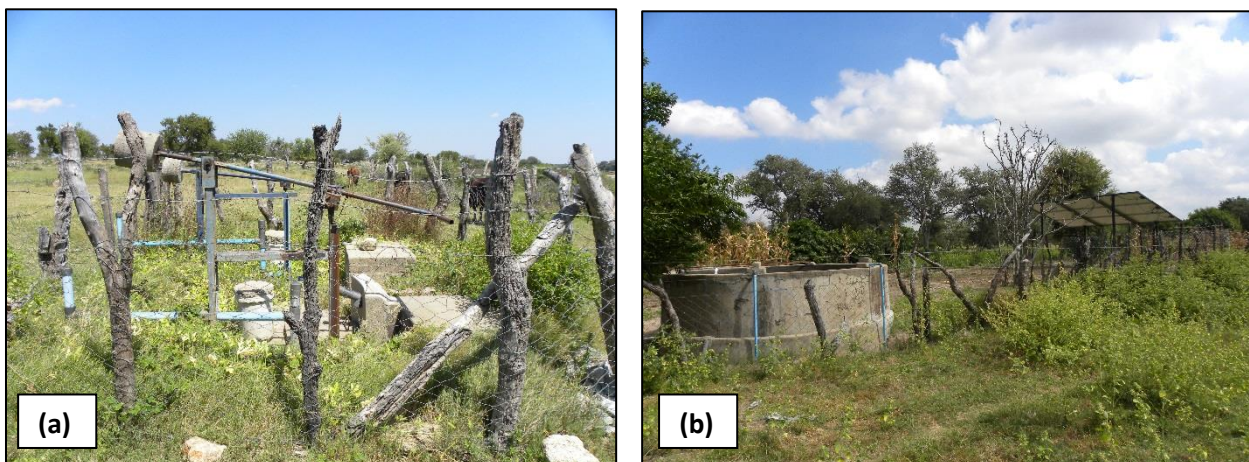


Figure 3-5: (a) Joma pump used to pump water to (b) collection tank in the nutrition garden

## CHAPTER 4

# Research Methodology

What has been done within the A4labs project?

The A4labs project initiated its hydrological work in Zim living lab in 2017 and performed by Blok (2017). The work had three objectives: (1) characterization of the aquifer, (2) establishment of a water balance and building a groundwater model, and (3) estimation of the volumes of water available for abstraction, in a study site of which the results can be later upscaled to the basin scale.

During the field work, the research team succeeded at installing a network of piezometers and a meteorological station. They also attempted to characterize the depth of the riverbed, however only probing was used and geophysics was further suggested to build a comprehensive model on the underlying bedrock and the presence of faults. The team also measured the hydraulic conductivity and the specific storage of the aquifer using Auger hole method but did not succeed in performing a pumping test which allows the estimation of the hydraulic properties and assesses the performance of the aquifer during intensive pumping.

For the desk work, both a water balance and GW model were built. For both models, all the parameters used were modelled which increases the degree of uncertainty in the results. The modelling was carried by many simplifying assumptions to overcome the lack of data. For instance, runoff was assumed to be 20% of the effective precipitation which was unable to re-saturate riverbed, also contribution of direct precipitation was not accounted for and abstraction assessed to be negligible. For the results, a decrease in storage of only 3% was measured during the driest month which did not correlate with previously measured groundwater levels drops of 1.5 m (a level drop equivalent to half of the sediment depth). A refinement of the water balance is suggested using the newly measured parameters and supported by a description of the dynamics between the hydrological components.

A groundwater model for the study area was built to assess the water level spatial distribution. The model was calibrated using only the one month measured data and therefore it is primal to recalibrate it with the longest available data. On the other hand, all the other input data must be re-evaluated, such as geometry, recharge, hydraulic conductivities, specific yield, runoff, and evaporation...etc. On the

other hand, since runoff presents the dominating portion of the recharge of the aquifer it is suggested to use discharge measurements when available.

The abstraction rates used currently by the gardens were considered to be negligible and therefore their impact cannot be observed. However, the region is intended to be developed further for agricultural activities and the alluvial aquifer would be relied upon more for water supply, therefore the impact of increased levels of abstractions will be evaluated both temporally and spatially.

To attain the specific objectives stated in Chapter 1, hence testing the hypothesis, the following formulated research questions will be answered:

- To further characterize the hydrogeology of the sand river aquifer, with an emphasis on the sediment depth and the subsurface layer in order to locate potential locations for abstraction.

*What are the characteristics of the aquifer (Porosity, hydraulic conductivity, specific storage, sediment depth, subsurface layering)?*

- To analyse the dynamics of the aquifer and the interaction of surface and groundwater and their impact on the storage of the aquifer

*How does the surface and groundwater interact, and how does this interaction influence the storage of the aquifer?*

- To assess the impact of increased water demand on the storage of the aquifer

*What is the impact of the increased water demand and thus abstractions on the spatio-temporal variation of the storage of the aquifer?*

## 4.1. Research design

To find answers to the questions highlighted in chapter 2, research was carried out following the framework shown in **Figure 4-1** and **Figure 4-2**.



Figure 4-1: Phases of research

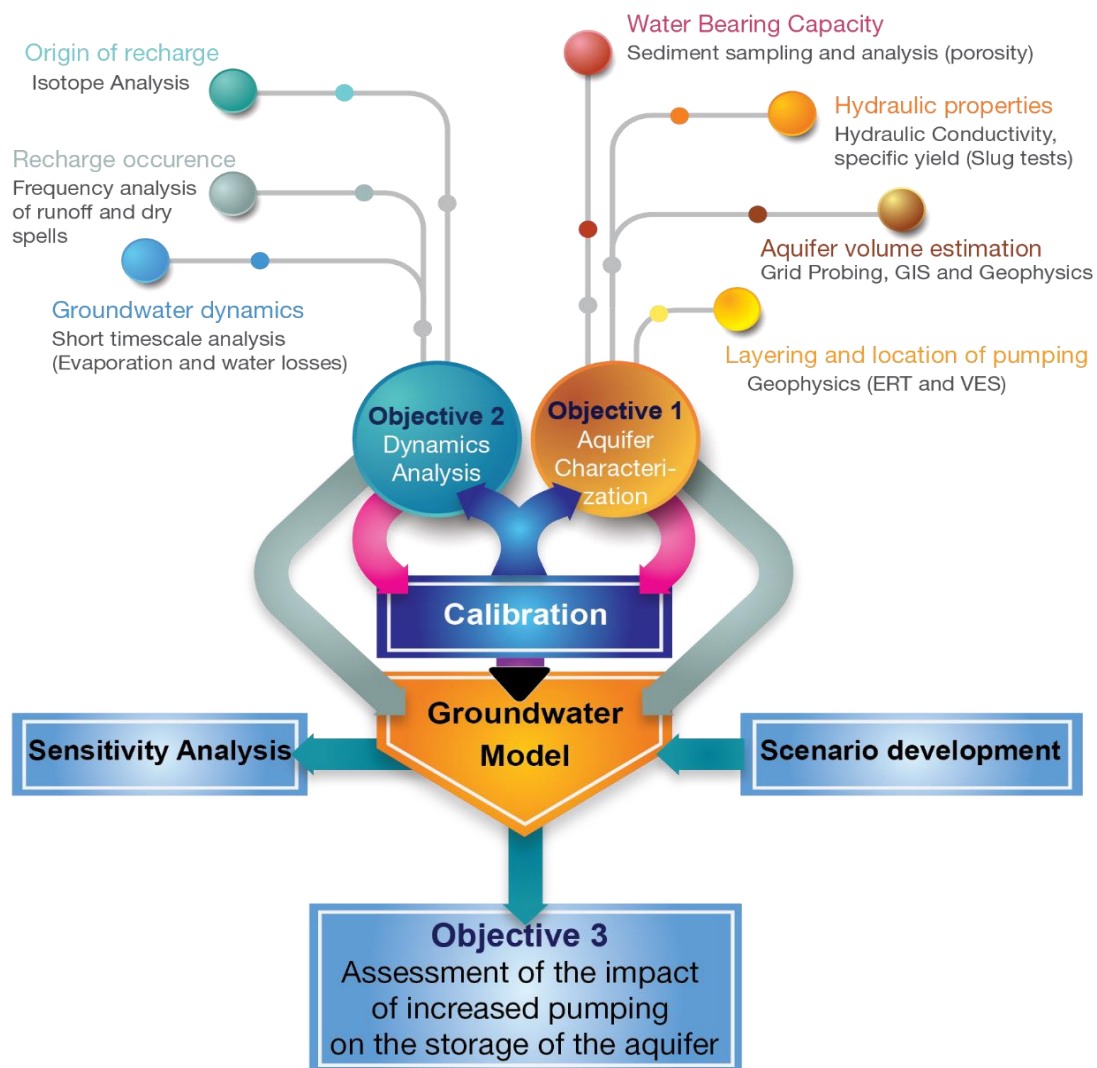


Figure 4-2: Framework of research methodology

## 4.2. Research techniques

### 4.2.1. Climatic data collection

The closest meteorological station to the study area is the « West Nicholson ». Other than that weather data are scarce. A small TAHMO third-generation telemetric weather station has been installed since April 2017 at Dabane's Processing Center with a measuring frequency of 5 minutes. The station ceased functioning months after its installation, which fortunately coincided with the dry season where rainfall rarely occurs. The station was reset in August 2017 and was able to capture the beginning of the entire following wet season with short periods of missing data. Rainfall data was not necessary for the study as surface water discharge is the dominant recharge mechanism of the aquifer, and field measurements were available.

Evapotranspiration estimations are on the other hand required for the modelling component of this study, as evaporation represents one of the main outflows from the sand river aquifer system. Average annual potential evapotranspiration values were considered to simulate the evaporation losses at the surface of the sand. The evaporation effect diminishes with depth until the extinction depth is reached and evaporation is ineffective. Values of 5 to 6 mm/day for PET were considered to be representative of the Northern Limpopo (EcoAfrica, 2015). Extinction depths for the sand were taken from the literature and vary between 0.8 to 1.2 m depending on the type of sand (Moyce et al. 2006; Mansell&Hussey, 2005; Hellwig 1973; Wipplinger 1958). The effect of evaporation from the surface of the sediment only becomes important if the water level remains close to the surface. Therefore the effect of the daily evaporation rates considered becomes less important almost a 100 days after the beginning of the dry season (Wipplinger 1958) , and any errors with the selection of the PET values will not affect the results significantly.

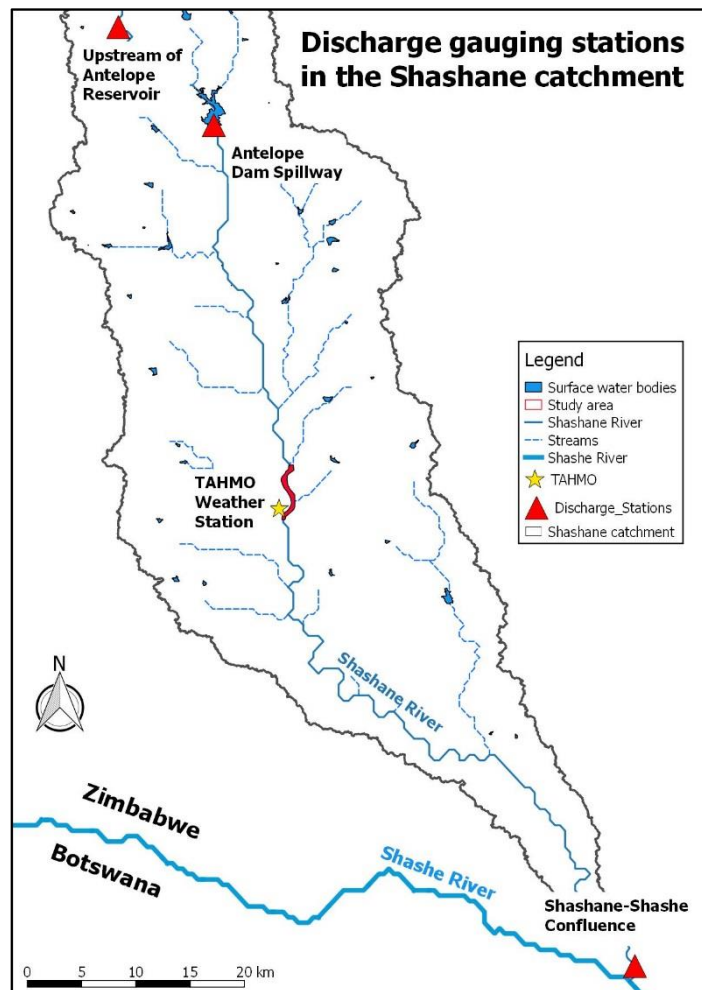


Figure 4-3: Location of the discharge gauges

Discharge data were obtained with a collaboration with the project partner ZINWA for three discharge measurement locations in the Shashane catchment (**Figure 4-3**). One measurement station is located just upstream of the Antelope reservoir to measure the incoming volumes to the reservoir. Another data set was consolidated from a discharge measurement station at the spillway of the Antelope reservoir which indicate events of both natural spills of the reservoir and events of artificial discharge. The third station is located at the outlet of the Shashane catchment a few kilometres upstream of the confluence of the Shashane with the Shashe River. This station measures the daily discharge variation for the catchment area downstream of the Antelope reservoir. The discharge observed at the outlet might not represent the natural hydrological behaviour of the catchment as this station is influence by the artificial releases from the reservoir. However, the magnitude of the releases is negligible compared to the concentrated discharge at the outlet of the Shashane catchment.

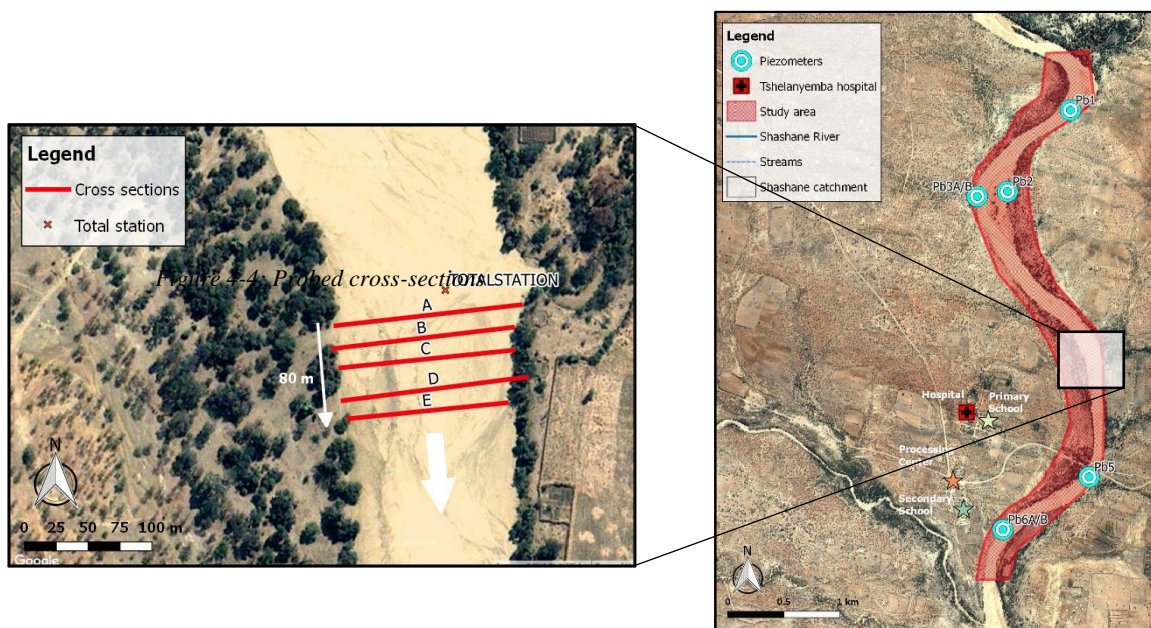
### 4.2.2. Total station survey

A length profile topographical survey was carried out by Blok (2017) starting from Pb1 to reach Pb6 with measurement points chosen to be in the middle of the cross section to cover the entire stretch of the study area (see **Figure 4-4**). This profile allows accurate estimation of the surface slope. On the other hand, a topographical survey was also performed on the probed cross sections for a more accurate 3D model of the subsurface. The elevations are relative and reported in reference to a random point at the most upstream stretch of the surveyed profile. A 3D model was developed using SURFER by interpolating the measurements points.

The geometry of the aquifer includes knowledge of width, length, depth and topography variation. The focus was intended solely for the study area and if necessary assumptions were made for the aquifer in the rest of the catchment. Lengths and widths of the aquifers as well as contributing areas of the catchments were determined using DEM data and satellite images.

### 4.2.3. Probing

Probing is an easy technique used in sand riverbeds to determine the depth of the riverbed layers and gauging the presence of water below the sediment surface. This is done by physically inserting a thin pointed steel rod into the sand until it reaches resistance. On removal of the probe, the moisture level can be noted. In addition, by assessing the difficulty required to insert the probe, an appreciation of the nature and consistency of the sediment can be gained (Hussey, 2005). The method is quick and easy but is blind, as the resistance can be attributed either to bedrock or to clay. With experienced use, a sense can be developed to make the difference between the two depending on the sound created between the steel probe and the resisting level. On the other hand, the length of the probe is limited which limits the knowledge of the depth to resistance in the main channel or in deep riverbeds.



Due to the limited access to geophysics tools, probing was used extensively to estimate the thickness of the aquifer. In the previous year, Block (2017) probed along 6 cross sections and a length profile upstream of the bridge (**Appendix E**). Topography was not surveyed along the cross sections, and both resistance and surface levels were referenced to the water level which was considered horizontal. While the assumption of horizontal level of the water is correct, measurements of the water level are prone to error especially in elevated sides of the riverbed, where they tend to be drier than the low levels and therefore the probe is dried up quickly and easily by contact with the dry sediment. For this study, a total number of 5 cross sections spaced by 20 m were probed in a grid setting with a topographical survey of the surface to build an approximate 3D model of the subsurface (**Figure 4-4**). This will serve as a basis to estimate the volume of the sand, hence the storage, but also to build a subsurface model to implement in the bottom layer of the numerical model. SURFER was used to interpolate the data and visualize the subsurface in 3D. Despite the irregularity of the subsurface, linear smooth interpolation was chosen so as to capture the general variation of the depth of the sand

#### 4.2.4. Geo-electrical surveys

Geophysical assessment techniques are important tools in searching for natural resources, specifically for groundwater occurrences.

Two main geo-electrical techniques widely used in groundwater exploration practices are the Vertical Electrical Sounding (VES) and Electrical Resistivity Tomography (ERT) (Nonner & Stigter, 2015). VES results are one dimensional and the measurements are representative only of the layers underneath the potential electrodes. ERT on the other hand, provides measurements that allow building a 2D subsurface model. However, the depth of interpretation is shallower than the VES (Nonner & Stigter, 2015). Another measurement that allows to resolve ambiguities in the interpretation of the results from resistivity methods, is induced polarization. Chargeability is a common parameter used to measure the potential decay after the current is turned off. While resistivity is a material parameter, chargeability is highly dependent on the measurement settings (Amaya, Dahlin, Barmen, & Rosberg, 2016). High values of chargeability are indicative of sediments with high clay content as well as mineralized rocks, while soils with uniform particle size of sand and gravel commonly yield lower chargeability values (Alabi, Ogungbe, Adebo, & Lamina, 2010). The interpretation is relative and therefore careful attention needs to be paid to interpreting the IP results.

Archie's law states that the ratio between the formation resistivity ( $\rho_f$ ) and the pore water resistivity ( $\rho_w$ ) is indicative of the formation type and inversely related to the porosity. The law is expressed with following equation:

$$F = \frac{\rho_f}{\rho_w} = a\phi^{-m}$$

Where F is the formation factor, and a and m empirical values defined respectively as the coefficient of saturation and cementation factor (Chandra, 2015). The coefficient of saturation and cementation factor



are taken respectively as 1 and 1.3 for unconsolidated loose material as suggested by (Archie, 1942; Kirsch & Yaramanci, 2009; Nonner & Stigter, 2015)

Time constraints restricted the work to two ERT measurements and one VES (**Figure 4-5**). One ERT was performed on a 216 m long cross section near the position of Pb4. This cross section A1 is located immediately downstream of a confluence with a tributary, includes the whole riverbed and extends to the inner bend of the river meander. A second ERT was performed at location A2 (**Figure 4-4**) to investigate the layering of the river bank with a measuring orientation parallel to the riverbed so as to omit the effect of the uneven level of the bedrock in the river bank perpendicular to the river flow

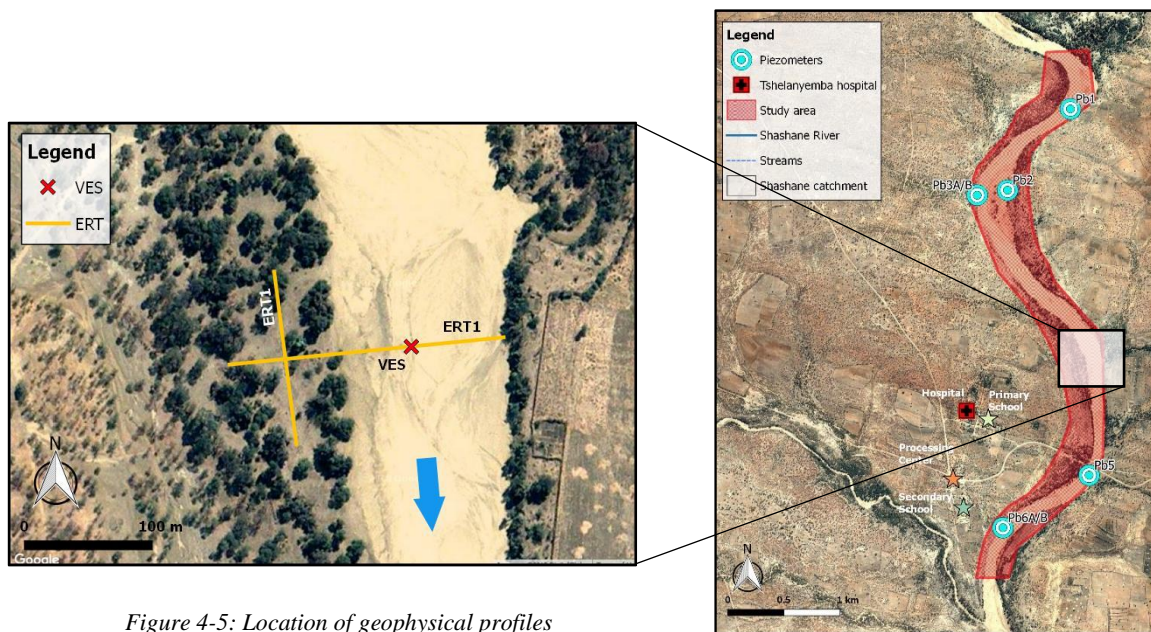


Figure 4-5: Location of geophysical profiles

direction. In the center of A1, one VES measuring sequence was done so as to be used to calibrate the ERT of the same cross section and increase the vertical resolution which lacks in ERT measurements. The topographical effect was included in the interpretation of profile 1, as the variation of the surface elevation can influence apparent resistivity values by altering the geometric factor (Kirsch & Yaramanci, 2009; Milsom & Eriksen, 2011).

A rule of thumb is that the interpretation is usually  $\frac{1}{4}$  to  $\frac{1}{3}$  of the length of the measured cross section. Small spacing between the electrodes allows to capture more details in the stratigraphy of the riverbed as this one is shallow but this depends mainly on the availability of short spacing resolution cables. Probing data indicate that the depth varies from 1 m to 3 meters which requires a very narrow spacing to capture accurately the variations of the subsurface. In this work, a spacing between electrodes of 3 meters was chosen with 48 electrodes leading to a maximum profile length of 144 m in one measurement set. A roll-along acquisition technique was performed to cover longer survey lines with limited electrodes in each run and survey a cross section of 216 m in total at once. Wenner-Schlumberger configuration was chosen as it offers a good compromise between lateral and vertical information. Finally, while cross section A2 is performed on a typically flat surface, the elevation in cross section A1 was surveyed so that its effect could be corrected during the model inversion.

VES interpretation was done using GEWin, which is an Excel-based application developed by N.L. van der Moot. ERT data was inversed using Geotomo's RES2DINV developed by Loke (1996).

Formation factors were classified for each formation type. Pore-water resistivity values were derived from EC measurements along the surveyed cross section, and information on the porosity and water resistivity was derived or also used to determine the underlying formations. In addition, considering representative values of the EC, formation types was classified for the rest of the subsurface material

In the scope of this research, geophysics will help answer questions related to the thickness of the sediments, the presence of clay layers in the riverbed, the layering of the river banks, the groundwater moisture content and quality, the aquifer subsurface boundaries and its interconnection with the remaining systems. However, the support is very limited given that the measurements were only done at one location within the riverbed and therefore upscaling needs to be further explored. Within limits of the data collected, the results will be then used as a basis to build the geometry of the numerical model.

#### 4.2.5. Aquifer properties

Sediment sample analysis were collected by Dabane Trust on multiple inspection campaigns carried out in different locations in the catchment. The sediments were sampled along the riverbed cross-section and for some locations, sampling was done in depth. Sieve analysis was performed and grain size distribution curves were developed by Dabane. The sediments were classified by the authors using the Unified Soil Classification System (USCS) which describes the texture and the grain size of most unconsolidated material. The distribution of the grains can also be evaluated by the uniformity coefficient and the coefficient of curvature to understand the gradation of the material. The results in combination with field observations shall serve as a basis to discuss the type of sediments, the uniformity, homogeneity and isotropy of the material forming the riverbed in the catchment. (Figure 4-6).

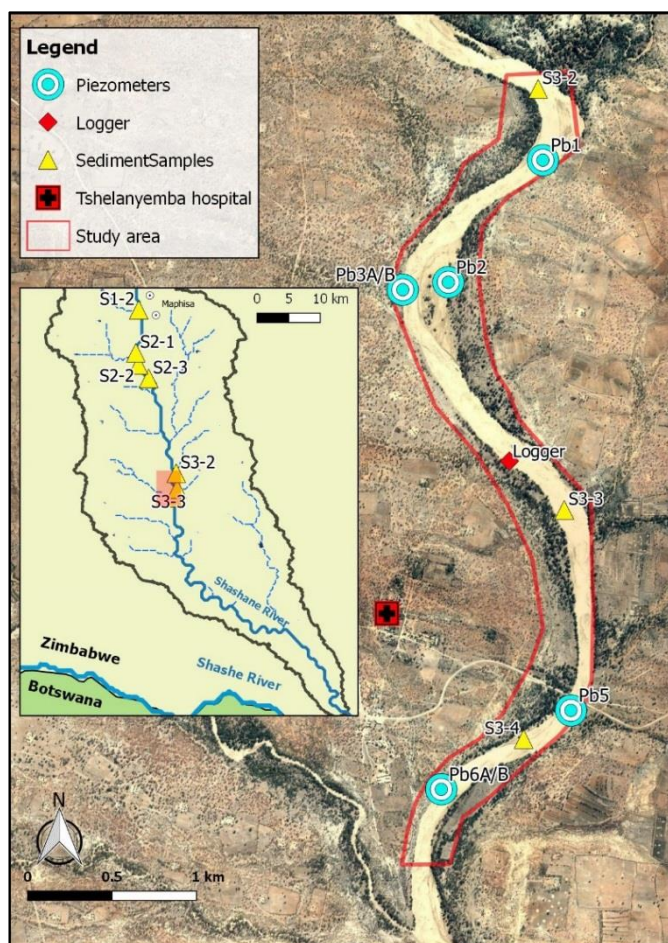


Figure 4-6: Location of sediment samples

Hydraulic conductivity can be estimated by different indirect or direct methods. Indirect methods to estimate the hydraulic conductivity such as the Hazen method (1893) are empirical and depend only on grain size distribution (Svensson, 2014).

$$K = C_H \times d_{10}^2$$

Where,  $K$  is the hydraulic conductivity in (m/s),  $C_H$  is an empirical constant taken as  $10^{-2}$  for sands (Leonards, 1962) and  $d_{10}$  is the particle size for which 10% of the material is finer (mm).

Direct methods span from regional to local tests. General and more representative values of the hydraulic properties of the aquifer could be determined by performing a pumping test. The narrow and thin geometric nature of the sand rivers combined with the irregular bedrock level as well as the presence significant clay layers present a unique set of problems which make the hydraulic situation very complex (Baker & Davies, 1997). It is essential for interpretations of pumping tests that no boundary effects interfere such as the location of the pump near the banks or recharge from surface water within the cone of depression especially since this one tends to be shallow and very wide in such excellent formation (Mulder, 1973). A pumping test was attempted, but no significant drawdown was recorded. In addition the conditions of the experiment were not favourable.

Local well tests were performed in Pb1, Pb3B, Pb5 and Pb6B. A slug test was performed by adding a known volume of water into the piezometer. The water level response in the well to the addition of water was measured using a diver set to measure every 0.5s interval. The measurements for each experiment started once the PVC pipe was filled entirely to the top level. The results were first interpreted using the Hvorslev method (Hvorslev, 1951) which assumes homogeneity, isotropy, incompressibility and infinite extent of the aquifer. However the method is initially designed for confined aquifer with possible use in unconfined aquifers if the well screen is not too close to the water table. The assumptions are valid for the aquifer material except the infinite extent and the confinement of the aquifer. For accurate interpretation AQTESOLV software was used to find the best method for estimating the hydraulic conductivity values which was revealed to be Bouwer method (Bouwer & Rice, 1976) designed specifically for unconfined aquifers.

Knowing the aquifer hydraulic properties ( $K$ ), the hydraulic gradient ( $\frac{\Delta H}{\Delta L}$ ), Darcy's velocity (in m/day) and the groundwater discharge (m<sup>3</sup>/day) can be computed by Darcy's law using equation:

$$q = K \times \frac{\Delta H}{\Delta L} \text{ and } Q = q \times A$$

Finally, porosity and specific yield of the aquifers sediments were not measured during this research. Their values were collected from literature (See section 2.1).

#### 4.2.6. Groundwater levels

As the piezometers equipped with divers installed last year in the study area were vandalized, a total of four new piezometers and two divers were installed in locations close to those of Pb3 and Pb6 to

measure the level of groundwater in the riverbed (**Figure 4-6 and Figure 4-7**). The upper part of two of the piezometers were left sticking out of the sediment by about 50 cm and capped on the top. This design allows to measure the groundwater at high levels of runoff before they get fully inundated. The piezometers will be monitored manually on a weekly basis by volunteers from the neighbouring gardens. This design of piezometers is unfortunately too attractive for passers and puts the monitoring point and specifically the divers at risk of vandalism. A defensive installation technique was adopted. The top of the second piezometer was submerged at a depth of 5 – 10 cm under the surface level of the sediments. The top part was slotted and covered with a filter to prevent sediment intrusion. The slots on the top also prevent the air in the piezometers from being trapped during high runoff levels and therefore measurements from the diver will not be disturbed. Divers were also introduced in the buried piezometers for computations of gradients and groundwater flowrates. Water levels were coupled with accurate elevation measurements using the total station. Manual measurements were performed during the observation period to cross-validate the diver measurements.

Short time-scale analysis was done on the recorded water level variation to estimate the losses that undergoes the storage of the aquifer. While the piezometer data indicate the total variation in WL, multiplying the losses by the effective porosity indicate the decrease in the amount of the water from the storage. Consequently, gross losses in the aquifer was estimated and compared with evapotranspiration

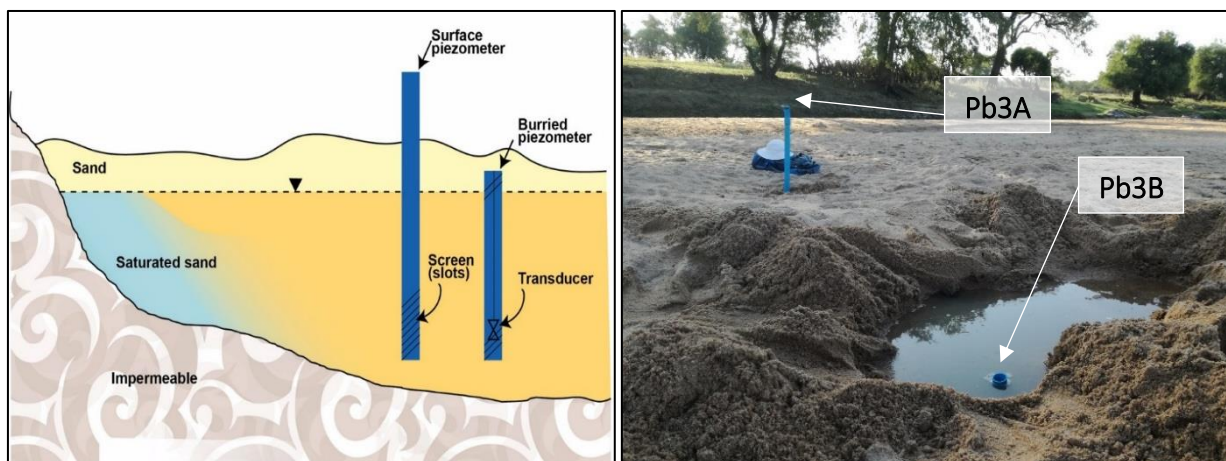


*Figure 4-7: Piezometers installed at location 3. Pb3A manual measurements and Pb3B for diver measurements rates to assess the predominance of each loss component.*

On a more detailed time-scale, diurnal groundwater fluctuations were used to determine daily evaporation rates using the Hays method (Hays, 2003) (**Figure 4-8**).

Water losses were compared to the potential evapotranspiration computed using the data from the installed meteorological station and using FAO's ETo calculator available for free download and use (see <http://www.fao.org/land-water/databases-and-software/eto-calculator/en/>).

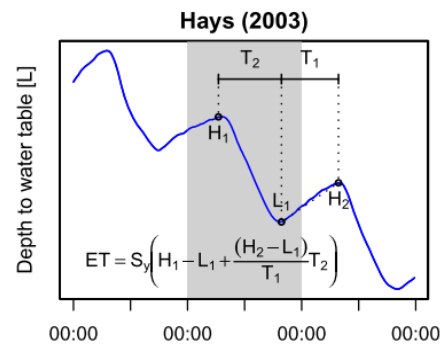


Figure 4-8: Illustration of estimation of daily ET based on groundwater fluctuation using the Hays method. (Fahle & Dietrich, 2014)

Dabane Trust also owns an hourly data logger installed about 500 m downstream of Pb3 and in operation since 2012 (**Figure 4-6**). The logger, measures a compensated water depth above the sensor, however there is no metadata available about its depth. Due to the importance of this data set in the calibration of the numerical model, the depth of the sensor (or the level of the surface level) had to be determined. This was achieved by comparing the values of the daily maximum measurements with the daily average. The properties of the ephemeral river suggest that surface water levels vary rapidly which makes the ratio of daily max with daily average measurements high, whereas groundwater level variations are slower and the ratio between max and average daily measurements should be small. This allows to determine with certitude the beginning and end of the dry season and differentiate between records of surface water and groundwater. The depths of the sensor were then easily deduced from the graph.

### 4.3. Groundwater model

In light of the previous methods including geophysics, topography, and field measurements, a groundwater numerical model was built to understand the dynamics of the aquifer system. The main objective of modelling a limited stretch of the aquifer is to assess its capacity to sustain development schemes in the neighbouring region. The developed model is transient and aims to provide the following information:

- Estimation of the recharge in natural and abstraction scenarios
- Assess the interaction of surface and groundwater
- Simulate local water management scenarios for agricultural development
- Determine the best spatial locations of abstraction wells
- Optimize the abstraction rates to sustain agricultural development
- Determine the potential area to be irrigated by the aquifer.

The modelling was accomplished using Aquaveo's GMS as a commercial graphical user interface to USGS MODFLOW.

### 4.3.1. Conceptual model

A conceptual model is a simplified presentation of the groundwater bearing system and the interaction between its units as well as its boundary conditions (**Figure 4-9**).

Conceptually, the Shashane riverbed is defined as a conduit composed of two layers of deposits. The upper layer of the alluvium is an unconfined aquifer formed of fine to coarse sand of depths varying from 1 to 5 meters. Probing and Geophysics data showed that this thickness varies depending on the location of the main channel. Closer to the riverbanks the riverbed is shallow and deepens in the middle or the opposite riverbank. The alluvium material becomes finer with depth and is underlayed by silty clay material of very low hydraulic conductivity. The system is assumed to be enclosed by an impermeable

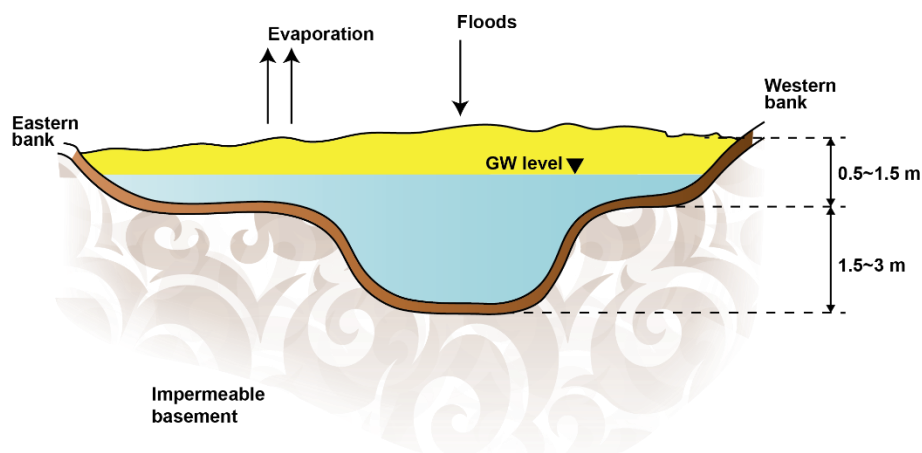


Figure 4-9: Conceptual model

rock basement that prevents vertical seepage.

Groundwater inflow and outflow occur at the upstream and downstream boundaries, respectively, where significant fluxes of water are expected due to the connectivity with the upstream and downstream extents of the alluvium aquifer. However, due to the low gradient, the fluxes remain insignificant in comparison with the evapotranspiration outflows. On the other hand, groundwater lateral inflow from, and outflow to the riverbanks is assumed to be insignificant due to the very low hydraulic conductivity of the clays that form the banks.

Recharge is derived mainly from surface river flow and rainfall contribution is insignificant. Discharge occurrence is considered as a signal of full saturation of the aquifer as surface water only occurs once the whole aquifer is saturated. Therefore, the model will not simulate accurately the mechanisms of recharge since these require an accurate characterization of the flow in the unsaturated zone. Discharge from the aquifer is mainly due to evaporation, outflow through the downstream (southern) boundary and direct groundwater abstractions.

The simplifying assumptions of the model under natural conditions can be summarized as follows:

- There is constant replenishment from the upstream independent of the season.

- Evaporation effect is observed up to a depth of 0.8 ~ 1.2 m with a maximum rate corresponding to the potential evapotranspiration rates uniformly to the whole area.
- No flow boundaries are assumed between the riverbed and the riverbank, even if the riverine vegetation indicates the two systems might be connected. The same is assumed between the riverbed and the underlying layers of clay and fractured bedrock. Vertical leakage is assumed to be insignificant and there is no presence of preferential groundwater flow due to secondary porosity, fracture or faults.
- Surface elevation is considered to be uniform within one cross section
- Discharge at the study area is considered to be the same as the catchment outlet without a delay in occurrence.
- Recharge to the aquifer is uniform across its area.
- Surface water infiltration is the main recharge component to the aquifer and direct precipitation recharge is insignificant.
- The riverbed is assumed to have uniform and isotropic hydraulic properties.
- The constant head boundaries vary in time according to a time-dependent relationship developed from logger data. The same trend is assumed to be observed everywhere in the aquifer. This means that the aquifer will never run entirely dry in the natural conditions as evaporation, being the major outflow component, extinguishes below 1 m of depth. In addition there is constant head inflow and outflow that maintains a balance in the dry season.

#### 4.3.2. Simplified tank model

The behaviour of the alluvial aquifer can be approximated to a rectangular canal containing sand to which a water balance can be applied (Hussey, 2005). Conceptually the water balance can be summarized in (**Figure 4-10**). The inflows comprise of the precipitation ( $P$ ), groundwater inflow ( $Q_{in,g}$ ) and surface water recharge ( $Q_{in,s}$ ), whereas outflows extend to groundwater downstream outflow ( $Q_{out,g}$ ), surface outflow ( $Q_{out,s}$ ), evapotranspiration ( $E$ ), downward seepage ( $G$ ), net lateral discharge or recharge ( $Q_L$ ) and artificial abstraction ( $Q_{abs}$ ). The water balance equation is expressed as follows:

$$Q_{in,s} + Q_{in,g} + P = E + Q_{abs} + G + Q_L + Q_{out,g} + Q_{out,s} \pm \frac{\Delta S}{\Delta t}$$

In the absence of all important components to close the water balance, the aquifer was conceptualized as a tank

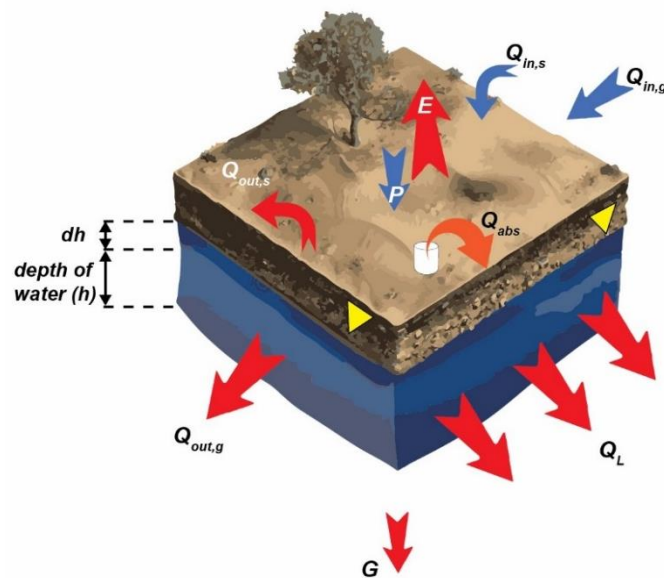


Figure 4-10: Idealized schematization of flow in the sand

(Figure 4-10 and Figure 4-11). Discharge occurrence is considered as a signal to full saturation of the aquifer. This means that when the discharge is observed, the volume of the aquifer is re-initialized at its maximum storage capacity. During dry days, the outflows are simulated using the WL time dependent relationship in section 4.2.6. This relationship is assumed to account for evaporation losses, and other unidentified outflow processes.

The tank model was defined for the 5.6 km long studied portion of the aquifer with the assumption that groundwater outflow from downstream is compensated by the same rate of groundwater inflow from the upstream. Abstractions and other losses are then added and the total storage at the end of the time step is computed as well as the corresponding height. Considering a uniform width of 120m and a length of 5600 m, the depth of the riverbed was taken to be equal to 3.85 m so that the storage of the aquifer approximates the storage of the 3D modelled riverbed. The maximum storage capacity of the tank and the volume of water available for use are defined in section 5.1.4.

The purpose of this simplified water balance model is to simulate the behaviour of the system in a lumped manner regardless of the spatial variations of the parameters. And compare the results to the numerical groundwater model.

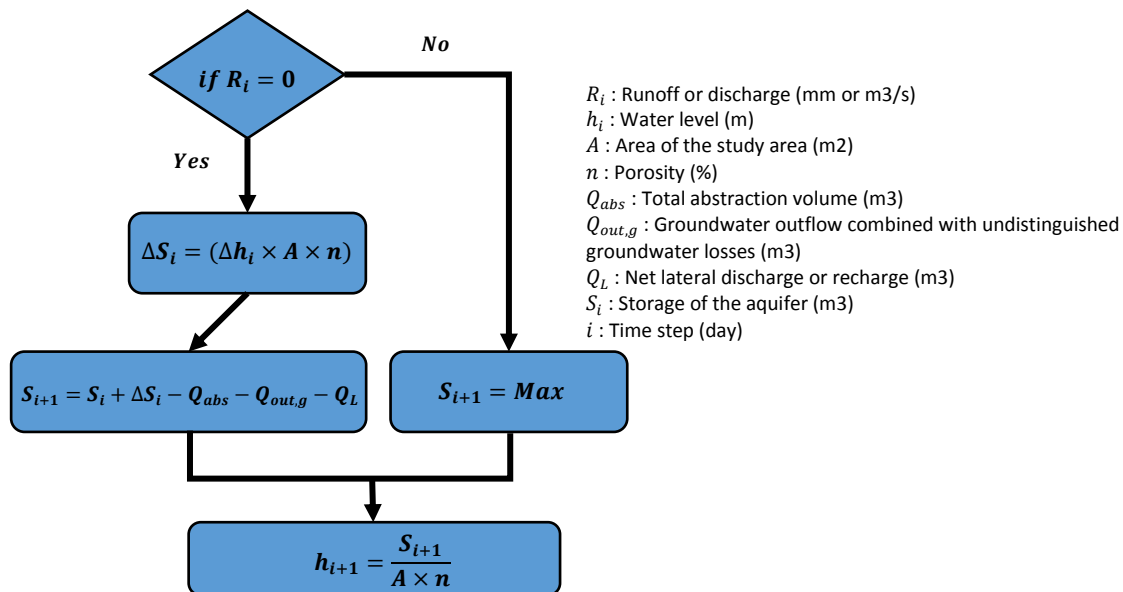


Figure 4-11: Simplified water balance model

### 4.3.3. Numerical groundwater model

#### a) Model discretization

MODFLOW is considered an international standard for simulating and predicting groundwater conditions and groundwater/surface-water interactions. The model requires both spatial discretization and time discretization. While refining the grids allows a more accurate representation of the behaviour of the system in interest area (for example: around obstacles and wells), for this work, no refinement was



necessary as the model was desired to be as simple as possible and detailed behaviour around abstraction wells was unnecessary as the simulations performed were independent of the method of abstraction.

Spatial discretization parameters are summarized in **Table 2**. The vertical dimension was added using one layer of varying bottom level. This was done assuming that the hydraulic conductivity of the clays was too low and no flow conditions were then assumed. This decision particularly decreases the number of layers and cells and therefore decreases computation time. However, such way of modelling the layer will create in some cases rough transition from one cell to another and increases the possibility of computation errors caused by geometrical complexity. Cells falling outside of the model boundaries are designated as inactive.

As the model is intended to be built in transient mode, MODFLOW requires the time dimension to be discretised into several stress periods. The recharge mechanism of the sand river systems as well as the decline in water levels during the dry season is fast and therefore a stress period of one day was considered. In addition, the spatial extent and discretization of the model justify the choice of such a high time resolution. MODFLOW computes the groundwater level at the center of each active cell in the model space for each time step of a stress period for the whole simulation.

Table 2: Model grid and time discretization parameters

Model grid specifications		Model time-discretization parameters	
South-west corner	(0,0)	Stress period length	1 day
No. of layers	1	No. of stress periods	Varying depending on the type of simulation. Min = 365 days; Max = 6000 days
No. of rows	265		
No. of columns	70		
Column width	20 m		
Row width	20 m		
No. of active cells	2565	No. of time steps	1 per stress period
Total cells (active + inactive)	18550		

The following surface elevation data sets are required to be specified in meters for the top and bottom of each active cell, in the current model to define aquifer geometry:

- Top elevation of surface of the aquifer
- Bottom elevation of the aquifer (varies from 1 to 5 meters)

Top level elevation of the riverbed surface were derived combining DEM data with a total station survey. Elevations were considered constant within a cross section profile. Bottom elevations were estimated by delineating the extent of the main channel using cross-sectional and longitudinal probing profiles. This allows the determination of the location of the deepest level of the aquifer. The form of the cross section was determined using the probing and geophysics. Shallow parts do not exceed 1 meter whereas the deepest parts reach up to 5 meters (**Appendix H**).

The simulation starts at the very beginning of the dry season of 08/04/1986 and the longest period of simulation is 16 years.

#### **b) Initial heads**

MODFLOW numerical model requires the modeller to indicate the initial head values for every active cell in each layer at the start of the first stress period. At the end of the last runoff event and after recession of the surface water the river bed will be fully saturated and therefore initial heads were assumed to be equal to the top surface elevation. This behaviour is observed in data retrieved from data loggers but is also an inner characteristic of this type of aquifers which saturates entirely before any surface water flow can occur on the surface (**Appendix H**).

#### **c) Aquifer parameters**

The knowledge of hydraulic conductivity and storage capacity of the aquifer at each active cell is required for each transient numerical model, in order to compute the flow between adjacent cells and the variations of the storage of the system. In general, values of the hydraulic conductivity and storativity vary across the model in length and depth and they are determined through in-field tests.

The material forming the alluvial aquifer was assumed to be uniform and isotropic of fine to coarse sand with expected hydraulic conductivity values varying from 80 to 140 m/day. This was observed in the field and estimated using bucket and slug tests. Additionally, values of the hydraulic conductivity were obtained from literature on aquifer systems in the Northern Limpopo or the Mzingwane which are in the same area and of similar conditions. These values were used as initial estimates for the model which eventually were varied during the calibration for the best fit obtained between measured and estimated values.

On the other hand, storage coefficients are assumed to be uniform across the model area. As the aquifer is unconfined, only specific yield needs to be specified in MODFLOW.

#### **d) Boundary conditions**

Boundary conditions determine where water enters or leaves the modelled area. Model boundaries on the river banks were defined as “no-flow” boundaries since lateral discharge is assumed to be insignificant. Boundaries in the northern (upstream) and southern (downstream) extents of the aquifer were designated as a constant head boundary (CHD) in which head varied with time (**Appendix H**). The variability in time was obtained using a time dependent relationship and the discharge data which define the water level in the aquifer during the dry season. During the wet season when there is observed discharge, the water level was assumed to be at the surface top elevation. The time relationship is

defined by an exponential decay that reaches a limit depth, therefore independent of the length of dry season. The water level at the boundaries never dries up providing infinite source of out- and in-flows. Imposing time-variable constant head boundary leads to forcing the system to behave accordingly and the inflows and outflows in and from the aquifer are not natural. This particular boundary condition creates a valid subject of debate on the validity of the model. (Miller 2000) (USGS) used injection wells to simulate the groundwater inflow upstream and abstraction wells downstream but this requires a clear estimation of the influxes.

Recharge events generated by river discharge cause full saturation of the aquifer which increase the head above the topographical surface level. In reality this excess head is translated to surface water and need to be taken out of the model. River package was intended to be used in order to simulate this surface water-ground water interaction. The River package cells are on top of the groundwater cells which means that the river is always a losing river. This created issues with the convergence of the model since the calculations are infinitely looped between groundwater excess that flows to the river and from the losing river to the aquifer. To overcome the issue and meet the description of the boundary condition, drains with a very high conductance were installed at the surface level of the aquifer, to make sure that at the end of the runoff event the head above the aquifer is at the topographical surface elevation.

#### **e) Recharge**

In this study, recharge is assumed to be a function of flood events only. Direct rainfall recharge is insignificant in comparison to the empty storage of the aquifer. Recharge in these alluvial aquifers is derived mainly from river flow where the full recharge of the aquifer occurs rapidly early in the beginning of the rainy season (Nord, 1985).

The recharge package (RCH) was used to simulate the recharge of the aquifer from the discharge values. Recharge data were increased and given in excess in order to ensure that the aquifer is fully saturated by the end of each runoff event. Any excess water was drained using the drains package (DRN). Recharge was defined on each cell uniformly. This was done to ensure that the sand level is saturated at the end of each discharge event. Recharge through side inflows of the tributaries was not included and was accounted for in the total flux recharge.

#### **f) Evaporation**

Evaporation is the major outflow from the aquifer in the absence of abstractions. In MODFLOW, evaporation is simulated using the EVT package which simulated the effect of direct evaporation in removing water from the saturated groundwater regime (Harbaugh, 1988)

The evaporation is implemented by specifying a maximum rate of evapotranspiration (ET) and the extinction depth below which zero evapotranspiration occurs. Between the two depths, evapotranspiration varies linearly.

Evapotranspiration was chosen between 0.0055 and 0.0025 mm/day which correspond respectively to an average potential evapotranspiration of 2000 mm/year and actual evapotranspiration of 912 mm/day (FAO). This value was maintained constant for all the stress periods. The extinction depth used had 1 meter value for sand materials. This value was corrected during the calibration to 1.2 m to simulate the same drop of the water level as the one observed in the field data as well as to obtain a better model fit.

#### **g) Well package**

The well package is designed to account for the water losses from the cells due to abstractions. Discharging wells have negative rates. For each cell only one value of the net discharge can be specified for each stress period.

Abstraction rates depend on the scenario to be simulated. On the other hand, a simulated pumping well is considered to be screened through the full saturated thickness of the cell. No refinement of the cells around the wells was performed which means that simulations performed will be independent of the abstraction method.

#### **h) Evaluation of the model**

- **Calibration of the model**

The calibration of the numerical groundwater model intends to determine the set of parameters, boundary conditions and external stresses that allow the simulated heads and fluxes to match field measured values within an acceptable range of error.

Calibration is only necessary during the dry season since the model assumes full saturation of the riverbed during the wet days. Due to the lack of data, calibration is performed over the dry season of the year 1986 which is representative of an average dry season with 263 dry days until the next major recharging event and assumes that the water levels drop in a similar way every year depending on the duration of the dry year only. Calibration was done by modifying the evapotranspiration maximum rate, extinction depth of evaporation and hydraulic conductivity. The degree of success of a calibration attempt was evaluated both qualitatively (visually) and quantitatively (statistically). As the model extent is small and the grid is refined, low discrepancies are expected between calculated and measured heads.

- **Sensitivity analysis**

Sensitivity analysis is a paramount step to justify the assumptions made for the model. The task was performed for the major input parameters defining the model and the changes on the output variable was assessed. The outputs could be displayed either by showing the variation of the head for the year of 1986 or in terms of the storage at the last day of the dry season as a percentage of the maximum available storage capacity.

The values of the parameters and the ranges of variations are given in **Table 3**. Ranges of the values of all the parameters were obtained from literature, except for the conductance which were defined specifically for the model. Max and min represent respectively the percentage of increase and decrease to the original value of the parameter.

Table 3: Parameter variation for the sensitivity analysis

Parameter	Value	Max %	Min %	Max value	Min value
Hydraulic Conductivity (m/day)	120	+100%	-50%	240	60
Specific Yield (%)	0.15	+66%	-50%	0.249	0.075
Max ET rate (m/day)	0.0025	+50%	-50%	0.00825	0.00275
Extinction depth (m)	1.3	+25%	-50%	1.5	0.6
Drains conductance (m <sup>2</sup> /day)	300000	-70%	-85%	90000	45000

#### 4.3.4. Scenario development

The scenarios developed in this section have the aim to assess the ability of the Shashane sand river aquifer to sustain agricultural development in the future, framed as such within the goals of the A4labs project. The assessment focuses on available water volumes as well as the locations of pumping and the effect of intensive abstractions on the storage of the aquifer.

The scenarios are built upon the baseline scenario (Scenario 0) which simulates the natural behaviour of the system without abstractions. A total of 4 strategies (1, 2, 3 and 4) were developed to assess the effect of the spatial distribution of abstraction wells on the yielded volumes. For each spatial strategy, increased abstraction rates are also simulated (A, B and C). The total demand is maintained constant between the pumping strategies (1, 2, 3&4) by reducing the abstraction rate per well and increasing the number of wells. This allows for a consistent comparison of the effect of the spatial distribution on the ability of the system to meet the demand. The wells were carefully positioned along the deep part of the subsurface (5 m) to avoid drying up due to shallow channel (**Figure 4-12**). Finally, Simulations are run on one year of 1986 as an

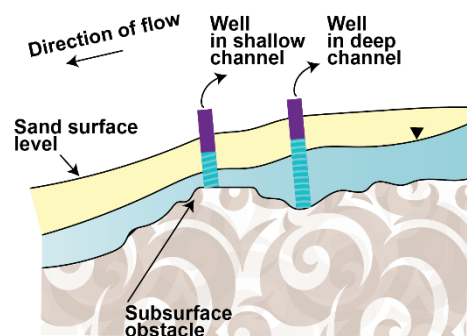


Figure 4-12: Illustration of the importance of positioning the abstraction wells

average dry year of 263 days. On the other hand, demand is considered to begin in the first day of the dry season. The scenarios are summarized in **Table 4 and Appendix H**.

Table 4: Summary of spatial strategies and abstraction rate scenarios

	Spatial Distribution				Total demand for each scenario (m <sup>3</sup> /day)
	Strategy 1	Strategy 2	Strategy 3	Strategy 4	
# of wells	11	15	21	30	
Spacing between wells (m)	500	350	250	150	
Scenario A: QA (m <sup>3</sup> /day/well) =	30	22.0	15.7	11.0	330
Scenario B: QB (m <sup>3</sup> /day/well) =	75	55.0	39.3	27.5	825
Scenario C: QC (m <sup>3</sup> /day/well) =	172.8	126.7	90.5	63.4	1900.8

- **Abstraction rate scenario justification**

- Scenario A: With moderate abstractions as defined by the development scheme of Dabane which dictates 3 mm for 3 ha every 3 days. Assuming 8 hours of pumping, this leads to 30 m<sup>3</sup>/day and a pump of 1 l/s. The modelling however, is independent of the abstraction method.
- Scenario C: It considers a solar pump of 1 l/s for every 0.5ha. This leads to 6 l/s for 3 ha, with a maximum of abstraction of 172.8 m<sup>3</sup>/day.
- Scenario B: Is simply an intermediate pumping rate to the previous scenarios.
- The total demand for each strategy is calculated by multiplying the abstraction rate per well by the number of wells.

- Optimizing pumping rate

For Strategies 3 and 4, the abstraction rate was varied to determine the maximum abstraction rate per well (hence total demand) which the system is able to sustain without any failure, for the entire dry season. With this, the potential irrigated area can be estimated. For this particular abstraction rate, the potential irrigated area is computed according to demand in Scenario A, Scenario C and also according to the suggested amount of water used by the Zimbabwean ministry of agriculture for planning irrigation developments which is defined by 41 m<sup>3</sup>/ha/day.

- Estimating Recharge

Recharge was artificially calculated using MODFLOW's flow budget, as the volume necessary to re-saturate the aquifer, therefore it is not simulated as a natural process. For Scenario 0, the recharge was computed for the entire observation period. The potential impact of increased abstractions on recharge and consequently on runoff was assessed by computing the recharge for selected years HY1990 to HY1999. The pumping strategy followed is Strategy 4 with a pumping rate of 26.6 m<sup>3</sup>/day per well (see 5.3.3).

## CHAPTER 5

# Results and Discussion

## 5.1. Characterization of aquifer parameters

### 5.1.1. Texture and permeability

- Texture

**Figure 5-1** illustrates sieve analysis results for samples from the study area (see **Figure 4-6**), sampled in the middle of the cross-section of the riverbed. It can be derived that the particle size distribution of the soil samples vary from 0.06 mm to 5 mm. The effective grain diameter ( $d_{10}$ ) varies between 0.28 to 0.45 mm whereas the median grain size diameter is 0.8 mm on average. Depending on the sampled location, between 50 to 75% of the grains pass through the 1 mm sieve and almost 99% of the alluvial material is larger than 0.0625 mm defining the lower boundary of the sand grains (Wentworth, 1922). 10 to 20% is the fraction corresponding to very fine to fine pebbles (higher than 2 mm) which was observed in the field on the surface of the riverbed and where the cross section enlarges and the flow slows down. The disparities between the distributions of the different samples are caused by the non-uniformity of deposition of the sediments as an effect to the increase or decrease of the bed shear velocity which depends on the flow regime (Lamb & Venditti, 2016). The distributions remain inter-

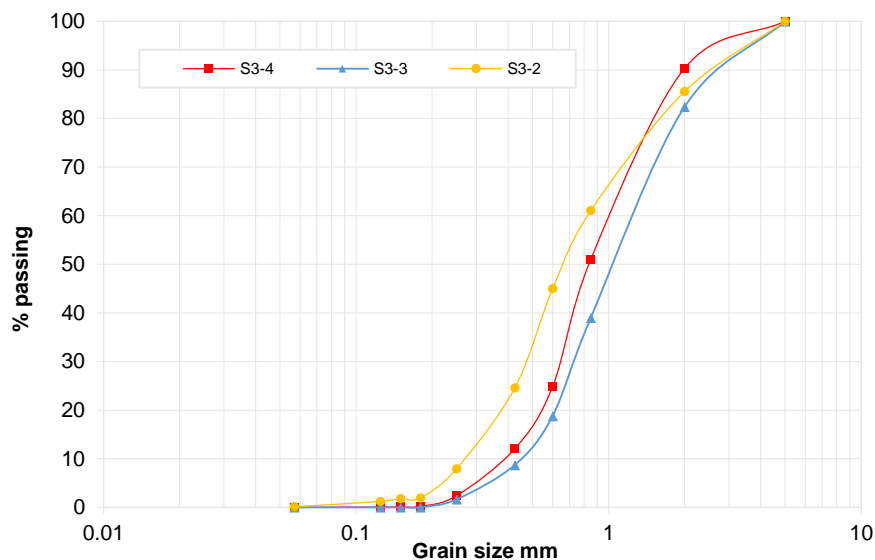


Figure 5-1: Grain size distribution of the sediment sampled in the study area.

comparable and fall within the same range of grain size which classifies the material as fine to coarse sand (**Appendix B**).

Values of the coefficients of curvature and uniformity in the study area vary respectively between 2.5 and 3, and approximating 1 for curvature coefficient. In other sparsely sampled locations upstream of the catchment (see **Figure 4-6 and Appendix B**), the coefficients have similar values except for S1-2. According to the Unified Soil Classification System (USCS), these alluvial deposits can classify as poorly sorted sands in contrast to the sand from sample S1-2 which is well sorted. However, its classification was determined at the limits of the criteria based on the uniformity and curvature coefficients.

Sand samples of unknown location, taken from the study site and sampled at a lower depth in the riverbed, were observed to contain a higher fraction of grains with a bigger sediment size, than those at the top surface (**Figure 5-2a**). The sediments get coarser in depth. This was observed as well during the installation of the piezometers where the drilling tool jammed several times on coarser angular grains with diameter between 20 to 25 mm. However, with this coarsening, the sediment remain within the boundaries of a poorly sorted sand and should not be considered as a separate layer. At a depth reaching 2.5 m, the sediments become finer as encountered frequently during the drilling. Mulder (1973), during an inspection campaign near Messina in the Limpopo, observed the occurrence of these lenses of fine sediments more specifically near the tributaries. This could be the result of slow sedimentation during recession of surface discharge (**Figure 5-2b**).

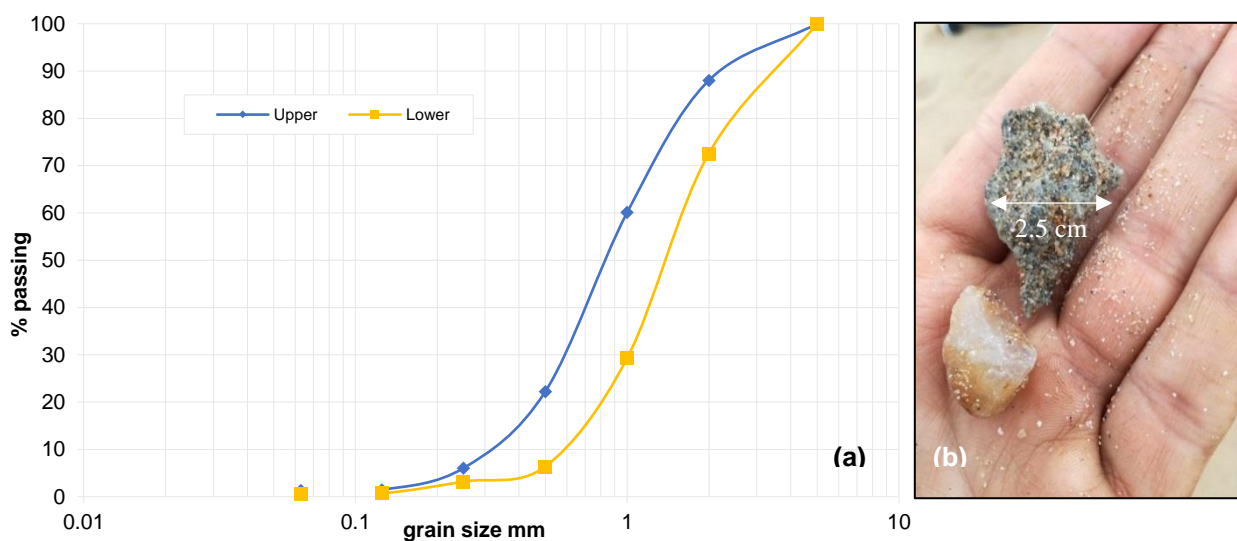


Figure 5-2: (a) Example of size grain distribution at different depths in the study area.(b) gravels encountered during drilling at 2 m depth

- **Hydraulic conductivity**

The results obtained from the two approaches to estimate the hydraulic conductivities are summarized in **Appendix C**. The Hazen (1892) method yielded an average hydraulic conductivity of 127 m/day, with a clear disparity between the upstream, midway and downstream samples. The Hvorslev (1951) method gave an average of 106.1 m/day whereas the Bouwer and Rice (1976) method yielded an average of 111.4 m/day. The slug method interpretations showed low variations between the samples as expressed



by a standard deviation of 9 m/day. Both approaches resulted in hydraulic conductivities within the ranges defined for sand aquifers of sand rivers. However, the Hazen method is sensitive to the square of the effective grain diameter which varies between the locations and depends significantly on the sampling method. On the other hand, slug tests do not disturb the grain distribution and unlike indirect methods, measure the horizontal hydraulic conductivity of the material within the vicinity of the well. The hydraulic conductivities obtained using slug tests are uniform and confirmed with repeated experiments. The assumptions of validity of the methods are almost entirely met except for the infinite extent of the aquifer. Finally, the Bouwer and Rice (1976) method provides the most reliable estimations of the hydraulic conductivity as it was designed for unconfined aquifers.

### 5.1.2. Average slope and hydraulic gradient

DEM data was used to develop the topographical profile of the 102 km stretch of Shashane River. The surveyed stretch shows a steady and uniform slope of 0.23% (**Appendix D**). Mansell and Hussey (2005) found slopes of 0.32% in the mid Shashane River, whereas, in the Mzingwane catchment, Moyce et. al (2006) found that the riverbed sloped by 1:500 to 1:1000 in the lower Mzingwane. In more detail, there are elevation spikes observed along the river which could either be the result of the low resolution of the DEM or the possibility of local variation in elevation explained by built-in sand dams or simply rock outcrops due to the non-uniform nature of the river sections. The local disparities in elevation decrease as the downstream stretch becomes flatter. The DEM profile was validated by a total station survey which indicated a similar value of 0.26% for the surface slope (Appendix).

The distribution of the channel is conditioned by the slope of the river channel. In areas characterized by steep slopes, the formation of the alluvial aquifer is discouraged as these sites favour erosion instead of deposition because of the high velocity flows generated. As a consequence, the formation of the alluvial aquifer is expected to be formed in flatter stretches where the slopes are gentle. At the low levels of the streams, the flow cross-sections enlarge, increasing the losses to evaporation and infiltration which reduce the sediment transportation energy and velocity of stream flow, thus, allowing more accumulation of the sediments and resulting in alluvial aquifer formation (Maspovo, 2008; RJ Owen & Rydzeski, 1991). Alluvial aquifers are typically present downstream of the center of the catchment where the slopes flatten to gradients less than 1:350 (R. J. Owen, 1989). Consequently, riverbed alluvial aquifers are expected in the Shashane and neighbouring catchments to occur around the southern edges of Zimbabwe.

### 5.1.3. Depth and thickness

#### Geophysical assessment

**Figures 5-3**, illustrate the results of geophysical ERT profiles (see **Figure 4-5**), including electrical resistivity and the formation factor. Profile 1 (**Figure 5-3a**) is perpendicular to the river, while profile 2 is performed on the western bank and parallel to the river (**Figure 5-3c**). Profile 1 extends for 216 m where

the start of the cross section is located at the most the western riverbank. The riverbed starts at 90 m and ends at 216 m.

From the profile three formations can be distinguished. A formation with resistivity below 80  $\Omega\cdot\text{m}$ , which forms the majority of the subsurface of the western bank as well as below the riverbed. These resistivity values correspond to saturated clay material of which resistivities range between 1 to 100  $\Omega\cdot\text{m}$  (Kirsch & Yaramanci, 2009; Loke, 1996). On the riverbed (90 m to 216 m), formation resistivity vary between 250  $\Omega\cdot\text{m}$  to more than 1000  $\Omega\cdot\text{m}$  to the left side of the riverbed. Resistivity ranging from 200 to 300 are typical for alluvial material of fine to coarse sand saturated with fresh water. The thickness of the material varies between 1 to 2.5 m in the centre and deepens to reach of 5 m of medium to coarse sand. At this depth, the sand starts mixing with finer material and clay as illustrated by the decreasing resistivity values of 100 to 130  $\Omega\cdot\text{m}$ .

Between 90 and 144 m, resistivity values vary between 400 to almost 2000  $\Omega\cdot\text{m}$ . These high resistivity values correspond to unsaturated to very dry sands (Nonner & Stigter, 2015). Probing results confirm this (**Appendix E**), although the estimation of the water table was inconsistent because of the friction between the wet probe and the dry sand on top. Finally, at a depth below 10 meters of the riverbed, there is an abrupt change of resistivity from values of 10  $\Omega\cdot\text{m}$  to resistivity values higher than 400  $\Omega\cdot\text{m}$ . As the subsurface is entirely saturated, such high resistivities obviously correspond to consolidated material identified according to the geology of the region as gneiss rock. This delineates the start of the unfractured rock basement. Finally, chargeability allows delineation of the weathered bedrock, where resistivities were low and chargeabilities are high. Such weathered rock is embedded with clay and silt and is weathered at varying degrees (**Appendix E**).

EC values were measured along the cross section until the water table was not reachable at the western side of the riverbed. EC values varied between 120 to 250  $\mu\text{S}/\text{cm}$  with an average of 192  $\mu\text{S}/\text{cm}$ . This leads to an average pore water resistivity value of 52  $\Omega\cdot\text{m}$ . Considering the average pore water and formation resistivity values, the formation factor was computed and plotted within the boundaries of Profile 1 (**Figure 5-3b**; see **Appendix E**). Layers identified as clays have formation factors varying between 0.5 and 1.2 which are indeed within the range of formation factor values for clay material. The top layers of the riverbank have formation factors below 2.5 which indicate an increase in the resistivity of the material due to the presence of silt. Formation factors are defined when the material is saturated which makes the values for the dry riverbed not representative for the analysis. The computed formation factor for the western side of the riverbed yields values of 4 to 5 corresponding to medium to coarse sand material. Finally, the bottom layer sees formation factor values of more than 10 indicating the basement formed by consolidated rock material. Formation factor values for the weathered rock are below 1.2 as the resistivity values are dominated by the low resistivity of saturated clays and silt.

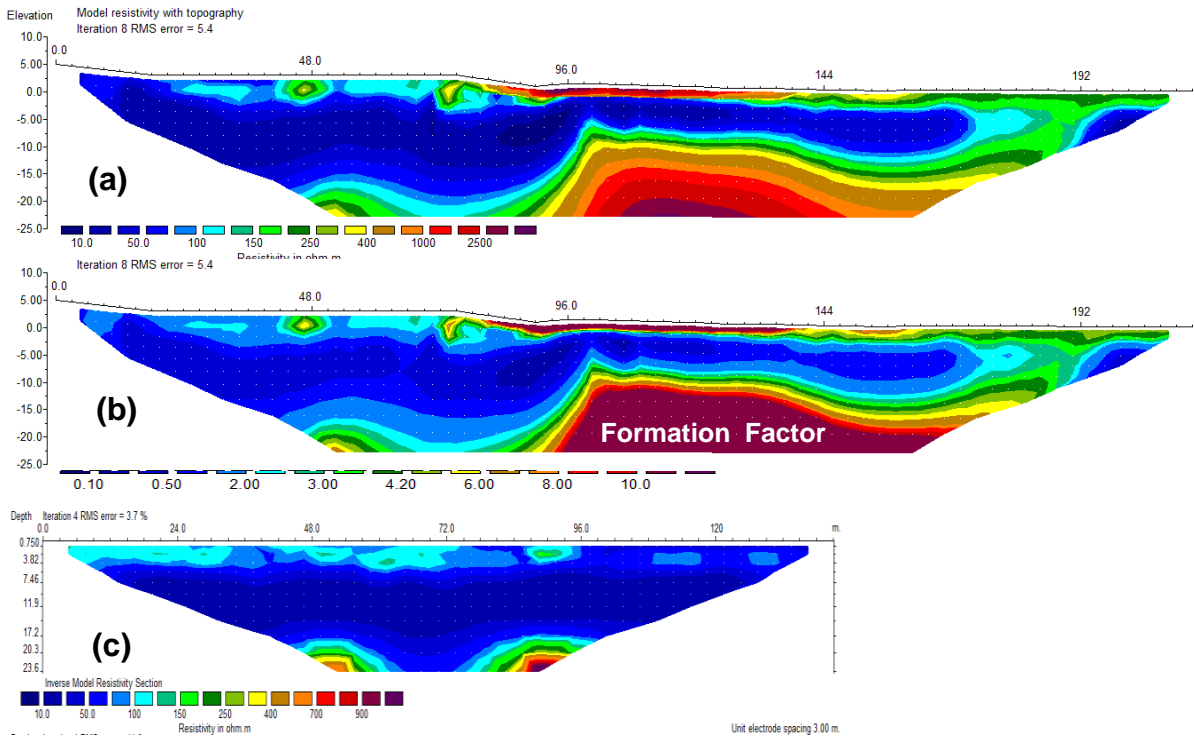


Figure 5-3: Geophysical longitudinal profiles. (a) ERT1: electrical resistivity (b) ERT2: Formation Factor (c) ERT2: electrical resistivity

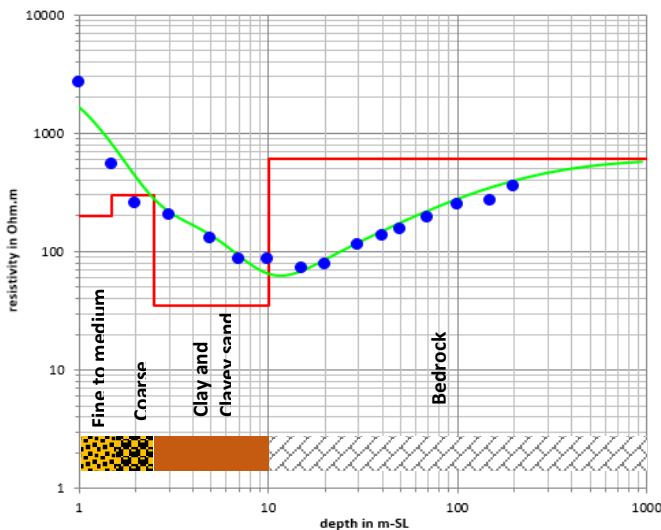


Figure 5-4: Interpretation of VES in the middle of the riverbed

A VES measurement was performed in the middle of the cross section to be used for calibrating the 2D measurements since this one provides a better resolution near the surface as compared to the low resolution of ERT of an electrode spacing of 3 m. The VES was carried in the riverbed, at a distance of +120 from the start of the western side of the cross section and the results are presented in **Figure 5-4**. The apparent resistivities can be explained by a five layer model for a better fit. The

first and second layers correspond to the saturated riverbed formed by sand material of fine to medium grains in the 1.5 m and coarsens to bigger grains down to 2.5 m of depth. The distinction between the two layers was necessary for a better fit of the model resistivity, although in reality the two are indistinguishable and there is simply more presence of the pebbles and gravels in depth. The third layer has a low resistivity of 35  $\Omega$ .m corresponding to material dominated by saturated to silty clay embedded in highly weathered and fractured rock. Below a depth of 10 m the resistivity increases significantly,

which defines the deepest layer of rock of resistivities higher than 700  $\Omega$ .m. For a better fit of the model, a layer with high resistivity was added at a depth of 0.5 m which indeed represents the dry sand of the riverbed.

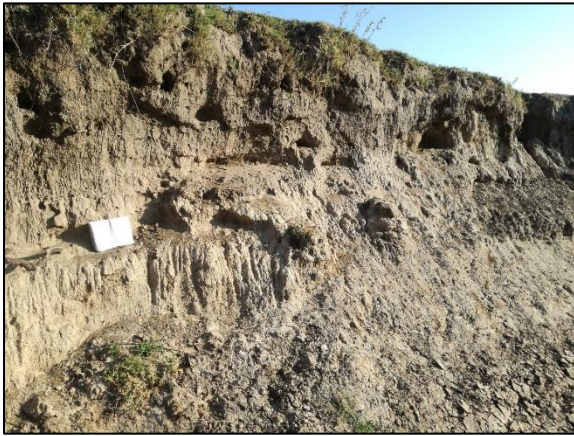


Figure 5-6: Profile of the bank along a gully

Profile 2 is parallel to the river and perpendicular at +48 m to Profile 1 (Figure 4-5). It is carried on a typically flat surface on the western riverbank. Inversed data for Profile 2 (Figure 5-3c) show uniform quasi-parallel formations of low resistivities. The top 3 meters have a slightly high resistivity values of 120  $\Omega$ .m corresponding to dry clays with silt content (Appendix E). The presence of silt is not uniform and occurs sparsely (Figure 5-5). The layer below 3 meters is formed with saturated unproductive clays with resistivities

below 50  $\Omega$ .m.. Such values are low for clay, although with pore water resistivities around 55  $\Omega$ .m, they are accepted and representative of the material (see Appendix). This clay layer shifts to a rock basement through a fringe of fractured and weathered rock.

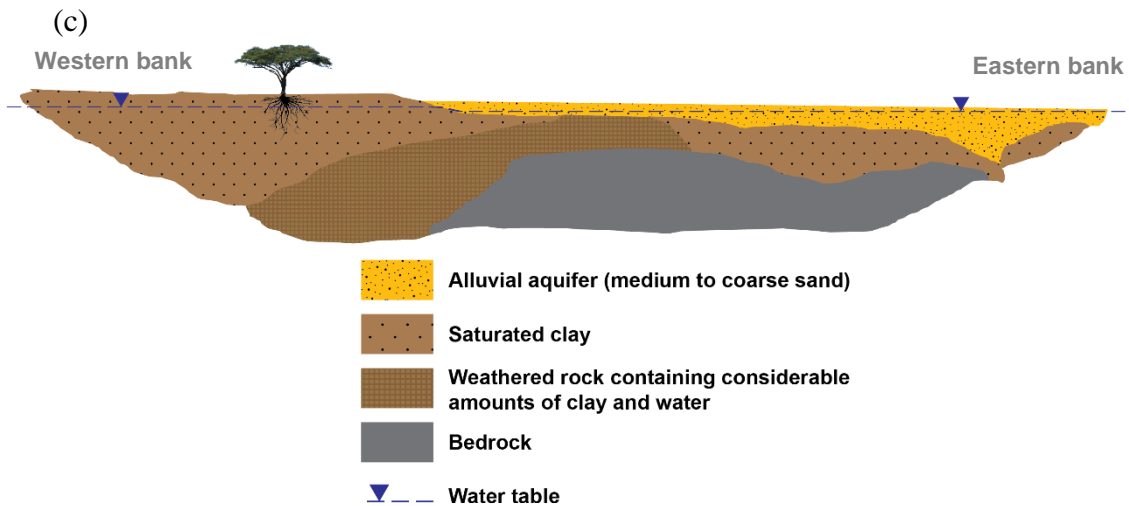


Figure 5-5: Interpreted subsurface model

Based on these results, Figure 5-6 shows the interpreted cross section of the aquifer subsurface. Combined with the probing and topography inspection of the riverbed, the results allowed the determination of a conceptual model of the subsurface upon which calculation will be made to estimate the storage capacity of the aquifer as well as building a subsurface model to be implemented for the numerical groundwater model.

The riverbed, is formed from fine to coarse sand of depths varying between 0.5 to 5 meters. The shallow part of the cross section is located at the inner beds whereas the thickest part of the riverbed is at the outer bends. The thickest part of the riverbed are observed along the main channel. The meandering effect of the river influences directly the topography and depth of the riverbed surface. A meandering

river tends to contain one main channel that cuts through the floodplain. Along its flow path, it deposits sediments on the inner bends through point bar deposits, and tends to erode the opposing bank on the outer bend of the channel creating thus a clear difference in elevation (Sutter, 2008).

As discussed above, such thicknesses of 5 m of sediment might only be observed at the level of the confluence of tributaries with the main river. Sand deposits also exist in the tributaries which form with the main river a parallel drainage system. These tributaries are narrow and typically shallow systems with a very rapid response to runoff, recharge and drainage. Consequently in these tributaries, levels of water drop quickly within the first month of the dry season and their contribution to the storage of the main river aquifer system is minimal (**Figure 5-7**). Where the tributary joins the main river, alluvial aquifers are expected to be developed since more sediment will be introduced into the main river (RJ Owen & Rydzeski, 1991). During a high intensity rainfall event, tributaries allow very fast surface water flow which can increase the erosion at the confluence level. This could have increased the weathering of the bedrock and increased the available empty volume for sediments deposits through the main river flow.



*Figure 5-7: Deep water level in a tributary*

#### **5.1.4. Probing**

In a previous study by (Blok, 2017), probing on five cross sections from the upstream to the downstream of the study area, revealed two main findings (**Appendix E**): i) there are changes in bedrock irregularity that make it difficult to locate good location for abstraction and ii) the differences in thicknesses of the riverbed within a cross-section, are linked to the occurrence of the main channel. The bedrock elevation varies both in cross section and in profile. In the cross sections by Blok (2017) (see **Appendix E**), of Shashane 5 (Pb1), Vusanani Tholoki (Pb3) and Siyazama (Pb4), the depth of the riverbed limited by the resistance of the probing indicates a presence of a shallow part located usually at the inner bend meandering river, and a deeper part located usually at the outer bend. The shallow part has a thickness of 1 m ( $\pm 0.5$  m) whilst the deeper part shows thicknesses exceeding 3m corresponding to the maximum length of the probe. The bedrock elevation is irregular and undulating by  $\pm 0.5$ m. At the bridge (Pb5), the depth to probing resistance, hence the thickness of riverbed is very shallow, because of a rock obstruction which is required to anchor the foundations of the bridge. At this level, the water was observed to be always above the surface level even if a few hundred meters upstream or downstream

water was below the sand surface. This indicates that the rock obstruction plays the role of a subsurface dam which blocks the water from flowing and creates at this level a water pocket during the dry season.

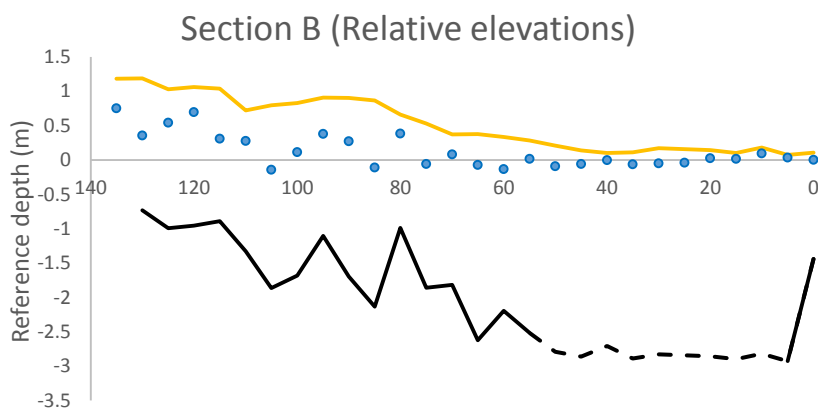


Figure 5-8: Probed cross section elevation and physical resistance profile

Figure 5-8, illustrates the resulting profile of the current research work for cross section B (see Figure 4-4 and Appendix E). The sand surface is elevated near the western bank (left) by 1 m in comparison to the eastern bank (right). Similar results were observed at other locations in the

Limpopo, where the elevation between the banks is significantly high at the inner bends forming local dunes (Abi, 2018). On the other hand, the bedrock elevation, is undulating with the thickest part of the riverbed located at the eastern bank. The recorded depths vary between 1 m and exceeding 3 m. When the probe is inserted into the sediments and resistance is reached, this can be both because of the presence of bedrock or clay. Therefore, even if the probing method is quick, the thicknesses estimated should be carefully considered.

### 5.1.5. Groundwater storage capacity

The riverbed of the Shashane River forms an unconfined groundwater unit of irregular varying thickness and width due to the irregularities of the bedrock underlying the alluvial material. Mansell and Hussey (2005) estimate the average thickness of the aquifer to be 3 m along the river. Probing and geophysical results show that the vertical extent of the aquifer varies from 0.5 to 1 m near the banks, to reach 5 m in the main channel.

The main river starting from the Antelope dam spans for 102 km until it confluences with the Shashe River downstream. Assuming an average width of 120 m and an average depth of 3 m, the river can contain approximately a total volume of 36.7 million m<sup>3</sup> of sand deposits which can store approximately 11 to 12 million m<sup>3</sup> of water at full capacity if a porosity values of 30 – 32% is considered. For a 5.6 km meandering stretch corresponding to the delineated stretch for the study area, the water storage volume varies between 605000 to 645000 m<sup>3</sup>.

To take into account the effect of the subsurface variation in depth, the storage capacity can be defined per 100 m length using the 2D grid probing survey. If a maximum probed depth of 3 m is considered, this results in 9600 m<sup>3</sup> of stored water per 100 m of length, or 537000 m<sup>3</sup> for the 5.6 km stretch. According to the geophysical interpretations in section 5.1.2., the deepest levels of the aquifer in the

main channel was 5m. Considering this depth, the aquifer can store 12250 m<sup>3</sup> per 100 m length, or 686000 m<sup>3</sup> for the study area stretch, which is 27% higher than the 3 m maximum depth. Because of the topographical variation of the sand surface, about 30 cm below the top surface is dry as it can only be saturated during a runoff event. The remaining of the storage decreases because of losses induced by evaporation, groundwater vertical and lateral seepage as well as anthropogenic abstractions for domestic and irrigation uses.

The water in storage is not entirely available for direct abstractions and depend on the specific yield of the aquifer material. For the study stretch, specific yield values of 15% characterize the sand material. This results in a volume varying between 322500 and 350000 m<sup>3</sup> available for direct abstractions.

Another factor to consider is the longitudinal undulating nature of the basement of the riverbed, usually caused by rock sills. Such rock sills form natural subsurface structures that separate the sand deposits into discontinuous micro-reservoirs which leads to a further reduction of the estimated storage (Hussey, 2007; Wekesa, 2017).

For comparison, **Table 5** summaries volumes available for direct abstraction per area of the channel, in study sites in Mara basin in Kenya, Mzingwane and Shashane in Zimbabwe. There is about 3400 m<sup>3</sup> available for direct abstraction per 1ha of alluvial channel in the Shashane as compared to 2833 m<sup>3</sup> in Mara and 4700 m<sup>3</sup> in lower-Mzingwane. Rivers in Mara basin are narrow and shallow which reduce the storage capacity. Sand rivers in the lower Mzingwane were more developed and wider therefore containing more water available for abstraction. The estimations made by Wekesa (2017) and Moyce (2006) were upscaled to the entire length of the river assuming uniformity in the thickness of the aquifer. The current estimations for the Shashane alluvial aquifer are more accurate for the local scale estimate, since the discontinuities of the riverbed were considered.

Table 5: Comparison of available volume per area of river channel in three different areas

	Moulahoum (2018)	Wekesa (2017)	Moyce (2006)
	Shashane	Mzingwane	Mara
<b>Specific yield (%)</b>	0.15	0.2	0.15
<b>Area of channel (ha)</b>	102	362.5	2345
<b>Volume per ha of channel (m<sup>3</sup>)</b>	3431	2833	4716

Considering the static characterization in section 5.1, a subsurface model was built (**Figure 5-9**). Each cross section is composed of two parts, a shallow part with a thickness below 1m, a thick part with a maximum depth of 5 m, and a transition depth interpolating the two. The thickest portion of the aquifer was build following the boundaries of the main channel which can be easily determined using a satellite image validated by the probing survey. Longitudinal discontinuities were also included using longitudinal probing section as observed in **Appendix E**, and previous work done by (Blok, 2017). The total storage capacity of this portion based on a porosity of 30% is **696360** m<sup>3</sup> which is similar to previous computations. The volume available for abstraction is **348180** m<sup>3</sup> with a specific yield of 15%.

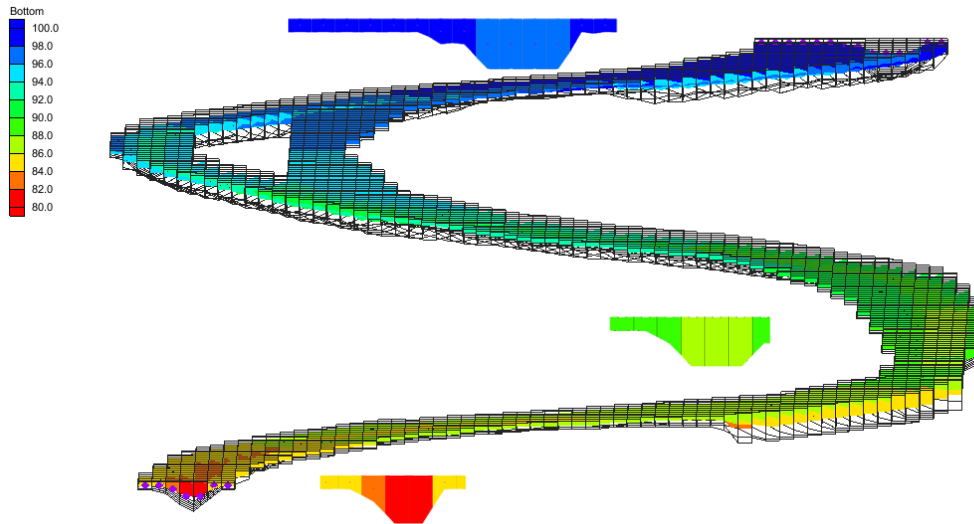


Figure 5-9: Developed 3D model of the riverbed in the Tshelanyemba study area

## 5.2. Dynamic analysis

### 5.2.1. Groundwater level dynamics

- Diver data

**Figure 5-10** presents the relative water level variations during 27 days (06/04/2018 to 03/05/2018) for piezometers Pb3B and Pb6B installed in the sand river (see **Figure 4-6**). The water level in Pb6B showed a total drop of 25 cm from an initial depth of 8-10 cm above the sand level, which corresponds to 8 cm of water loss considering a 32% porosity. In Pb3B the water level only dropped by a total of 8.7 cm, from an initial depth of 10-12 cm below the sand surface level, which corresponds to 2.88 cm of water loss, further confirmed by manual measurements. Drops in the water level in the sand river are controlled by three main discharge components: direct abstractions, evaporation and lateral discharge to the riverbanks. Groundwater outflow downstream could influence the decrease, but at the beginning of the dry season its effect is minimised by groundwater inflow at a similar rate.

Daily potential evaporation fluxes were calculated using the data from the weather station and plotted in **Figure 5-10** to provide a reference to the impact of the evaporation on the losses observed. If evaporation from the water table is considered to occur at the maximum potential rate (varying between 2.8 mm/day to 4.5 mm/day) without a depth reduction effect, the water table would decrease at a rate of 1.18 cm/day, translating to a water loss of 3.5 mm/day. The loss induced by maximum ET without accounting for the depth effect, depletes the water faster than observed. If a linear model is assumed for the variation of evaporation up to an extinction depth of 1 m (Hellwig, 1973), then the WL drop rate is closer to the observed data of Pb6B. Taking into account the uncertainty associated with the extinction depths in sands, this can indicate that the WL losses in Pb6B could be explained to a great extent by



the evaporation effect. On the contrary, decrease rates in Pb3B are much lower than expected from ET, indicating that the losses are minimized. This could be explained by the location of Pb3B in a shaded area where radiation is reduced. Another hypothesis is based on an increase in the groundwater inflow at Pb3B. Pb3B is situated at a meandering outer bed and the riverbed is separated into two systems by a local elevated island. Weekly manual observations during the same period indicate that water level in the inner bend system (Pb2) drops significantly faster indicating a lower replenishment rate. It could possibly indicate that groundwater flow is concentrated towards the outer bend part of the aquifer, however the groundwater flow velocities are too slow to generate such an effect. Finally, at that location, a subsurface obstacle could prevent the groundwater downstream outflow and therefore accumulates water operating as a dam. Therefore, the WL will not decline fast as there is more replenishments than losses.



Figure 5-10 : Relative water level drop for diver Pb3B and Pb6B compared to simulated water level drop caused by evapotranspiration

Daily fluctuations of the groundwater level can be observed (see Appendix F). For Pb3B, water level drops during the day by approximately 1.3 cm and recovers during the night by approximately 0.8 cm. On the other hand, groundwater levels in PB6B show a diurnal variation with different duration for loss and replenishment. Water level drops by 1.84 cm in 18 hours including night time, and replenishes rapidly by 1 cm in the following 6 hours. The longer hours lead to a higher WL drop. It remains unclear how WL drop continues during night time where evaporation effect should be negligible. Interestingly, the water groundwater level fluctuations are inversely related to the groundwater temperature. Water level drops when temperature of the water increases and vice versa, indicating an accumulation of the required energy that triggers evaporation.

Diurnal groundwater fluctuations can be used to estimate the daily evaporation rates. ET estimates based on the Hays Method, are on average 7 mm/day for Pb6B and 2.5 mm/day in Pb3B (see Appendix F). These are very high in comparison to the evaporation rates estimated by the ETo calculator which correspond to potential evapotranspiration. These estimated values appear to correspond to the Water head dropping rates which are not representative of the water volume loss.

- **Logger data**

**Figure 5-11** shows computed daily average water level data retrieved from the logger installed by Dabane Trust in 2012 to monitor the Groundwater level hourly variations in the sand rivers and the corresponding ratio between daily max and mean of groundwater level.

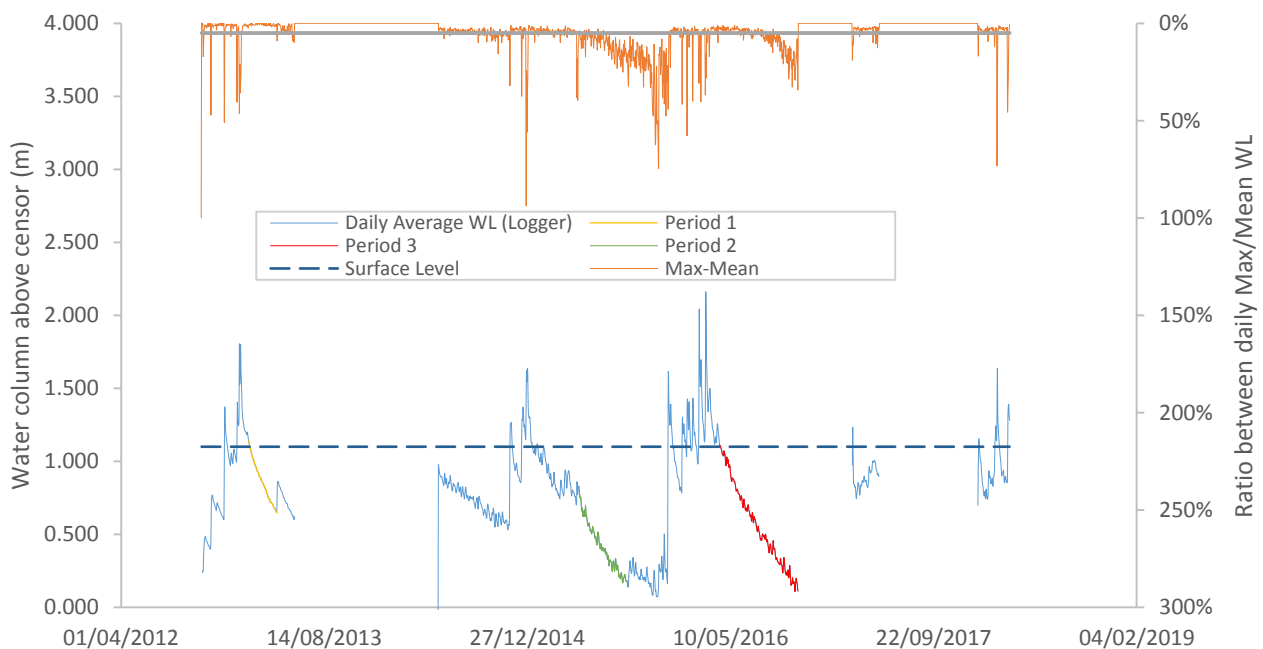


*Figure 5-11 : Logger groundwater level reading and daily max-mean water level ratios for the recorded period from 2012 to 2018*

Analysis of the data indicate a clear difference between the variation patterns of the wet and the dry season. The high peaks between November 13<sup>th</sup> and 14<sup>th</sup> of the year 2014 and 8<sup>th</sup> and 9<sup>th</sup> of December 2015 are indicators of the first storm events of the wet season. These events are rapid and increase quickly the groundwater level to reach the surface and thus saturation of the riverbed within a period of two days. In contrast, the beginning of the dry season is characterised by a gradual undisturbed decrease in the water level between the months of March-April to October-November.

The WL dropping rates for most of the dry periods between March-April of all the 3 years, vary between 2 to 5 mm/day on average (see Appendix F). For the long period, WL drop compares with the WL drop observed at the piezometers since these are both measured during the beginning of the dry season where groundwater levels are still high and so is evaporation. On the other hand, water levels between

23/01/2013 to 26/01/2013 shows a drop of 50 cm in a period of 4 days which corresponds clearly to a surface water level drop behaviour.

The observations indicate that the sensor was approximately installed at a depth of 1.15 m. This depth is not sufficient to capture the WL drop in very dry years where the WL is suspected to drop more due to consumption from riparian vegetation. It also approximates the distinction depth of the effect of soil on evaporation. It is not possible to clearly state if the WL drop can be entirely attributed to losses due to evaporation.

Three periods of continuous undisturbed monitoring of the WL can be distinguished. Two of the periods are in sequence. A fourth period of observation of GW corresponding to 2014 was disregarded as it starts after a period of malfunction of the sensor as well as low voltage in the batteries. Therefore these values are not reliable. Interestingly, the three periods are observed to have approximately the same drop rate. An exponential model fits the drops and gives a relationship between the WL drop and time in the dry season (**Appendix F**). This relationship will be used to model the head drop at the boundary conditions after each flood event. It accounts for the contribution of all the mechanisms that lead to the WL drop. It also omits the effect of low and short rainfall/runoff events during the dry season which might increase the water level without causing full saturation of the riverbed as observed at the end of the period 2. This exponential relationship adapted to the 3 to 5 m deep riverbed, will plateau after a certain period of time and therefore considers that the riverbed never dries up no matter how long the dry season is.

### **5.2.2. Groundwater flow**

This section presents results of rough calculations to estimate the groundwater dynamics within the riverbed aquifer and analyse the importance of the relevance of groundwater flow in the aquifer's water balance.

Darcy equation was applied for an average hydraulic conductivity value of 100 m/day and a slope 0.26% to estimate the average groundwater flow velocity. The calculation yielded a velocity of 0.26 m/day or 0.1 km/year which is very low for an aquifer with such a conductive aquifer where high capacity of water transport is expected. The calculation assumes that the water table has a similar slope to the sand surface and omits the local variations of the water table induced by the bedrock irregularities. Assuming a uniform thickness and width of respectively 3 to 5 m and 120 m, the maximum possible groundwater flow rate is 93.6 to 156 m<sup>3</sup>/d. This flow rate is maximum when the groundwater level is close to the surface which corresponds to the days subsequent to recharge events. Considering the study area of 5.6 kilometres, this means that the aquifer is replenished naturally from the upstream extent of the aquifer at a maximum rate of 93.6 to 156 m<sup>3</sup>/d while possibly losing the same amount downstream. This transforms the narrative of the problem to be static and a portion of the aquifer could independently be studied as a tank.

The hydraulic conductivity and hydraulic gradient are the two main controlling factors of the downstream movement of the groundwater within the aquifer. Unlike the slopes at the starting point of the river upstream of the Antelope dam, where the area is characterized by steep hills and sediment deposition is low, the slopes at the flattening part of the river significantly decrease the groundwater flow rates since the hydraulic gradient is constrained by the channel slope. As calculated above, the water from the downstream tends to move 100 m per year and is typically replenished by groundwater from the upstream, part of the aquifer. Therefore, discharge is not a significant component in discharge (Owen, 2000).

In the hypothetical case of infinite duration of drought, and in the idealized conditions of a sealed bedrock preventing deep or lateral seepage, it would take approximately 337 years for the drought to reach the study area located 32 kilometres downstream of the Antelope dam. It means that the aquifer at the study site is replenished from the upstream for this entire period. However, this does not mean that the portion of the aquifer at the study area can be exploited for all this duration. It takes in fact less time for the storage to drop below the abstractible level. Flow in the aquifer is argued to be made up of hydraulically isolated sections separated by irregularities in the bedrock (Mansell & Hussey, 2005). With these irregularities, independent groundwater ponds can be created if the water drops below the level of the subsurface obstacle (rock sills), in which case the time it takes for a portion downstream to dry is accelerated. The assumption of perfect no-flow boundaries as well increases the time of complete drought since the riverbed is connected to the fractured bedrock maintaining a vertical seepage, while riparian vegetation could contribute to the acceleration of drought as a dependent ecosystem on the water of the aquifer.

### 5.2.3. Surface water dynamics

The Shashane sand river is ephemeral in nature and is characterized like in all the other sand rivers by variable flow regime of rainfall storms that are short and intense followed immediately by dry periods. The rainfall-runoff reaction is rapid and runoff is quickly generated once the riverbed is entirely saturated. Occurrence of discharge is a clear indicator of entire recharge of the riverbed, and therefore analysis of the discharge allows a thorough understanding of the recharge occurrence of the aquifer.

Three data sets of discharge measurements were retrieved from the Zimbabwe Water Authority (ZINWA) (see **Figure 4-3 and Appendix F**). The longest time series is the one measuring the inflow discharge to the Antelope dam from October 1969 to October 2005, whereas the gauging station at the Shashe confluence has the shortest record of 18 intermittent years, with almost 8 years of missing data between 1976 and 1984 (a common hydrological gap period corresponding to the social and economic instability caused by the Rhodesian civil war (MacDonald, 1990)). The maximum recorded spillway discharge of 1.4 m<sup>3</sup>/s is negligible in comparison to the magnitudes of the discharges measured at the outlet of the catchment in the same period (543 m<sup>3</sup>/s) and makes the effect of spills or artificial releases

minimal and limited to a few kilometres downstream of the reservoir. Therefore, the discharge measurement at the outlet of the Shashane sub-catchment could be considered to be the sole product of the natural response of the draining area of the rainfall event downstream of the Antelope dam. The Shashe confluence data with a draining area of 1686 km<sup>2</sup> (**Appendix F**) allow estimations of the annual surface runoff which leads to an average of 33 mm per year, similar to the values reported by (Ncube et al., 2010) and (David Love, Uhlenbrook, Twomlow, & van der Zaag, 2010).

The surface flow events occur erratically, with high flood pulses followed by dry spells of varying duration (**Appendix F**). As flood levels were not gauged, appreciation of the flood impact of each event cannot be observed. The highest discharge peak of 543 m<sup>3</sup>/s was observed in February 1991 allowing 47 Mm<sup>3</sup> to flow out of the Shashane catchment, which accounts for almost 25% of the runoff of that year. Other discharge pulses between 1984 and 2001 had peaks less than 130 m<sup>3</sup>/s similarly accounting for almost 23% of the runoff of that year. This difference in flood peaks is illustrative of the variance in the flow regime resulting from variable received rainfall. Low flow peaks could be both the product of low rainfall

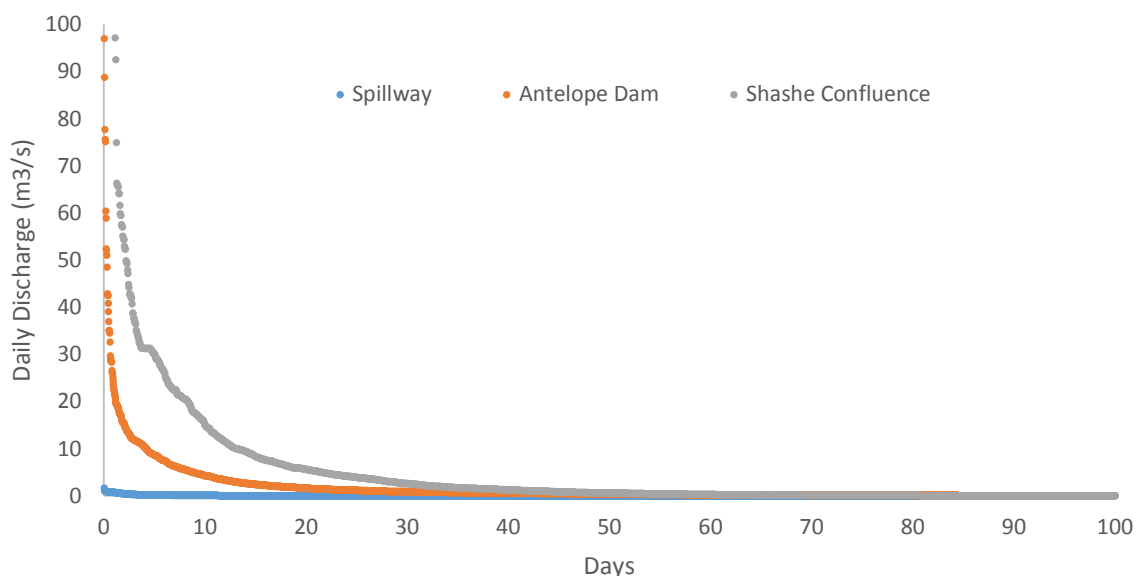


*Figure 5-12: Flow duration curve for the daily discharge (m<sup>3</sup>/s) measured between October 1973 and February 2001 for the discharge gauging stations at the upstream of the Antelope dam, the Antelope spillway and the outlet of the Shashane catchment (confluence with Shashe)*

events or sustained by groundwater as the slopes tend to flatten and consequently perennial groundwater tends to concentrate at the outlet of the catchment. However, the groundwater contribution to base-flow remains negligible. In the upstream sections, the river is dry during most of the time of the year with water stored in the sand deposits and surface flow immediately ceases after the rainfall events are over.

**Figure 5-12** illustrates the frequency duration curve of the discharge data for the three time series of discharge. As stated above, the magnitude of the spillway releases is insignificant in comparison to the discharge events at the Shashe confluence gauging station. Similarly, the discharges occurring upstream of the Antelope reservoir are of lower magnitude mainly due to a lower draining area as compared to the drainage area producing surface runoff downstream of the Antelope dam. Discharge

events of high magnitude ( $> 30 \text{ m}^3/\text{s}$ ) are very short and last fewer than 5 days. These events contribute from 5% to 70% of average yearly runoff. Higher magnitude discharge events are shorter and have a duration that does not exceed 2 days. These events are very intense and contribute significantly to the total yearly runoff. Discharge events, higher than  $1 \text{ m}^3/\text{s}$  (0.1% contribution to the total yearly runoff) are exceeded 40 days per year on average. This indicates that the number of days of river flow per wet season is very small and therefore surface flow is never reliable for use.

#### 5.2.4. Dry spells and dry season

- **Dry spells**

**Figure 5-13** illustrates the length and the frequency of discharge dry spells for each rainy season. The 1991 Hydrologic Year (HY) observe a high yearly runoff of 120 mm and a cumulative of 50 days of dry spells separated in 9 events of 5 days on average. In contrast, HY1986 recorded 3 mm of runoff with a cumulative of 55 days of dry spells divided in 2 major dry spells that persisted 25 days on average. In HY1987, the wet season is continuous and no dry spells are recorded, whereas in HY1974 and HY1993 the dry spells are long and less frequent despite the high level of runoff which is an indicator of very intense rainfall events that produce high discharge. In general, wet years are characterized by short and frequent dry spells whereas in dry years dry spells are less frequent but of long duration and separated by short duration, low intensity rainfall events. Frequency analysis of the dryspells indicated that the maximum recorded dry spells could reach up to 63 days whereas the average maximum duration of dry spells per year is 22 days. A statistical analysis was performed to assess the frequency occurrence of maximum dry spells however. The data fit a uniform distribution, and therefore maximum dry spells are equiprobable (**Appendix F**). This could be due to the insufficient length of the time series or mainly a consequence to the erratic occurrence of rainfall.

This analysis is based on a fast reaction of the runoff to rainfall without considering the spatial variability of the rainfall regime in the draining area, therefore, discharge dry spells are indicative of rainfall dry spells (Hussey, 2005; Wekesa 2017). With this assumption, the characteristics of the dry spells indicate that rain fed agriculture in the region is clearly not sustainable. This was demonstrated by a reduced millet crop yields in some regions in sub-Saharan Africa, accompanied by a very low development of the grass cover which resulted in important consequences for (rainfall-dependent) agro-pastoral production during seasons with an increase in dry spells longer than 5 days (Boubacar, 2012). During the dry spells that follow after a surface flow event, the aquifer level is saturated and the groundwater level starts dropping until the next surface flow event. This available groundwater provides a potential

source for irrigation to sustain nearby agriculture during the dry spells. The impact of dry spells on the storage variability of the aquifer will be assessed further in the numerical modelling section.

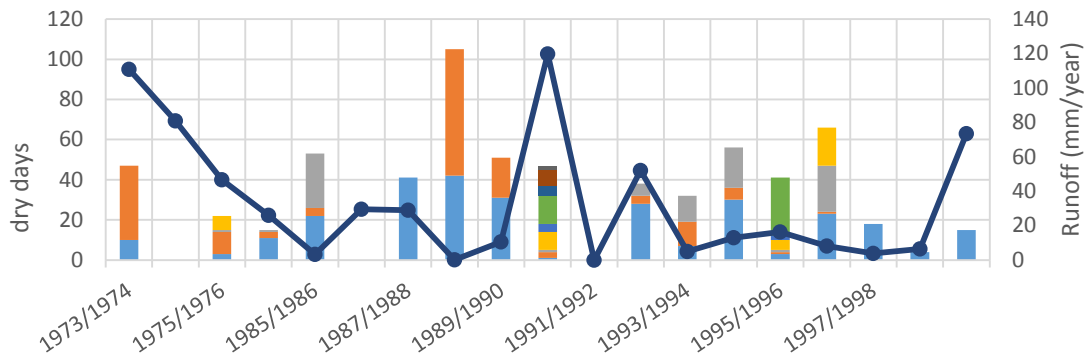


Figure 5-13: Duration and frequency of the dry spells, and yearly runoff from HY1974 to HY2000. Number (1 to 10) are indicative of the order of occurrence of the dry spell

- **Dry season**

The short, intense and intermittent wet season is followed typically by a long dry period during which there is no surface runoff and perennial groundwater provides the major accessible water source for drinking and irrigation water supply. As indicated in **Figure 5-14**, the dry season on average starts late March and early April and ends in October with an average duration of 255 dry days. The dry season of 1986 started very late in June and lasted for 4 months only, until the next event of runoff occurred in October corresponding to the start of the next hydrological year and saturation of the aquifer. However, the wet season of 1987 was also short with an interrupted flow event that lasted for two months until December. This was followed by a dry season (1987) that started late in December and lasted for the next 12 months. In a few other years, the dry season starts late and extends to the following year disturbing any plantation plans. This is observed in an extreme way for HY1991 which was wet with a recorded runoff of 110 mm, however, the dry season extended to the following year of 1992 where not a

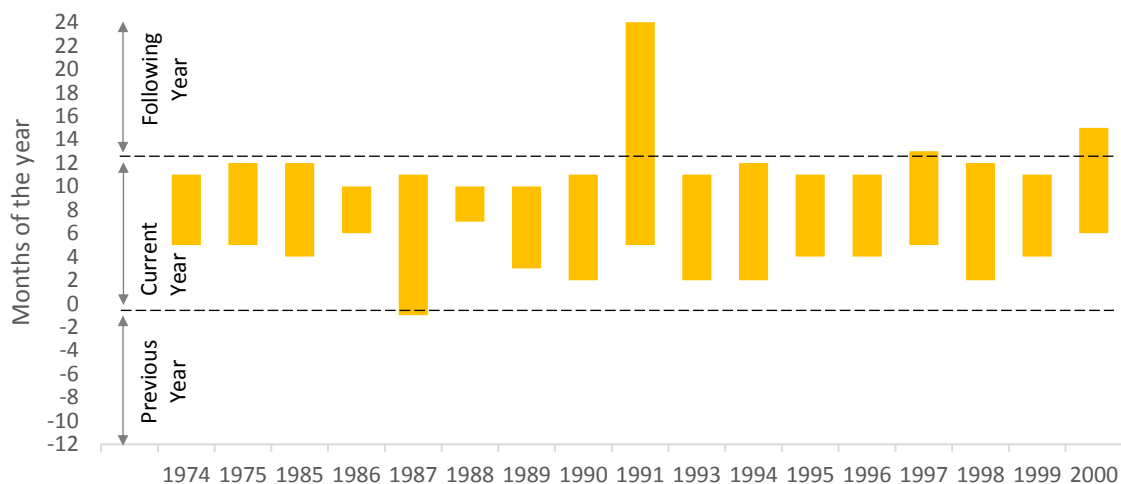


Figure 5-14: Duration of the dry season between HY1974 and HY2000 in the Shashane sub-catchment

single runoff was observed for a total of 554 days. In general, the starting and ending of the dry is unpredictable and the duration is irregular with possible drought duration exceeding 365 days.

The impact of the dry season is direct on the storage, as the groundwater levels starts immediately dropping as soon as the surface flow dries up. The longer the duration of the dry season, the lower the water levels are expected to drop and the storage of the aquifer is naturally depleted. The level of decrease of the aquifer storage conditions the recharge of the following year as there is more available storage space to be recharged. As runoff is expected to occur every year, the aquifer system is resilient and storage might be exploited entirely unless this will impact the surrounding dependent ecosystems downstream and in the riparian banks.

The first observed discharge measurement which indicates the kick-off of the wet season is an indication of the full saturation of the riverbed. The process of saturation is dependent on the permeability, the porosity but also the rainfall intensity and the degree of saturation prior to the rainfall event. Wekesa (2017) observed a time lag between the rising limbs of groundwater and surface water levels indicating that that the riverbed saturates before surface water begins to rise, which is an indication that flow cannot pass until the entire unsaturated sand beds are filled. Depending on the intensity of rainfall, this typically happens within hours of the start of the rain event. Logger data of the groundwater level in the Shashane riverbed aquifer indicate that the levels of surface water is an extension to the level of the groundwater during a surface flow event and the saturation of the riverbed typically occurs within a day or two after the first rainfall event, and thus the riverbed is entirely saturated at the beginning of the first major rainfall-runoff event.

## 5.3. Abstraction potential

### 5.3.1. Simplified tank model

The variation of the storage as the percentage of the maximum storage capacity for a period of 16 years of available discharge data, is presented in **Figure 5-15**. The simulation, included 3 scenarios, of groundwater outflow only, artificial abstractions and no-abstraction scenario.

In the basic scenario where no abstractions nor groundwater outflow is considered, the storage starts dropping immediately after the last discharge event of the wet season and reaches a minimum storage capacity at the end of the dry season. The level at which it drops depend on the length of the dry season. For the first year of simulation, the storage drops to 70% of its available storage capacity after 263 dry days. The longest dry year lasted for more than 556 days (between D2374 and D2930) and the storage dropped to 65%. For the longest dry period, and after a period of 250 days the storage decrease slows down and reaches an equilibrium state. This result is the consequence of assuming that losses in the aquifer are only controlled by evaporation which has no effect below the extinction depth.



Losses controlled by downstream groundwater outflow, vertical seepage and lateral seepage, were all combined to amount to 120 m<sup>3</sup>/day. The effect of these losses reduces the storage to a minimum of 54% for the longest dry season whereas in the first dry season (D263) the storage dropped by only 5% compared to the no-flow/no-abstraction scenario. On an average length of a dry season of 250 days, if no water is abstracted, there would be almost 60% of the storage available for use at the end of the season.

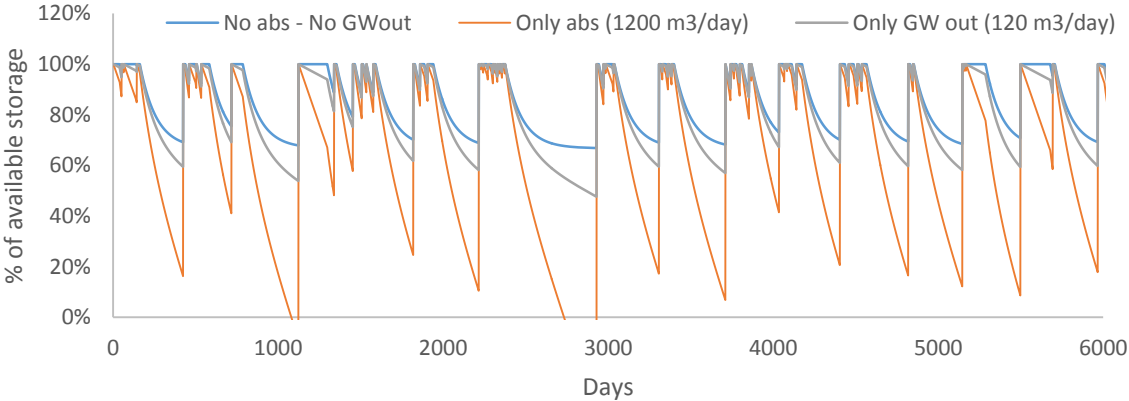


Figure 5-15: Storage variation using the simplified water balance for 16 years of available data

To account for the impact of abstractions, a total abstraction rate of 420 m<sup>3</sup>/day was introduced in the water balance in addition to the seepage losses. This demand was calculated considering 14 gardens with 30 m<sup>3</sup>/day as need for irrigation (See section 4.3.4 and results in section 5.3.3). Simulations show that the storage is depleted faster. For the first year, the storage level drops to 20% after 263 days of drought. While the second year (< day 730) was very wet, the following year saw a longer dry season of almost 375 dry days at the end of which the storage was entirely exhausted. The storage of the aquifer is completely depleted 175 days before the end of the longest dry season (556 days). If there is enough rainfall every year to generate runoff, this means that the aquifer is recharged with one intense rainfall event, providing high resilience potential. It means that with certainty that the aquifer will be completely recharged the following year, the use of the storage can be maximized with consideration of the dependent ecosystems.

With these rough calculations, the aquifer is then able to sustain a water demand of 420 m<sup>3</sup>/day for an average dry year of 250 with a storage of 20% remaining at the end of the dry season. The capacity of full use of the storage of the aquifer is acceptable since the aquifer is recharged entirely on a yearly basis. However, these results need to be carefully considered. The water balance model assumes that naturally the aquifer will not dry as a consequence to evaporation losses only. It also does not consider the spatial variability of the thickness of the riverbed, which reduces the abstraction capacity of the installed wells. In addition, it assumes that aquifer recharge any discharge event is able to recharge the entire aquifer since surface flow only occurs after the saturation of the riverbed. Finally, the model does not consider the interaction between the hydrological components where the losses dynamically adapt to the abstractions. Therefore, abstraction rates with the same impact, should be higher in the numerical model.

### 5.3.2. Numerical groundwater model

- **Calibration**

The parameters used for final calibration are ET, extinction depth and hydraulic conductivity (**Table 6**). ET rate was 2.5 mm/day while the extinction depth was increased to 1.3 m to compare with the maximum drop observed in the Logger data. The hydraulic conductivity value that gave the best fit was 120 m/day which corresponds to the measured hydraulic conductivity values in the field (**section 5.1.1**). **Figure 5-16**, indicate that the calibration of the model is very satisfactory with heads above 80 cm of depth in the aquifer are simulated accurately. Heads below 80 cm are higher in the model simulations than in the observation. This is a direct result to the evaporation which is the dominating outflow component in the model. Its effect becomes irrelevant around the extinction depth. For the simulated period, the difference between simulated and observed lower heads is less than the tolerated error and the impact would only be significant when the duration of the dry seasons are above average. ET rate and extinction depth control the outflows rate whereas hydraulic conductivity controls the groundwater flow rate. Lower hydraulic conductivity values would lead to slower flow of groundwater and therefore more exposure to the effect of Evaporation which leads to a lower drop of GW levels. Such very good results of calibration are expected for a model of such scale and with such boundary conditions.

Table 6: Summary of the parameters used for the calibration

Parameter	Hydraulic Conductivity (m/day)	Specific yield (%)	Max ET rate (m/day)	Extinction depth (m)
Value	120	15	0.0025	1.3

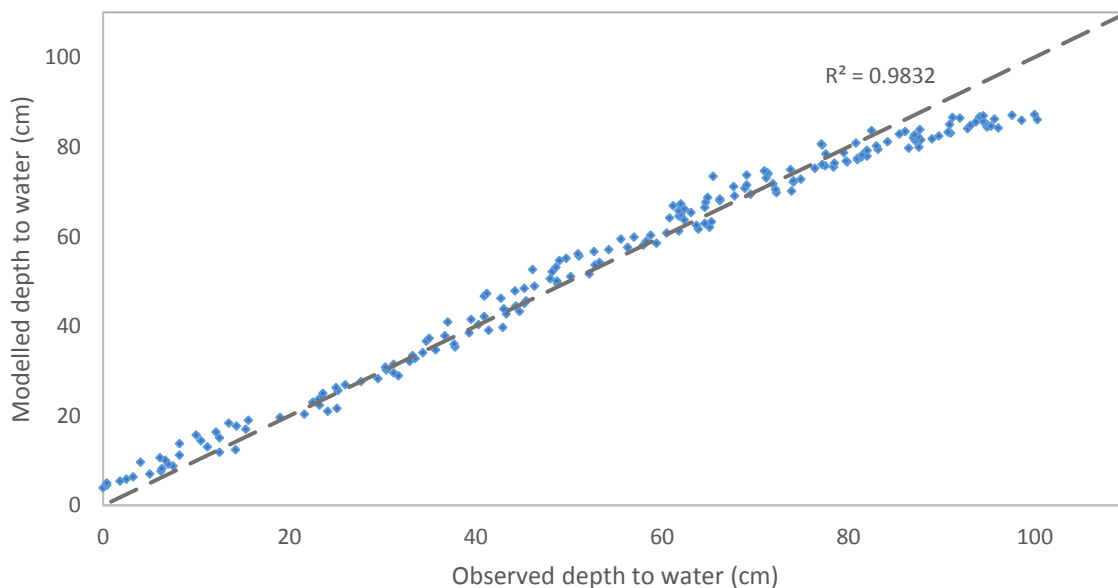


Figure 5-16: Performance of the calibrated model heads in comparison to the measured heads

- **Sensitivity Analysis**

**Figure 5-17** illustrates a summary of the sensitivity of the storage of the system at the end of the dry season (D263) to a variation in the input parameter (see **Table 3, section 4.3.3.**). In general, a decrease in the value of any the input parameter leads to an increase in the storage at the end of the dry season, whereas the opposite might not be true.

To start with, the model is insensitive to variations in the values of conductance of the drains installed to simulate surface water flow. Drains define a head dependent flux boundary conditions, and are conditioned both by the values of the conductance and the head of the water on top. As long as conductance is not too low (representative of silts or clay), the drained flux only depends on the head above the drain which is caused by excess recharge. The higher the recharge is given, the slower it takes the drains to eliminate the excess water out of the model. Nevertheless, to make sure that the effect of the drains does not influence the results, excessively high values of conductance were given. This parameter is purely a modelling hack and does not mimic any natural parameter that could be measured.

On the other hand, doubling the horizontal hydraulic conductivity results only in a 3% decrease in the total storage of the aquifer. The hydraulic conductivity is a parameter that conditions the ability of flow of the water in the porous material. The storage decrease indicates that there is more water lost. This could be explained by the ability of a high conductive material to replenish the system faster and therefore more water is available for evaporation loss. Although, hydraulic conductivities of 240 m/day were not observed in the Shashane River therefore lower increase will lead to an even insignificant decrease in the storage. Such a result indicates that any errors associated with the choice of the hydraulic conductivity will not significantly impact the output of the model.

A reduction in the maximum ET rate and the extinction depth lead to a significant increase in storage, hence less water is evaporated. The extinction depth's effect on storage is more pronounced than ET. In addition, while a deeper extinction depth depletes the storage more, a higher ET rate surprisingly does not significantly affect the storage. This is a direct result to the choice of the model representative output parameter. A higher ET rate will lead to a faster drop in the water table, however, the final level will be similar as it is already conditioned by extinction depth (**see Appendix I**). Actual evapotranspiration was used as the ET rate which is already an over-estimation of the actual ET calculated in the study area by ETo, therefore the uncertainty in the output caused by ET is small. However, there is significant uncertainty associated with the extinction depth as these values are withdrawn from literature of other sediments of similar nature.

Finally, the model output presents a high sensitivity to the specific yield. Higher specific yield values result in a decrease in the storage observed at the last day of the dry season and vice versa. An increase in the specific yield means that there is more water available to flow in or outside the cell when the water

balance for each cell is solved and therefore any increase in the specific yield allows more water to flow out of the model. There is a lot of uncertainty associated with determining the specific yield for the sand river aquifers. While the best method to obtain the values is through field tests, these might amount to be expensive. In this research only values of specific yield that were measured were considered, although the measurement methods were unreliable and need to be improved.

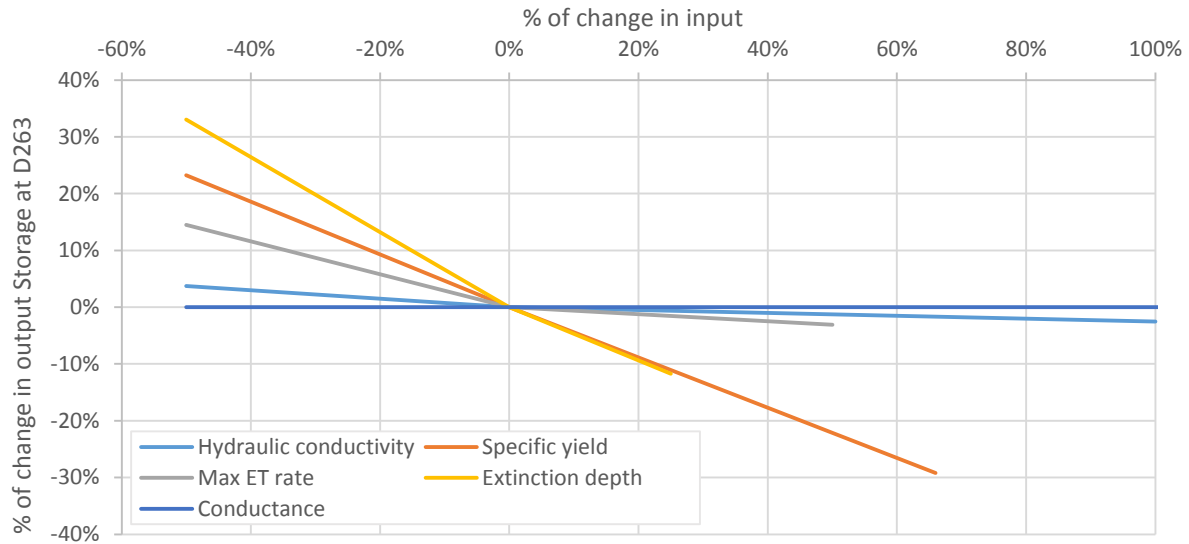


Figure 5-17: Summary of the sensitivity analysis results

- **Storage variation**

After assessing and calibrating the model, the model was run on a period of 16 years. The water budget was calculated from the output of the model. The available storage variation was computed and presented in **Figure 5-18** as available storage percentage. The storage variation occurs in a series of wet and dry seasons varying in length. The storage drops gradually to reach on average 45 to 50% of

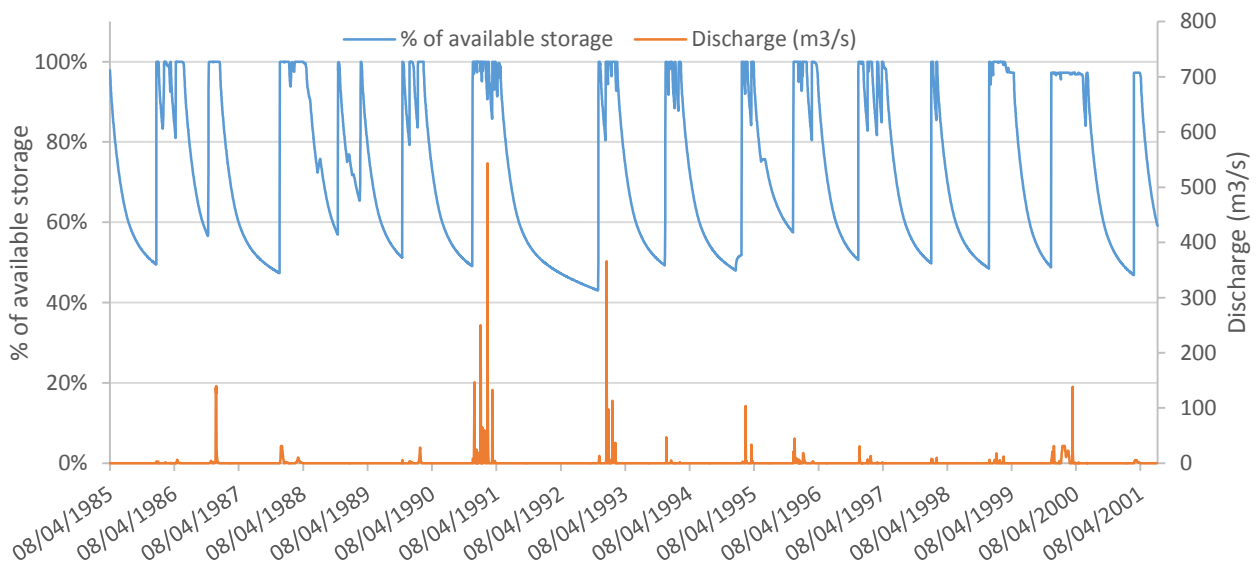


Figure 5-18: Simulation of the variation of storage in the natural scenario - no abstraction -

the maximum storage capacity at the last day of the dry season. This is observed for instance in 1985, 1990 and 1993. Years 1991-1992 show a more intense storage drop where storage at the end of the dry season drops to reach 40% of storage. These periods have a drought duration typically above average which could in some cases last for two years in a row. The natural depletion of the aquifer is lower in the numerical model as compared to the simplified water balance in section 5.3.1. since the losses in the numerical model are more realistic and correspond to actual evapotranspiration rates. Moreover, the spatial irregularities in the bedrock, create local ponds at which point evaporation losses are higher. After 300 days storage capacity will not vary much even if the entire following year is dry as observed. This is a direct consequence of the assumptions made the outflow components. As the evaporation is the main outflow component of the model, the effect of evaporation ceases when the water level drops below the extinction depth. As a consequence, the storage decline stops after the evaporation effects ceases, and is maintained by the upstream head boundary condition only. The relatively large depletion leaves a small volume available for abstraction, which could be increased if abstractions are initiated early in the dry season, as less volume water would be available for evaporation from the riverbed.

During the wet season, the majority of the days are dry since the discharge events are usually, short. During these dry days defined as dryspells, the water table decays with the same patterns as in the dry season until the next surface flow event occurs. As seen in in section 5.2.2, the maximum dry spell duration could reach up to 63 days during which time the storage could drop down to 70% of its available storage capacity. Rainfed crops could be severely damaged when such long dryspells persist, however the aquifer storage at that level provides significant amounts of water that can sustain irrigation during that time

- **Recharge estimation**

The simulation of the variation of the storage for the period of 16 years show that the aquifer system recharged almost certainly every year except for the 1992 where no discharge occurred indicating extreme drought conditions. A beneficial application of the model would be to use the storage variation results to estimate the recharge of the aquifer in the boundaries of the study area. Calculated recharge as a flux per hydrological year is presented in **Figure 5-19**. Recharge volumes vary between 150000 m<sup>3</sup> to 380000 m<sup>3</sup> per year. The magnitude depends on the length of the dry season of the previous year in addition to the frequency and duration of dry spells during the wet year. HY1987 observed the

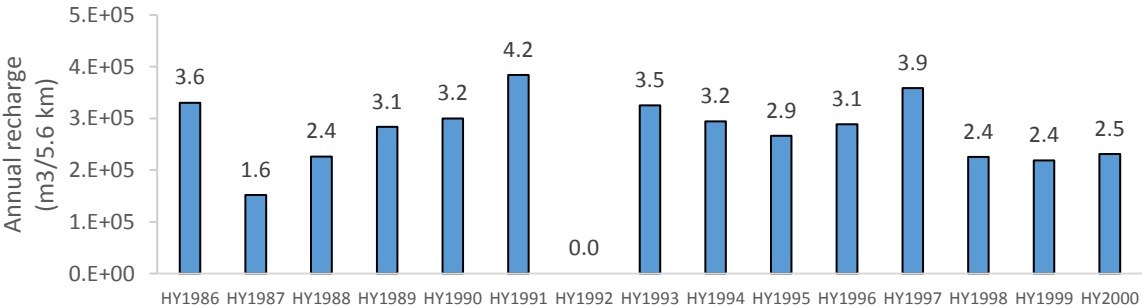


Figure 5-18: Calculated recharge for the Tshelanyemba study site. Volume are reported on the y axis and the labels in mm

lowest recharge since the dry season was very short and no occurrence of dry spells (**Figure 5-13**). The highest recharge occurs during HY1991 and HY1997 where the volumes reach a cumulative of 380000 m<sup>3</sup>. These volumes exceed the maximum available capacity of the aquifer and suggest that recharge is cumulative and a function of the occurrence and duration of dry spells. Indeed, both years had a cumulative duration of dry spells between 50 and 70 days with shorter but more frequent dry spells. During the dry spells, the storage naturally depletes as an effect to evaporation losses, which is immediately re-saturated in the next discharge event. The depletion-recharge cycles increase the cumulative amount of recharge for a given hydrological year.

Recharge is distributed during a hydrological year (**Figure 5-19**). At the beginning of the hydrological year which follows the beginning of the wet season, almost 55% of the total recharge occurs. This amount depends on the degree of storage depletion of the previous dry season. With the occurrence of dry spells during the wet season, the storage level depletes naturally and is recharged at the next discharge events. Recharge following a single dry spell event contribute between 8% and 25% of the total recharge of the considered hydrological year. Dry spell recharge occurs as frequently as the dry spells do and the total accumulates to almost 45% of that annual recharge.

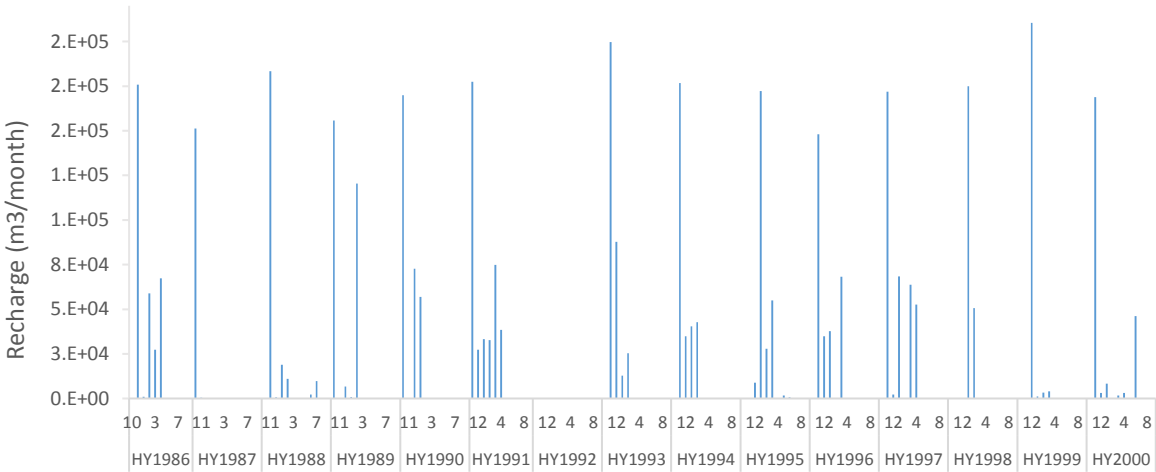


Figure 5-19: Calculated monthly recharge flux to the study area

These estimations are only valid for the study area stretch of 5.6 km. It is therefore difficult to generalise these calculations as diffuse areal recharge from rainfall if the mechanism is actually concentrated recharge from infiltration of runoff water. If we assume however, that recharge can be uniform for the entire stretch of the river in the drainage area, the recharge values computed above can be rescaled to the entire area of the drainage so as to compare its magnitude to other components of the hydrological cycle (**Figure 5-20**). This would lead to recharge values varying between 1.6 and 4.2 mm per year. This is considerably lower than the average annual runoff of 33 mm. On a yearly basis, sometimes, recharge observed was higher than runoff of that year (example of HY1986, 1989, 1994, 1998). This results from the model assumption that any discharge events was considered an indication of the saturation of the riverbed, regardless of the magnitude of the discharge measurements which sometimes was measured at 0.001 m<sup>3</sup>/s. A threshold value could have been applied to account for a reliable detection threshold, however, in the absence of stage data this was not possible. Stage data would have been more appropriate to estimate the relevance of the flood event in recharging the aquifer (Gustar & Demuth, 2008; Loucks & Beek, 2005).

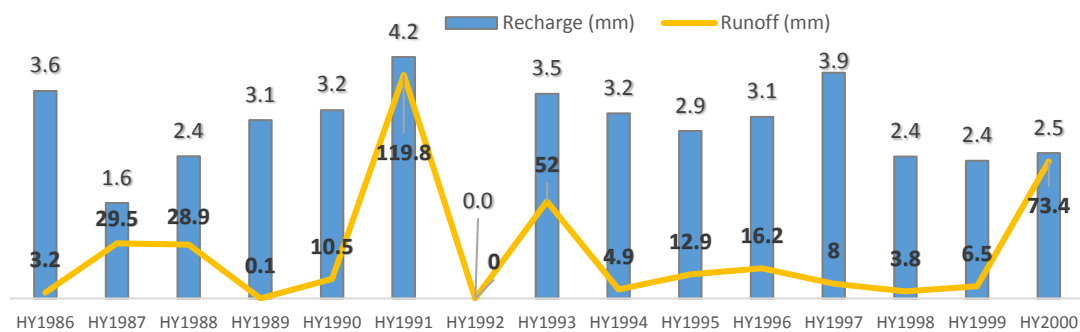


Figure 5-20: Comparison of annual recharge of the alluvial riverbed and annual runoff for the catchment

### 5.3.3. Scenarios simulation

- **Effect of the strategies storage and on meeting the daily demand**

Figure 5-21, illustrates the percentage of meeting an assigned demand defined by the number of wells and the pumping rate per well for scenarios 1, 2, 3 and 4 and for both cases of scenario B and C (See section 4.3.4). The total demand is fully met for the entire dry season for all A scenarios, therefore the results were not presented. For the B scenarios where the total demand is 825 m<sup>3</sup>/day, all distributions fail at meeting the daily demand at different durations after the beginning of the dry season. In strategy 1B, failure is observed after 130 days of the beginning of the dry season and continues until the last dry day where the total daily demand is met at 40%. For the remaining strategies 2B, 3B and 4B, failure occurs around 40 days after the failure of 1B, with a higher percentage of meeting the daily demand as compared to 1B, however, failure is increased rapidly in the remaining days. This shows a clear advantage of using sparse pumping strategy midway the dry season. A strategy with distributed wells and decreased pumping rates per well should cause less local over-exploitation and therefore is expected to perform better than concentrated pumping. This is dependent on the location of wells with regard to the depth of the aquifer as well as any other obstacles in its upstream or downstream. In these simulations of sparse located wells, wells positioned downstream of rock sills dry up quickly as the water level drops below the obstacle, preventing any replenishment of the downstream. The closer the well to the upstream obstacle, the quicker it will dry and therefore the total daily demand decreases at higher rate than a scenario where the wells are located a bit downstream of the obstacle.

For scenarios C, the system fails at delivering the total daily demand of 1900 m<sup>3</sup>/day, after the first 72 days of the dry season. Even though strategies 2C, 3C and 4C fail after 97 days, the decrease is more pronounced and the system provides less water per day for these sparse strategies as compared to concentrated pumping strategy. This is an expected result for high pumping rates per well, which will induce more drawdown that leads to interference between the neighbouring wells.

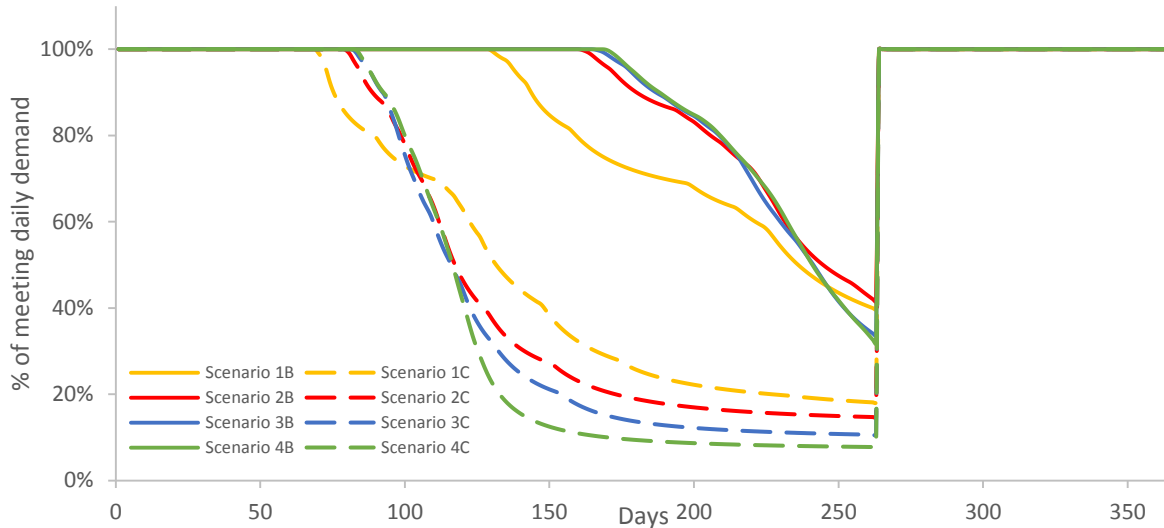


Figure 5-21: Percentage of meeting the daily demand for an average hydrological year

The total demand associated with Scenarios A, reduces the storage of the aquifer at the last day of the dry season to 35% of the maximum storage capacity as compared to 45% in the no-abstraction scenario (**Figure 5-22**). In scenario B, and at the same dry day, storage reaches 10% whereas in Scenarios C, the storage is almost entirely depleted. The pumping strategy influences the total storage of the aquifer. The sparser the distribution of the wells is, the more depleted is the aquifer, which indicates clearly the advantage associated with a more distributed strategy. The wells when strategically and sparsely positioned allow abstraction of more water from the aquifer.

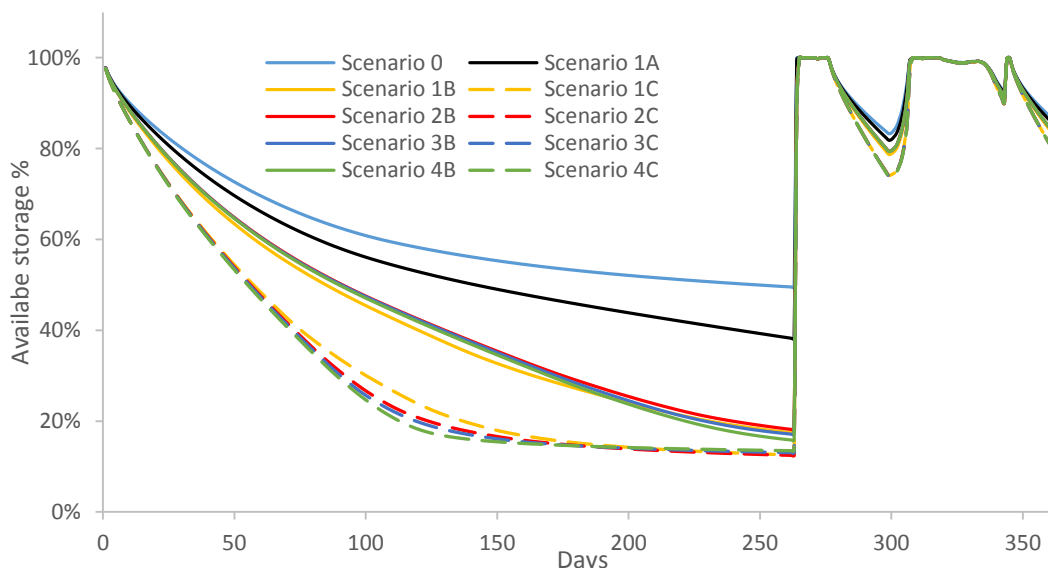
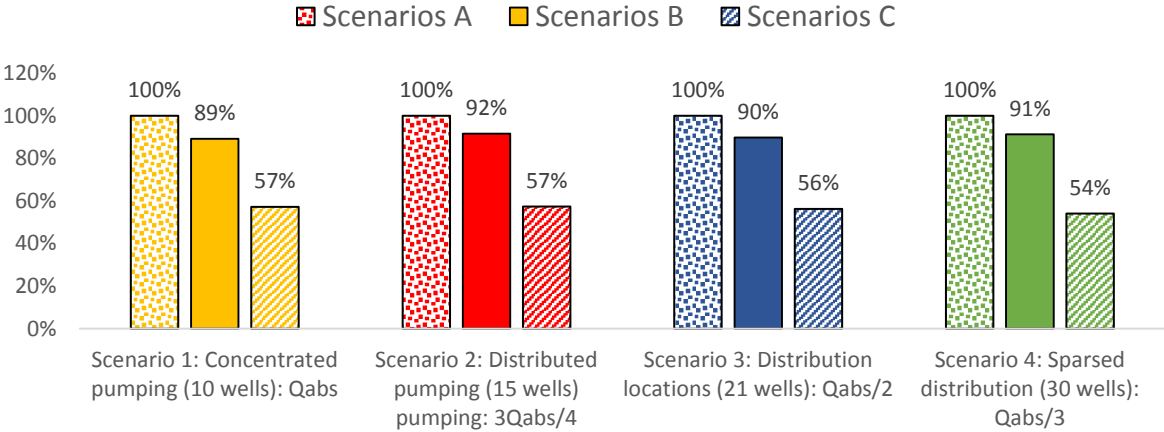


Figure 5-22: Variation of storage for an average hydrological year for the different scenarios. Maximum available storage is 350000 m<sup>3</sup>



**Figure 5-23** illustrates the percentage of meeting the total demand during the dry season for the different scenarios simulated so far. Scenarios C lead to meeting the total demand in the dry season by up to 50% only. This is due to the high abstraction rates per well which increase the depressions around the abstraction wells creating local overexploitation effect. For this case strategy 1 of concentrated pumping



*Figure 5-23: Percentage of meeting the total demand in the dry season (263 days)*

offers an advantage in which wells are far from each other therefore minimizing the interference between the drawdowns. In scenarios A, a total demand of 330 m<sup>3</sup>/day is met entirely. Simulations of scenarios B, show that of the spatial distribution of wells and reduction of their abstraction rates improve the degree at which the system is reliable to be used for a defined demand. While it was expected that the sparser the distribution the better the performance of the system in providing more water, scenario 2B shows that a distribution of 15 wells spaced by an average of 250 m are able to meet the total demand at a higher rate than Scenario 4B. This is highly dependent on the choices of locating the wells and the longitudinal irregularities in the bedrock which separates the entire system into disconnected micro-reservoirs that deplete faster than a system that is constantly replenished from the upstream when no sublayer obstacles are observed.

- **Effect of abstraction on evaporation losses**

**Figure 5-24**, illustrates the relationship between the supplied volumes to meet the demand and the total evaporation from the aquifer as a cumulative flux for the entire dry season for a specific daily demand. With increasing daily demand, the total cumulative evaporation during the dry season decreases. When no abstraction are applied, evaporation losses are equivalent to 53% of the available storage. This percentage decreases as the abstraction increase. For instance, an abstraction of 800 m<sup>3</sup> per day lead to a 20% reduction in the evaporation rate and more water of the storage is available for use. For management strategies, more abstractions is favoured as it allows to maximize the use of the available water in the storage instead of losing to natural evaporation.

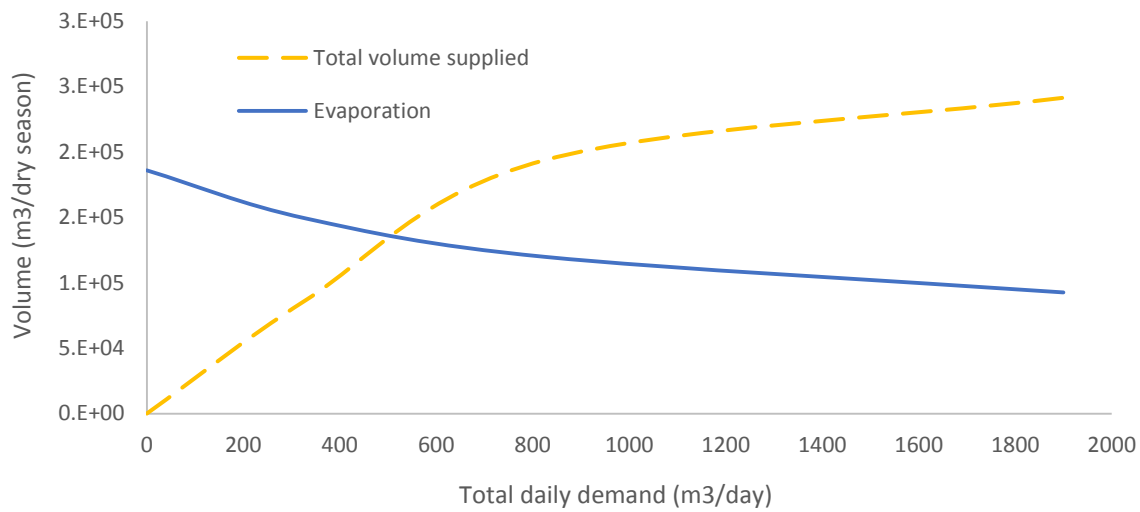


Figure 5-24: Total annual evaporation in comparison to the abstracted volumes as a function of a specified daily demand

- **Optimization of pumping rate and potential irrigated area:**

If we consider that meeting the total demand of the entire dry season as the criteria of the success of the system then determining the maximum abstraction rate per well which meets this criteria helps determine the maximum extractable volumes and thus the degree of agricultural development in the region. For this, the best abstraction strategy would be either strategy 3 or 4 even if strategy 2 showed better results. The reason behind this choice, stems in the distribution of gardens in the region which are distributed on both sides of the river banks. A sparse well network minimizes the distances of the pipes and installations and could possibly reduce the associated costs. Since the optimized daily pumping rate is intended to meet the total demand at 100%, this means that the strategy is not relevant especially since no significant differences between the strategies in terms of the percentage of meeting the total demand was recorded (Figure 5-25).

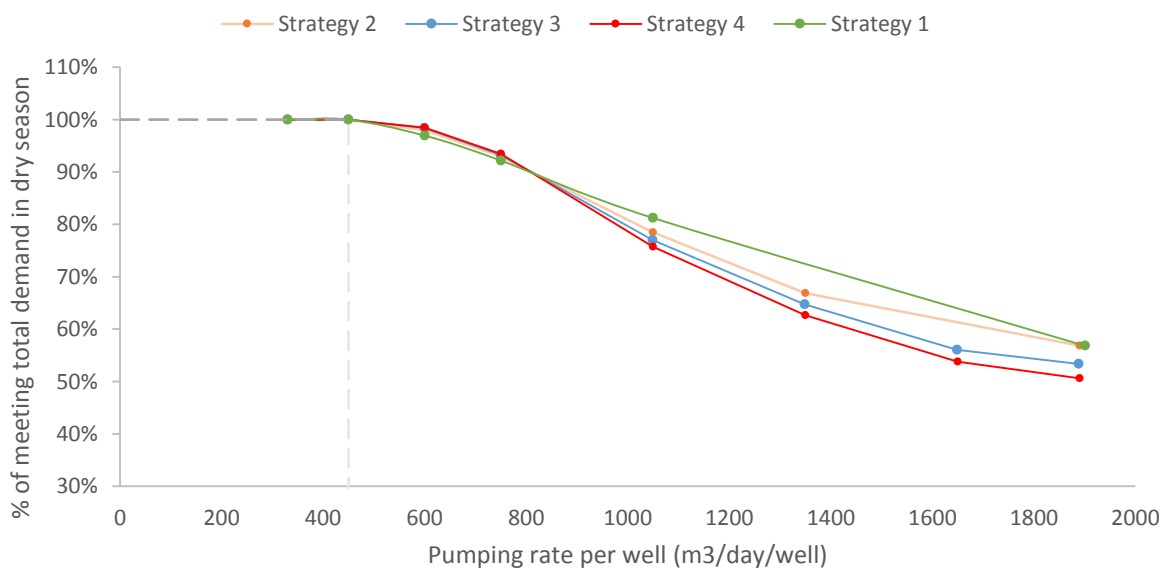


Figure 5-25: Percentage of meeting demand for Strategies 2, 3 and 4

The maximum total demand that could be entirely satisfied by either one of the abstraction strategies 3 or 4 without any drying up of the wells is 450 to 800 m<sup>3</sup>/day. There is not a significant difference between the two scenarios for the abstraction rate. Such volume will be used in the majority for irrigation of the neighbouring gardens, as abstractions for drinking water consumption are assessed to be negligible. This estimation is based on the assumption that irrigation starts immediately at the beginning of the dry season. Any delays in the start of the irrigation season results in more available water for abstraction at the end of the dry season, although evaporation losses might reduce the amount. **Table 7** summarizes the potential area that the determined abstraction rate can irrigate.

Table 7: Potential irrigated area for an average dry season for the 5.6 km studied stretch

	Dabane plan		Zimbabwe, Ministry of agriculture		Based on plant demand	
	High deficit irrigation				Full irrigation	
m <sup>3</sup> /day/ha	30		41		57.6	
Daily available water (m <sup>3</sup> /day)	450	800	450	800	450	800
Potential irrigated area (ha)	15	26.7	11.0	19.5	7.8	13.9
Potential irrigated area (ha/km)	2.7	4.8	2.0	3.5	1.4	2.5
Surface of irrigation scheme (ha)	3		3		3	
Potential number of irrigation schemes	5	9	4	7	3	5

- **Effect of pumping on recharge and runoff**

Recharge was calculated for a selected year’s representative of average, medium and extreme drought duration, defined by the duration of the dry seasons (see section 5.2.4). The year selected area, HY1986, HY1988, and 1991/1992, and HY1995. The pumping strategy followed is Strategy 4 with a pumping rate of 26.6 m<sup>3</sup>/day per well and total demand of 800 m<sup>3</sup>/day.

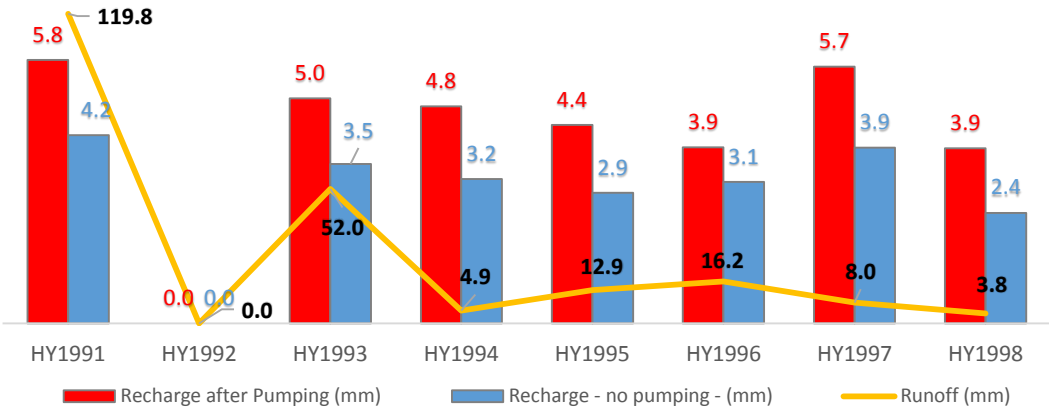


Figure 5-26: Annual recharge for scenarios with pumping and without pumping, compared to annual runoff

**Figure 5-26**, illustrates the annual recharge, computed for no pumping scenario and a pumping scenario corresponding to 800 m<sup>3</sup> per day. The annual recharge is higher in the pumping scenario as the storage

is depleted, and therefore there is more available empty volume to be recharged in the next surface water runoff event. As surface runoff is the main recharge source, increasing abstractions might lead to a reduction in surface water flow produced. For years with high runoff, the increase of the recharge will not disturb the surface flow regime as much as it could do for years with low runoff. For example, in HY1994, recharge in the pumping scenario increases by 1.6 mm more than the recharge in the no-pumping scenario. If this amount is solely taken from runoff, the yearly runoff of that year could then be reduced by roughly the same amount. Runoff could be as low as 3.8 mm for HY1998. Increased pumping might significantly decrease the discharge if a low runoff is to be recorded in the next year in the case of such large scale irrigation.

- **Limitations of the model**

As the famous saying goes: “All models are wrong, however, some are useful”. The model developed for this research was intentioned to provide a tool to understand the riverbed aquifer behaviour in natural conditions, and assess the extent at which agricultural development in the region can rely on for water provision. There were many simplifying assumptions followed and their justifications were presented. The assumptions adopted for the modelling have direct impact on the validity of the results and their implications will be discussed.

As the modelled study site is only a portion of a 102 km river stretch, head boundary conditions needed to be defined in the upstream and downstream of the study area to simulate the extent of the aquifer. Constant head with time variation was chosen for this exercise. The variations of the head was build using the discharge data and a simple assumption that any occurrence of the discharge brings the head to the saturation level. This might be a valid assumption considering the used time step, however, imposing the head in the upstream and downstream, will be forcing the system in the middle to react accordingly. In fact when simulations were run without any evaporation losses, the water table still decreased as a reaction to the drop in the heads at the boundary conditions. This could explain the low calibrated evaporation rate compared to the potential evaporation rates (see section 5.2.1.).

The constant head boundary conditions have no significant impact on the storage as inputs/outputs are negligible compared to the storage of the aquifer. In fact, simulations were performed were pumping stopped during the dry season and after the water level dropped below the extinction depth. The storage remained constant and was as expected not replenished by the constant head boundary conditions. Still, an alternative to these conditions would be to simulate a larger extent of the area (20 km for example) in a free draining condition by installing drains at the downstream extreme. This will mimic the natural behaviour of the system and allow the boundaries to react freely to the stresses within the study area.

No flow boundaries were considered on the riverbanks and the underlying bedrock. Such assumptions were justified because of the low conductive fine material which limits the losses. Since the processes

in the aquifer are rapid, it is safe to make such an assumption. However, in the presence of undetected faults, the losses might be exacerbated.

During the flood event and after saturation of the riverbed, the water head exceeded the sand surface level. It was unable to use MODFLOW to simulate surface water flow. A modelling hack was adopted by installing drains at the level of the sand surface and therefore anytime the water head exceeds the sand surface level, the excess is eliminated out of the model. The use of drains for such a purpose was not found in literature before, perhaps due to the lack of small scale groundwater model. There are still some issues observed with their use. At the beginning of each simulation the drains seem to drain out water is not in excess even in the dry season. This creates extra losses in the storage and underestimate the real values of the storage. Therefore correction on the flow budget need to be done, or an improvement of the drains performance is suggested.

Modelling the abstractions was done without consideration of the method of abstraction and its feasibility. It assumed that the wells operate at a high efficiency and no issues are to be expected with the pumps. Besides, no refinement of the cells was applied around the wells and therefore drawdowns are expected to be more severe in the vicinity of the wells.

Finally, the optimized pumping rate using the numerical model is higher than that obtained by the tank model. The simple explanation is that the losses in the tank model were predetermined and conditioned by the logger data, therefore are not influenced by the hydrology of the system. Whereas in the numerical model, increased pumping allow more water to be pumped that would have otherwise be lost to evaporation. If the tank model adopts a linear model for the evaporation, similar results could be obtained from both.

## 5.4. General discussion

**Objective 1:** *Characterization of the hydrogeology of the sand river aquifer with an emphasis on the sediment depth and the subsurface layers in order to locate potential locations for abstraction.*

The aquifer is formed of material identified as poorly sorted fine to coarse sand with the presence of pebbles and gravels. For such material, have a porosity of 30 to 32% which indeed falls within the range of poorly sorted sands (Das, 2008). The spatial distribution of the sediment in the riverbed is not uniform across the channel as this is mainly related to the flow regime, where high velocities generate high shear forces which can erode bigger grains, whereas lower velocities tend to favour depositions or erosion of small grains only (Lamb & Venditti, 2016). Slope also is a controlling factor in the deposition of the sediments. In the upstream stretch of the river, slopes are steeper and the channel is narrow, therefore less deposition occurs and the riverbed aquifer tends to be shallow. In opposite, the more to the downstream, the slopes become gentler and the channel wider and therefore the riverbed thicknesses are enhanced as more deposition is favoured (Moyce et. al, 2006; Maspovo, 2008). Despite these disparities, the sediment remains within one class which does not alter significantly the hydraulic

properties. Soil gradation gives an indication to other material properties such as hydraulic conductivity and porosity, hence the sediment material in the study area provides good storage and drainage capacity for the aquifer.

The material forming the riverbed of the Shashane River is highly conductive with conductivities varying between 90 and 120 m/day. Such values are representative of ephemeral riverbeds in the regions of southern Africa as reported by Owen (1991), Moyce et. al (2006) and Masnell & hussey (2007). Although the low values compared to well-graded sands might be indicative of presence of clays or silts. Flow velocities are dependent both on hydraulic conductivity and the very gentle slopes slow down the groundwater flow significantly. In the Shashane, the groundwater front was estimated to advance by 100m per year as compared to 1km per year reported by Owen (2001) in the Lower Mzingwane river channel. This has three implications: (a) the aquifer can be studied as an isolated tank as the replenishments or losses of the groundwater component are negligible compared to the storage capacity of the aquifer, (b) the slow movement of the water allows for an improvement of the quality of water for drinking water, mimicking a sand filter purification system, and (c) such slow flows reduce the source vulnerability of the aquifer to pollution events as the conductive transport of contaminants is slow.

Specific yield is a hydraulic parameter that conditions the available amount of water available for abstraction from the aquifer. No measurements of this parameter were done during this research, however, values were taken from relevant studies in neighbouring regions in southern Zimbabwe. Accepted reported values range from 10 to 20% (Moyce et. al. 2006; Nord, 1985; Owen, 1994). Such values are relatively low for a sand formation which vary typically between 20 and 33% for the same material (Heath, 1983; Morris & Johnson, 1967). Low values of specific yield are indicators of heterogeneity and mixing with finer material such as silt or clay. Disparities with specific yield values increase the uncertainty in the groundwater estimations.

Hydraulic conductivity and specific yield are better estimated by pumping tests which revealed to be difficult to execute in the complex settings of the riverbed alluvial aquifers. In addition to costs associated with such tests, considerable pumping might result in very wide cones of depression which makes the drawdown at the observation wells hard to detect the parameters unreliable to estimate. As a consequence, the pumped water has to be discharged far from the aquifer to avoid return flow to the aquifer and alteration of the cone formation (Mulder, 1973; Karanth, 1987).

The geophysical assessment in this study was limited to one cross-section of the river, nonetheless it helped characterize the local subsurface of the riverbed and its extension to the river bank. The lateral extent of the riverbed is delimited by the riverbanks which are delimited either by silts and clays or outcropping rocks (**Figure 5-27**). The riverbed is shallower near the banks at the inner bend of the meander and thickens at the outer bends. The thickest part of the riverbed are observed along the main channel. A meandering river tends to contain one main channel that cuts through the floodplain. Along its flow path, it deposits sediments on the inner bends through point bar deposits, and tends to erode the opposing bank on the outer bend of the channel creating thus a clear difference in elevation (Sutter, 2008). At the entrance locations of the tributaries, the registered thickness reached 5m as the rapid velocities associated with surface flows in the tributaries, deepened the hard rock through deposition during low flow regimes. The thicknesses might not be as deep in other cross sections, and therefore a detailed investigation using geophysics is required.



*Figure 5-27: outcropping rock at the riverbank*

The riverbed formation gets finer in depth as more silts and clay are encountered. Underneath the fine sediments, unfractured bedrock is encountered at a depth of 10 m, upon which fractured and weathered rock is embedded with saturated clays and silts. Weathered bedrock increase the downward movement of water whereas less weathered bedrock limits these losses (Maspovo, 2008).



*Figure 5-28: Roots penetrating the sand deposits*

The riverbanks are formed by saturated silts and clays which are not suitable for water extraction. This formation was initially hypothesised to be a paleo channel formed from sand that receded because of the migration of the meanders. However, the geophysical survey indicates, that this material is clayey with presence of silt which is unproductive even for small scale abstractions. Despite the low productivity of the material in the banks, it is an extension to the riverbed and the clayey material is kept saturated by the riverbed groundwater. This is illustrated by the presence of the undisturbed riparian vegetation. Accessing water is a key factor for the riparian vegetation to be sustained. As the river is dry most of the time of the year, roots of the trees extend in depth to tap in water from the underlying formation (**Figure 5-28**).

**Objective 2:** *Analysis of the dynamics of the aquifer and the interaction of the surface and groundwater and their impact on the storage of the aquifer*

The studied portion of the riverbed alluvial aquifer provides a maximum storage capacity of almost 700000 m<sup>3</sup> of which only 50% is available for use. There is however a high uncertainty regarding this estimation related to the values of the hydraulic and geometrical parameters of the aquifer. The deepest point of the channel was chosen from the geophysics to be uniformly 5m, with the exception of locations of subsurface obstacles. This assumption cannot be generalized as the geophysical assessment was limited to one cross section. Besides, the cross section was at the level of a tributary which generally favours erosion and therefore thicker riverbeds are expected compared to cross-sections away from the tributaries. In addition, the 3D subsurface model relied on many sparse interpolations between the probed cross sections despite the extreme irregularity in the bedrock. Considering 3.85 m as the average thickest depth of the main channel decreases the estimated total storage capacity by 12%. On the other hand, disparities with regard to the specific yield values which conditions the available volume for abstraction, will give gross differences in the estimations of groundwater. This work may be overestimating the potential of the aquifer.

The results of scenario 0 showed that the system's water losses are dominated by evaporation as illustrated in the groundwater dynamic analysis (see section 5.2.1.). Gonzalez-Carballo (2018) following the same approach, concluded that water level drops could be explained to a high extent only by evaporation. In opposite, Wekesa (2017) pointed out the existence of an additional loss to evaporation which he attributed to seepage into the underlying fractured bedrock. While vertical and lateral seepages might affect the water table decrease, their impact is localised as the weathering degree of the rock is irregular and cannot be generalized. In another hand, at locations where the water is trapped behind subsurface rock obstacles, volumetric evaporation losses tend to increase. As the water cannot flow downstream, the only way out for it is through evaporation which is enhanced by the shallow depth of the water table and the upstream constant replenishment. Finally, losses to evapotranspiration of the riparian vegetation were clearly observed through the diurnal fluctuations of the water table (see section 5.2.1.) and a clear indication that the riverbed aquifer system is connected to the banks. Gonzalez-Carballo (2018) modelled this connection with aquifer system and the riverbanks and quantified that these losses are insignificant in comparison to the direct losses to evaporation. This supports the assumption of no lateral flow in the model.

The natural depletion of the aquifer is recharged almost certainly at the beginning of the first or second surface flow event of the next wet season. This is highly dependent on the water content in the aquifer, the level of the water table, the hydraulic conductivity of the sediment and the intensity of the rainfall and the size of the system. Recharge from direct rainfall is generally almost negligible for small to medium systems, and runoff is considered by many authors as the main recharge mechanism. Wekesa (2017) for instance showed that indeed the surface water is only recorded once the groundwater level entirely saturated. Although the system he studied is shallow of 2 m depth and therefore bigger systems



will require more intense events for their saturation. Studies on ephemeral rivers in Australia estimated that 25% of the discharge are infiltrated in the riverbeds, and the total recharge to the sand rivers amount to 4% of the total catchment recharge. While the ratio of infiltrated water from the discharge was not considered in this study, estimated recharge values from the model varied between 2 to 4 mm per year which account between 2 and 5% of the total catchment recharge (Nyagwambo, 2006; Sangwe, 2001). Note that the upscaling of the results was performed for indicative purposes only and recharge cannot be considered as a uniformly diffusive mechanism along the entire river. A more thorough estimation of recharge for the catchment's alluvial aquifer is recommended.

Despite the assumption that the recharge occurs in tandem with discharge events, there are still some years that go without a single drop of water to recharge the aquifer. According to the data, this occurred once every 20 years, although the length of the data series was too short for a strong affirmation. In the case of these long durations of the dry season, one of the advantages of the sand aquifer is that evaporation does not affect the losses once the water level drops below the extinction depth, and only slow losses to deeper aquifer or the river banks persist. This allows for water to be available for drinking purposes at specific locations where water tends to accumulate behind subsurface obstacles. However, the quality of the water for drinking purposes might deteriorate due to increased salinity (Gonzalez-Carballo, 2018) and large scale irrigation cannot be sustained during such prolonged dry seasons since the storage will be depleted through pumping in the previous year. Dependent vegetation on the other hand, should not be affected significantly as the plants can still access water beyond the retained fraction until the moisture content reaches the wilting point.

The dominance of evaporation results in a natural depletion of the aquifer to half of its available storage. This is particularly an issue with wide and shallow systems. Love et. al. (2007) indicates that shallow aquifers less than a meter in depth can dry up due to evaporation losses within 24 hours of a river flow. Nord (1985) estimated that evaporation losses account for a total of 25% of the available water in the aquifer in Botswana. This water should then be utilized immediately after the river flow as this will reduce the available water to evaporation and allocates it for other uses. Following this, if the water is utilized entirely during the dry spells or the beginning of the dry season, the water level will decline creating more available empty volume to be filled in the subsequent wet event, and thus maximizing the use of the aquifer water.

Maximizing the amount of water used from the aquifer can be achieved by intensively pumping the entire available storage and waiting for it to be recharged with the first flood event of the next wet season, however, this might have implications on the riparian vegetation and the generated runoff if the pumping is intense. The yearly runoff is highly variable where some years could observe 110 mm whereas others observe runoff as low as 3 mm. On the other hand, pumping directly increases the recharge volume of the following year as it creates more empty storage for the runoff to refill. If runoff in the following year happens to be low, an increase of recharge of 1.8 mm because of pumping (see figure 5-31) might reduce the generation of the runoff to an extent that it affects other users downstream. In the absence

of any particular study that supports this finding on the scale of sand river, Sapriza-Azuri, Jódar, Carrera, and Gupta (2015), using a global model in the semi-arid southern part of Spain, indeed found that intensive pumping reduces runoff generation by up to 50% throughout the entire year.

**Objective 3:** *Assessment of the impact of increased pumping on the storage of the aquifer and the potential area that the system can irrigate.*

On an average dry season of 255 dry days, the studied stretch of 5.6 km of the aquifer has the potential of providing between 450 and 800 m<sup>3</sup> per day without failure of the system in the entire dry season. Higher volumes will lead to drying up of some wells before others. When the water level drops below the level of a subsurface obstacle, the system will be separated into discontinuous micro-reservoirs and the micro-reservoirs downstream of the obstacle will not be replenished from the upstream. Therefore, the wells located at the immediate downstream of such an obstacle are most likely to dry up first. In contrast, wells located upstream of an obstacle are likely to remain productive for longer periods, as these obstacles work as subsurface dams that prevent downstream losses (see **Figure 5-29 and Appendix G**). At these levels, the water depth is shallow and easily accessible and therefore well installations should be targeted in the vicinity of such areas. Determining these localities, groundwater can be used to support local scale commercial irrigation.

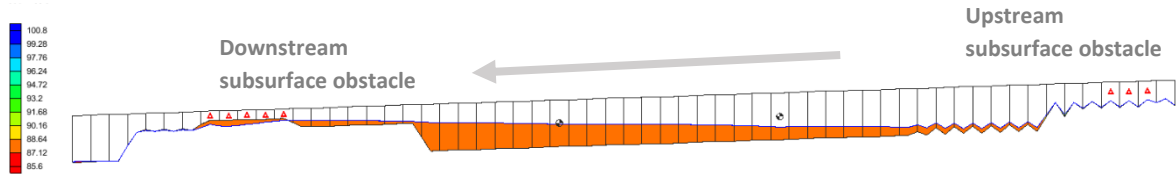


Figure 5-29: longitudinal cross section of a portion of the modelled riverbed illustrating the effect of the subsurface obstacles on the water level variation locally.

The spatial pumping strategies were evaluated with the model. A strategy with sparsely located wells and reduced pumping rates was expected to be more reliable. It was revealed that this might be true when the abstraction rates are not relatively high. When pumping rates are low (i.e. meeting the total demand without failure), there is no observed difference between the strategies. For medium pumping rates (i.e. when failure is minimized) the sparse strategies are indeed more reliable than concentrated pumping, although the difference is only 3% (see **figure 5-23**). Higher pumping rates are better achieved using fewer wells because the interference between wells is minimized. Mulder (1973) reported a radius of influence of wells of 750 m for an optimum pumping rate of 1900 m<sup>3</sup>/day in the Limpopo riverbed aquifer system. Mulder’s (1973) findings are for a system that is three times larger than the study area. Since for low pumping rates, the spatial strategy is not important, it is however suggested to opt for the distributed pumping network if small and more irrigation schemes are planned.

The optimized pumping rate could be allocated mainly to agricultural uses since domestic use demand was estimated to be negligible (Mansell & Hussey, 2005). Such abstracted volumes will be able to

irrigate a potential area between 8 and 27 ha per 5km stretch or 1.4 to 4.8 ha/km depending on the followed irrigation strategy. This compares with the estimations made by Maspovo (2008) which approximated a potential irrigated area of 11.8 ha/km for an aquifer that is twice as big as the Tshelanyemba study site. Dabane's perspective is to develop gardens of 3ha of area using an irrigation scheme of 3 mm every 3 days. This is a very high deficit irrigation that stresses crops and therefore yields are expected to be low. On the other hand, the Ministry of Agriculture suggests a daily irrigation of 41 m<sup>3</sup>/day with which an average of 2.5 ha can be covered per km of river. A lower area can be covered by full irrigation, as this strategy aims to meet the entire demand of the crop which is higher than the potential evapotranspiration for crops like wheat, citrus, vegetables and sugarcanes, commonly planted in communal areas in Zimbabwe (Acquah and Masanzu, 1997; Mhlope 2017; Hussey 2005).

Sand river abstraction methods vary from traditional to technologically advanced methods. For limited abstractions, the local dwellers rely on hand dug wells in the sediment which are deepened depending on the drop of the next water level. These wells are seasonal and need to be reinstalled in the next season. Modern methods on the other hand are either humanized or motorized and vary in scale depending on the purpose of the abstraction. In the study area, users rely on scoop holes, whereas garden owners either use rower pumps, diesel pumps or solar pumps. Rower pumps allow for a low pumping rate that does not suit large irrigation schemes. Diesel pumps are the commonly used as they are portable and easily operated. Solar pumps installed by Dabane in the recent years are the favourites as they reduce the energy costs. However, their operation still creates a maintenance dependency on the supplier. On many occasions installed solar pumps were disconnected as a consequence to flooding events and require the intervention of Dabane for maintenance which sees the farmers switching back to diesel pumps as they are more reliable for them for the time being. Conveyance structures are more suitable to divert water from the river channel to the arable lands (Owen, 1989).

## CHAPTER 6

# Conclusions and Recommendations

## 6.1. Conclusions

This research aimed at characterizing the riverbed shallow alluvial aquifer of the Shashane River on a first step and evaluating its potential for use in agricultural development projects in the neighbouring areas on a second step.

To characterize the water bearing units of the aquifer and their capacity of storage, sieve analysis of the sediments associated with geo-electrical methods were performed. The ability of flow and transportation of aquifer was tested through field slug tests to determine in-situ undisturbed values of the hydraulic conductivity. Recharge occurrence was evaluated through frequency analysis of the measured discharge data. Finally, the previously inquired information were incorporated in a groundwater numerical model to assess the potential of abstraction. The results revealed that the aquifer has a good development potential and is currently underutilised.

The riverbed aquifer is formed by homogenous highly conductive fine to coarse sand, however, the gentle slope slows down the groundwater flow to 100 m per year. The sand layers are very irregular all over the river and tend to deepen around the main channel and outer bends where thicknesses can reach up to 5m. The irregularities in subsurface due to the presence of natural bedrock barriers, divide the subsurface system into disconnected pools every 600 to 1000 m. The disconnection between the pools limits the groundwater replenishment and reduces their exploitation potential. However, the subsurface obstacle create location with a shallow water level easily abstracted.

The riverbank plains extend to a 100 m away from the main channel and are formed by silts and clays. These plains are elevated by an average of 3m and present material with low potential for abstractions. It forms however an extension to the main channel system as is illustrated by the presence of vegetation and the diurnal fluctuation in the groundwater table, although the losses from the main channel aquifer to the banks remain negligible.

On the bottom of the aquifer, the sand material is underlayed by saturated weathered and fractured gneiss rocks embedded with silts and clays. The low conductive fine material limits the vertical seepage losses, however, this is highly irregular in space and depend on the degree of weathering and the rock.

The studied portion of the aquifer has a maximum storage capacity reaching around 0.7 Mm<sup>3</sup> of which only 0.35 Mm<sup>3</sup> per 5.6km available for abstractions. Naturally, evaporation is the dominant outflow mechanism, which accounts for almost 50% of the available water in an average dry season. It is conditioned by the extinction depth which is as deep as 1m for sands. Evaporation losses persist through the dry season in location where the water table is high, generally where the water accumulates behind subsurface obstacles. Another loss mechanism is the downstream groundwater flow which is only observed locally at the level of the created pools. In the entirety of the system, the upstream extent of the aquifer, allows for replenishment of the groundwater although its contribution is almost entirely negligible.

The aquifer systems underlays an ephemeral river system that serves as its main recharge input. It flows only a limited number of days during the short wet season. It is characterized by highly variable flood pulses that are interrupted by dry spells of almost 63 days of length. Generally, each flood pulse transports a volume much superior to the storage capacity of the entire riverbed aquifer of the catchment. Typically, the aquifer is re-saturated almost entirely with the first or second flood event of the wet season. Recharge estimates established by an upscaling of the local results varied between 2 and 4 mm. Such values were artificially calculated as the volume required to refill the aquifer and were up-scaled over the entire aquifer considering the recharge mechanism as diffusive. Recharge however, is not ensured on a year to year basis. Some years pass by entirely dry without a single recorded discharge. This occurred once only in the 20 years of data available, which provides a significant certainty in recharge occurrence. Increased pumping might significantly reduce runoff generation if the following years have a low runoff. This could impact the dependent ecosystems, the local dwellers and the downstream users.

Simulation of abstractions to determine the best spatial abstraction strategy as well as the sustainable abstraction rates were performed on an average dry year. It was hypothesised initially that a distributed network with lower abstraction rates per wells would maximize the exploitation potential of the aquifer storage. However, it was revealed that the spatial distribution does not seem to have a big influence for relatively low abstraction rates, whereas for high abstraction rates, fewer wells operate for longer before drying up. This occurs as a direct consequence to the discontinuity of the aquifer into micro-reservoirs where wells at the upstream of these obstacles are more likely to dry up, than those at the downstream.

The portion of the studied aquifer is able to cover a demand of 450 to 800 m<sup>3</sup> of water without any registered failure of the system over an average dry season. Such volumes are able to irrigate an area between 1.5 and 5ha per km of stretch depending on the considered water demand of the crops.

The research demonstrates that the riverbed aquifers have a good groundwater development potential as it showed that significant quantities of water for irrigation and water supply are available and their distribution meets the rural settlements in economically deprived communities in arid to semi-arid regions.

## 6.2. Recommendations:

This research was done in the fulfilments of the A4lab project which aims at improving accessibility to water for deprived communities in semi-arid and arid sub-Saharan Africa. It aimed to characterize the aquifer and quantify its potential for future agricultural development. The area is scarce in data and any work achieved in this is a step further towards a complete characterization of the system. Building upon previously done research is a step further.

The previously installed divers were vandalized and no data was collected during this research. The two new installed buried piezometers equipped with divers in combination with the extended logger data should provide more data to allow for a better calibration of the model. In combination with the weather station, a dynamic analysis between the climatic records can be performed to increase the knowledge on the hydrologic characteristics between the interaction of surface and groundwater.

As the TAHMO weather station is installed in the center of the yard of the processing center, it is suggested to be moved and reattached to one of the buildings in order to avoid any accidents that might damage the station. In addition, it is always suggested to discuss with the local communities the research steps and any new equipment installations.

It is suggested as wells to take a sand and clay auger drill equipment in order to investigate the layering of the riverbanks to confirm the findings with the geophysics. In addition, it is crucial to perform more geophysics measurements along the stretch in areas upstream of tributaries, where the river narrows and enlarges.

Due to the deficiency of the equipment, no chemistry samples were collected from the area. It is therefore important to analyse the water chemistry in the riverbed, and the banks and all along at multiple locations upstream and downstream of the study area. Similarly, stable isotope analysis is suggested, with an addition of more samples to the western part of the catchment. It is important to take temperature as well as EC measurements at the sampled locations.

The modelled aquifer area could possibly be enlarged to account for the interaction with the riverbanks and the bedrock and allow a more accurate quantifications of the losses. The evaporation at the banks should be modelled differently than the riverbed and account for future scenarios of agricultural development.

The boundary conditions must be re-evaluated and could perhaps be simulated using a free head condition. In addition, as the runoff is assumed to be the main recharge source for the aquifer, it is recommended to model the runoff generation and its evolution along the entire 102km stretch so as to account for the effect the intensity of the rainfall events as well as the spatial variability of the recharge.

Rower pumps seem to suffer from a recurrent problem with the disconnections of well point. After a flood event, the pipes seems to float back up due to buoyancy of the pipes. It is therefore suggested to simply attach a weight to the pipe to prevent them from surfacing on the top and allow for longer periods of use.

# References

- A4labs. (2016). *DUPC2 Integrated Research for Development - A4Labs full proposal*. Retrieved from Delft: <http://a4labs.un-ihe.org/a4labs>
- Abi, A. (2018). *Assessing the groundwater dynamics, recharge and storage potential in the Limpopo river sand deposits*. (MSc thesis), UNESCO-IHE Delft Institute for Water Education,
- Alabi, A. A., Ogungbe, A. S., Adebo, B., & Lamina, O. (2010). Induced polarization interpretation for subsurface characterization: A case study of obadore, lagos state. *Arch. Phys. Res*, 1, 34-43.
- Amaya, A. G., Dahlin, T., Barmen, G., & Rosberg, J.-E. (2016). Electrical Resistivity Tomography and Induced Polarization for Mapping the Subsurface of Alluvial Fans: A Case Study in Punata (Bolivia). *Geosciences*, 6(51). doi:10.3390/geosciences6040051
- Archie, G. E. (1942). The Electrical Resistivity Log as an Aid in Determining Some Reservoir Characteristics. *Society of Petroleum Engineers*, 146(1), 54-62. doi:10.2118/942054-g
- Ashton, P. J., Love, D., Mahachi, H., & Dirks, P. H. G. M. (2001). *An Overview of the Impact of Mining and Mineral Processing Operations on Water Resources and Water Quality in the Zambezi , Limpopo and Olifants Catchments in Southern Africa* (ENV-P-V 2001-042). Retrieved from Harare, Zimbabwe:
- Awuah, E., Nyarko, K. B., Owusu, P. A., & Osei-Bonsu, K. (2009). Small town water quality. *Desalination*, 248, 453-459.
- Baker, J. A., & Davies, J. (1997). Exploiting Groundwater from Sand Rivers in Botswana Using Collector Wells. *30th International Geological Congress (Conference Paper)*, 22, 235-257.
- Blok, T. (2017). *Groundwater storage in sand rivers: A case study of Shashani, Zimbabwe*. Retrieved from
- Boubacar, I. (2012). *Caractérisation des saisons de pluie au Burkina Faso dans un contexte de changement climatique et évaluation des impacts hydrologiques sur le bassin du Nakambé*. (PhD), Université Pierre et Marie Curie,
- Bouwer, H., & Rice, R. C. (1976). A slug test method for determining hydraulic conductivity of unconfined aquifers with completely or partially penetrating wells. *Water Resources Research*, 21(3), 6.
- Chandra, P. C. (2015). *Groundwater Geophysics in Hard Rock*. CRC press.
- Chinoda, G., Matura, N., Moyce, W., & Owen, R. (2009). *Baseline Report on the Geology of the Limpopo Basin Area, a contribution to the Challenge Program on Water and Food Project 17 "Integrated Water Resource Management for Improved Rural Livelihoods: Managing risk, mitigating drought and improving water productivity in the water scarce Limpopo Basin"*. Retrieved from WaterNet Harare:
- Davies, B., Thoms, M., & Walker, K. (1994). *Dryland Rivers: Their Ecology, Conservation and Management*. Wiley.
- EcoAfrica. (2015). *Climate Change for the Limpopo Province, South Africa*. Retrieved from [http://www.ecoafrika.co.za/sites/default/files/project\\_resources/3%20LEO%201st%20DRAFT%20Chapter%201%20Climate%20Change%2020151209\\_0-3.pdf](http://www.ecoafrika.co.za/sites/default/files/project_resources/3%20LEO%201st%20DRAFT%20Chapter%201%20Climate%20Change%2020151209_0-3.pdf)

- Fahle, M., & Dietrich, O. (2014). Estimation of evapotranspiration using diurnal groundwater level fluctuations: Comparison of different approaches with groundwater lysimeter data. *Water Resources Research*, 50, 273-286. doi:10.1002/2013WR014472
- Gonzalez-Carballo, A. (2018). *Assessing Groundwater Recharge And Storage Enhancements In The Alluvial Aquifers Of The Tigray Highlands (Ethiopia)*. (MSc thesis), IHE-Delft Institute for Water Education.,
- Gustar, A., & Demuth, S. (2008). *Manual on Low-flow Estimation and Prediction*. Retrieved from Geneva, Switzerland:
- Hamer, W. D., Love, D., Owen, R., Booji, M. J., & Hoekstra, A. Y. (2008). Potential water supply of a small reservoir and alluvial aquifer system in southern Zimbabwe. *Physics and Chemistry of the Earth*, 33(8-13), 633-639. doi:10.1016/j.pce.2008.06.056
- Harbaugh, M. G. M. A. W. (1988). *A modular three-dimensional finite-difference ground-water flow model*. Retrieved from <https://pubs.er.usgs.gov/publication/twri06A1>
- Hays, K. B. (2003). *Water use by saltcedar (Tamarix sp.) and associated vegetation on the Canadian, Colorado and Pecos rivers in Texas*. (PhD), Texas A&M Univ,
- Hellwig, D. H. R. (1973). Evaporation of water from sand. *Journal of Hydrology*, 18, 317-327.
- Herbert, R. (1998). Water from sand rivers in Botswana. *Quarterly Journal of Engineering Geology and Hydrogeology*, 31(2), 81-83. doi:<https://doi.org/10.1144/GSL.QJEG.1998.031.P2.01>
- Huisman, L. (1974). *Slow Sand Filtration*. Retrieved from
- Hussey, S. W. (2007). *WATER FROM SAND RIVERS: Guidelines for abstraction*: Water, Engineering and Development Centre, Loughborough University.
- Hvorslev, M. J. (1951). *Time Lag and Soil Permeability in Ground-Water Observations*. Retrieved from U.S. Corps of Engineers, U.S. Army, VICKSBURG, MISSISSIPPI:
- Interconsult, A. S. (1985). *National master plan for rural water supply and sanitation*. Retrieved from Ministry of Energy and Water Resources and Development:
- Kirsch, R., & Yaramanci, U. (2009). *Geoelectrical methods, in: Groundwater Geophysics*. Berlin, Heidelberg: Springer.
- Lamb, M. P., & Venditti, J. G. (2016). The grain size gap and abrupt gravel-sand transitions in rivers due to suspension fallout. *Geophysical Research Letters*, 43(8), 3777-3785. doi:<https://doi.org/10.1002/2016GL068713>
- Lasage, R., Aerts, J., Mutiso, G.-C. M., & de Vries, A. (2008). Potential for community based adaptation to droughts: Sand dams in Kitui, Kenya. *Physics and Chemistry of the Earth*, 33, 67-73. doi:10.1016/j.pce.2007.04.009
- Leonards, G. A. (1962). *Foundation Engineering*: McGraw Hill Book Company.
- Loke, M. H. (1996). *2-D and 3-D electrical imaging surveys*.
- Loucks, D. P., & Beek, E. V. (2005). *Water Resources Systems Planning and Management: An Introduction to Methods, Models and Applications*. Paris: UNESCO.
- Love, D., Uhlenbrook, S., Twomlow, S., & van der Zaag, P. (2010). Changing hydroclimatic and discharge patterns in the northern Limpopo Basin, Zimbabwe. *Water SA*, 36(3).



- Love, D., van der Zaag, P., Uhlenbrook, S., & Owen, R. J. S. (2011). A water balance modelling approach to optimising the use of water resources in ephemeral sand rivers. *River Research and Applications*, 27(7), 908-925. doi:10.1002/rra.1408
- MacDonald, T. W. B. U. M. (1990). Sub Saharan Africa Hydrological Assessment ( SADCC Countries ), Country Report: Zimbabwe.
- Mansell, M. G., & Hussey, S. W. (2005). An investigation of flows and losses within the alluvial sands of ephemeral rivers in Zimbabwe. *Journal of Hydrology*, 314, 192-203.
- Maspovo, T. H. (2008). *Evaluation of the groundwater potential of the malala alluvial aquifer, lower mzingwane river, zimbabwe*. (MSc thesis), University of Zimbabwe,
- Milsom, J., & Eriksen, A. (2011). *Field geophysics* (3rd edition ed.): John Wiley & Sons.
- Moyce, W., Mangeya, P., Owen, R., & Love, D. (2006). Alluvial aquifers in the Mzingwane Catchment: their distribution, properties, current usage and potential expansion. *Physics and Chemistry of the Earth*, 31, 988-994.
- Mpala, S. C., Gagnon, A. S., Mansell, M. G., & Hussey, S. W. (2016). The hydrology of sand rivers in Zimbabwe and the use of remote sensing to assess their level of saturation. *Physics and Chemistry of the Earth*, 93, 24-36. doi:dx.doi.org/10.1016/j.pce.2016.03.004
- Mulder, M. P. (1973). *WATER SUPPLY FROM RIVERS AND LIMPOPO RIVER AT MESSINA*. Retrieved from
- Ncube, B., Manzungu, E., Love, D., Magombeyi, M., Gumbo, B., & Lupankw, K. (2010). *The challenge of integrated water resource management for improved rural livelihoods: Managing risk, mitigating drought and improving water productivity in the water scarce Limpopo Basin*. Retrieved from
- Nissen-Petersen, E. (2006). *Subsurface dams built of soil*. Retrieved from Kenya:
- Nonner, J., & Stigter, T. (2015). *Groundwater Exploration: Lecture Notes*. Delft: UNESCO-IHE.
- Nord, M. (1985). *Sand rivers of Botswana, Phase 2*. Retrieved from
- Nyagwambo, N. L. (2006). *Groundwater Recharge Estimation and Water Resources Assessment in a Tropical Crystalline Basement Aquifer*. (PhD), TU Delft and UNESCO-IHE, Delft.
- Owen. (2000). *Conceptual Models for the Evolution of Groundwater Flow Paths in Shallow Aquifers in Zimbabwe*. (Unpublished PhD thesis), University of Zimbabwe,
- Owen, R., & Dahlin, T. (2005). *Alluvial aquifers at geological boundaries: geophysical investigations and groundwater resources*. Rotterdam: AA Balkema Publishers.
- Owen, R., & Rydzeski, J. R. (1991). *Shallow groundwater as a resource for small-scale irrigation development, in techniques for environmentally sound water resources development*. London: Pentech Press.
- Owen, R. J. (1989). *The use of shallow alluvial aquifers for small scale irrigation with reference to Zimbabwe*. Retrieved from
- Richards, K. (1982). *Rivers: Form and process in alluvial channels*. London and New York: John Wiley & Sons.
- Sangwe, K. M. (2001). *Recharge map of Zimbabwe and validation of rain gauges for country wide total atmospheric chloride deposition studies*. (MSc thesis), University of Zimbabwe,

- Sapriza-Azuri, G., Jódar, J., Carrera, J., & Gupta, H. V. (2015). Toward a comprehensive assessment of the combined impacts of climate change and groundwater pumping on catchment dynamics. *Journal of Hydrology*, 529, 1701-1712. doi:<http://dx.doi.org/10.1016/j.jhydrol.2015.08.015>
- Sutter, A. (2008). Sedimentology, Depositional Environments and Sequence Stratigraphy. In.
- Svensson, A. (2014). *Estimation of Hydraulic Conductivity from Grain Size Analyses A comparative study of different sampling and calculation methods focusing on Västlänken*. (Masters), CHALMERS UNIVERSITY OF TECHNOLOGY,
- Svubure, O., Gumbo, T., Soropa, G., Rusere, F., Ndeketeya, A., & AMoyo, D. (2011). Evaluation of the Sand Abstraction Systems for Rural Water Supply: the case of Lupane District, Zimbabwe. *International Journal of Engineering Science and Technology (IJEST)*, 3(1), 757-765.
- Wekesa, S. S. (2017). *Analysis of Groundwater Potential and Interactions with Surface Water in the Sand River Region, Mara Basin Kenya*. (MSc), UNESCO-IHE,
- Wentworth, C. K. (1922). A Scale of Grade and Class Terms for Clastic Sediments. *The Journal of Geology*, 30(5), 377-392. doi:10.1086/622910
- Whitlow, R. (1985). Conflicts in land use in Zimbabwe: Political, economic and environmental perspectives. *Land Use Policy*, 2(4), 309-322. doi:10.1016/0264-8377(85)90029-8
- WHO. (2016). *Safely managed drinking water - thematic report on drinking water* (CC BY-NC-SA 3.0 IGO). Retrieved from Geneva Switzerland:
- Wipplinger, O. (1958). *The storage of water in sand : an investigation of the properties of natural and artificial sand reservoirs and of methods of developing such reservoirs*: Windhoek : South West Africa Administration, Water Affairs Branch.
- World Bank. (2017). The World Bank in Zimbabwe: Overview. Retrieved from <http://www.worldbank.org/en/country/zimbabwe/overview>

# Appendix

## Appendix A Sediment analysis

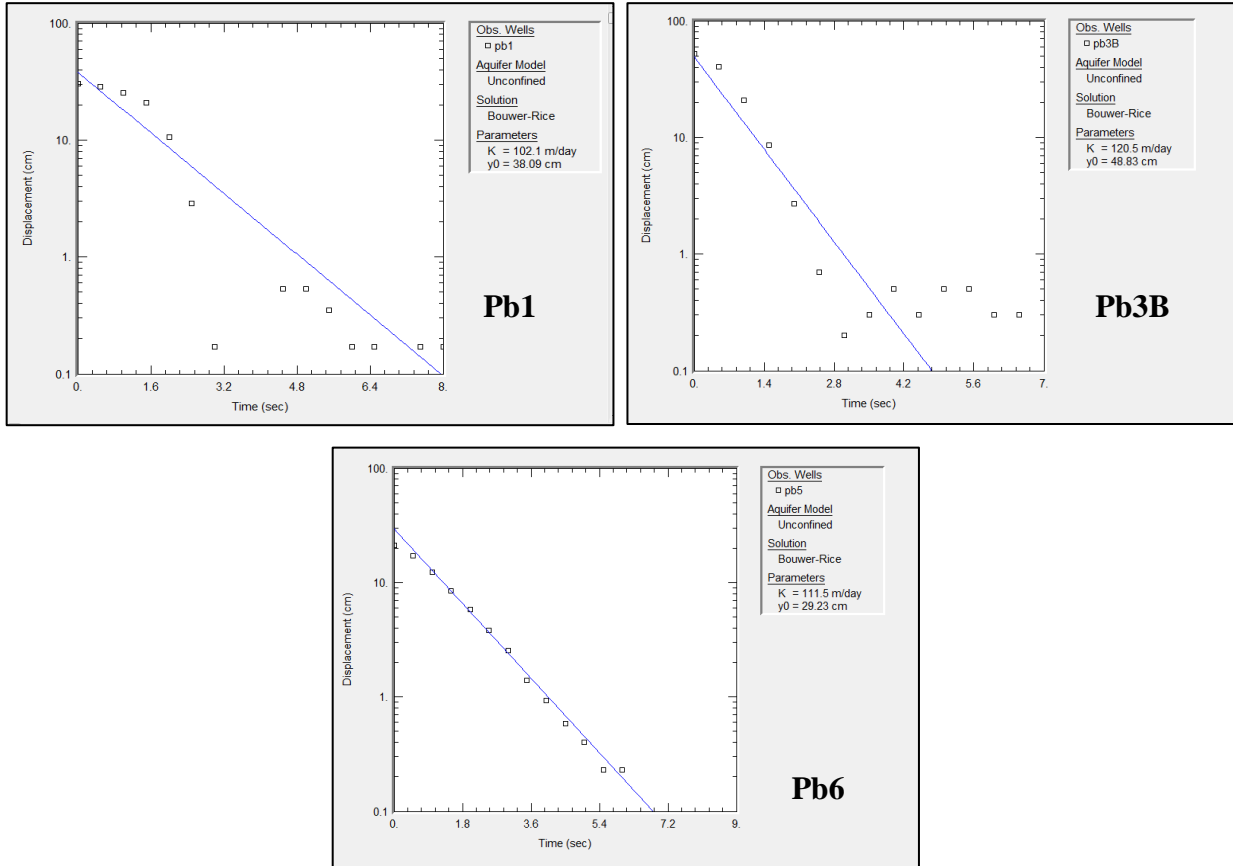
Geometry of the aquifer in the study area

	Dimension	Comment
Average length	5 to 5.6 km	From pb1 to pb6
Average width	120 m	110 m – 300 m
Average depth	0.5 to 5 m	Depth to the surface of the sediment
Average height of the banks	2 to 3 m	From the river bed to the river bank
Area	1.02 km <sup>2</sup>	
Other features		Bridge, nutrition Gardens (3 equipped with solar pumps) from Dabane, a number of other individual very small gardens, hospital.

Sample	Cu	Cc	USCS classification
S3-4	2.5	1.06	SP
S3-3	3	0.81	SP
S3-2	3	0.98	SP
S2-3	2.79	1.1	SP
S2-2	3.14	0.69	SP
S2-1	2.73	0.98	SP
S1-2	5.63	1.34	SW

Uniformity and curvature coefficients and the classification of the sediment according to USCS

## Appendix B Slug tests

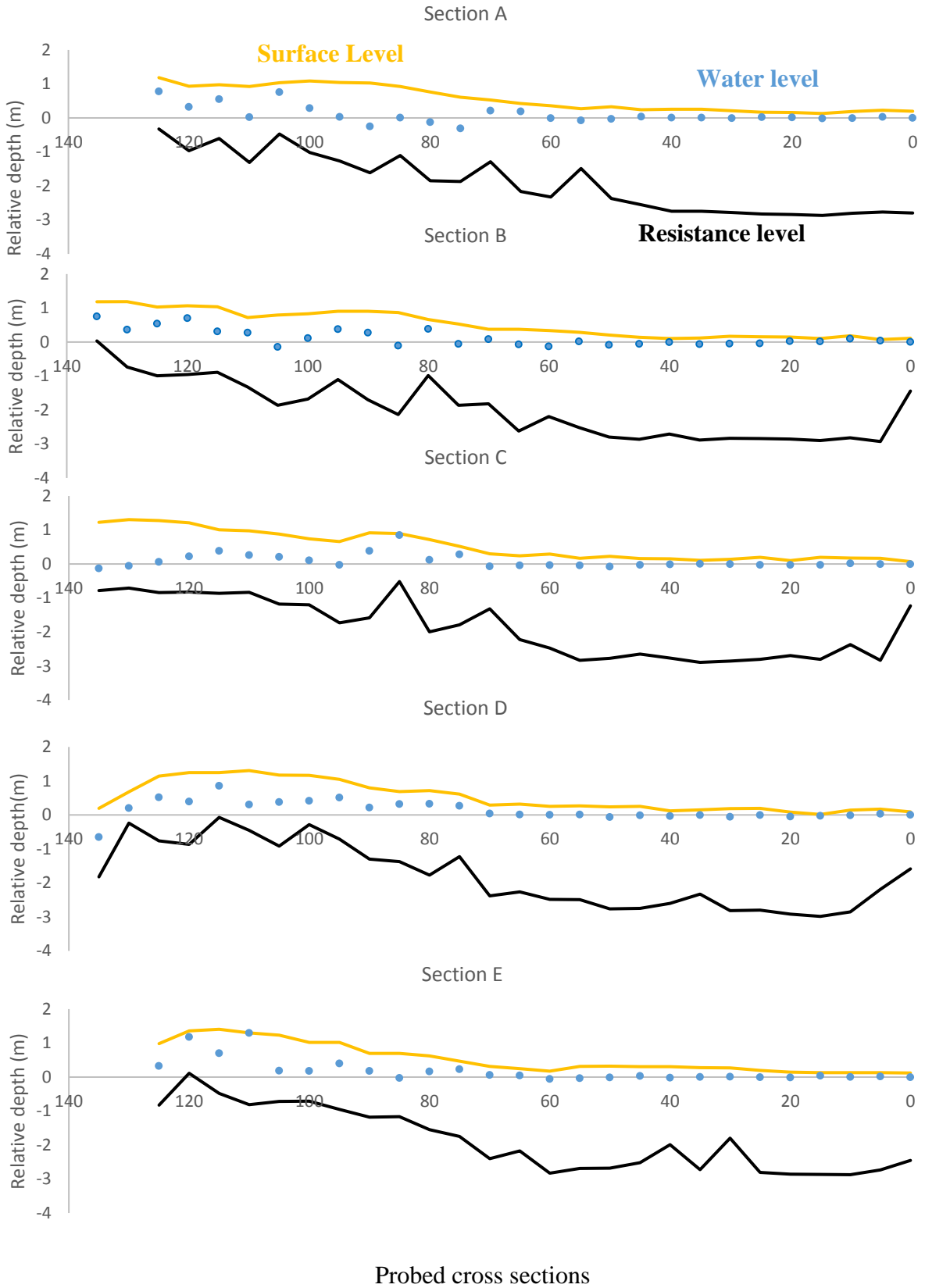


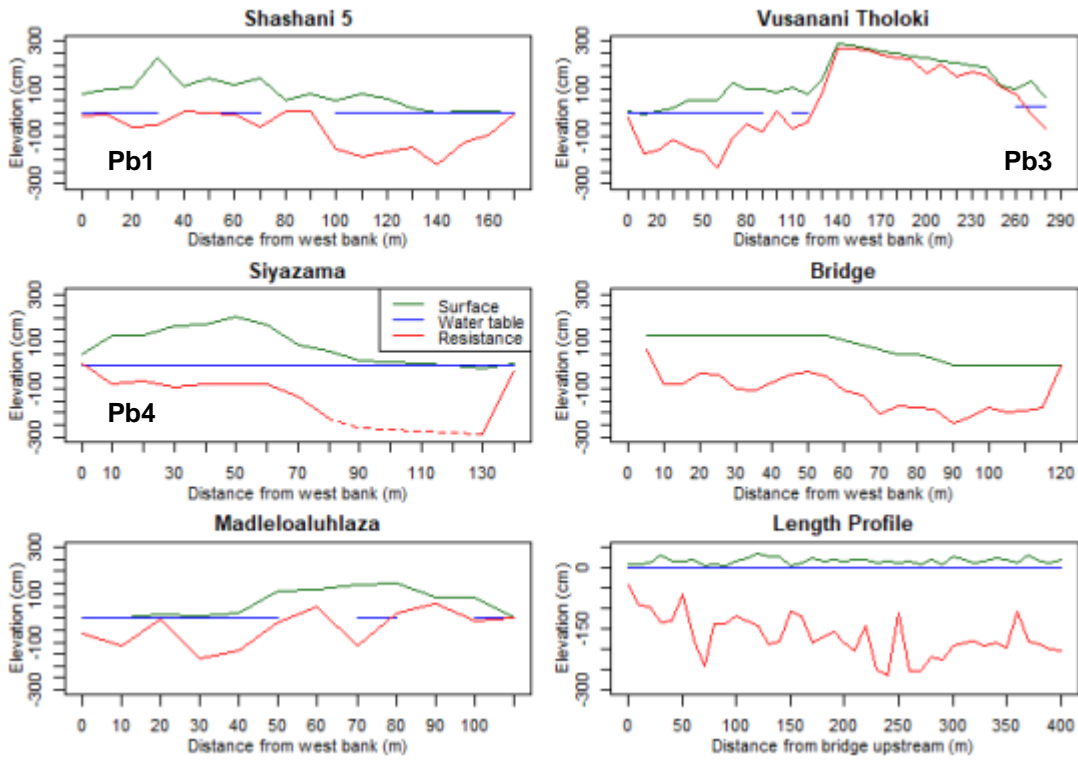
Location	Pb1	Pb3	Pb5	Average	STDV
Method (m/day)	Upstream	Midway	Downstream		
Hvorslev (1951)	99	117.2	102	106.1	9.7
Bouwer & Rice (1976)	102.1	120.5	111.5	111.4	9.2
Hazen (1893)	67.7	175	138.2	127	54.5

### Summary of aquifer parameters

Parameter	Blok, 2017	Hussey, 2003	Mansell & Hussey, 2005
Porosity (%)	34	32	42
Specific Yield (%)	15	-	-
Kh (m/d)	98	96 - 100	98
Kv (m/d) riverbed	41	-	-
Kv (m/d) river bank	3.4	-	-

## Appendix C Probing and Geophysics





Probed cross sections by Blok (2017)

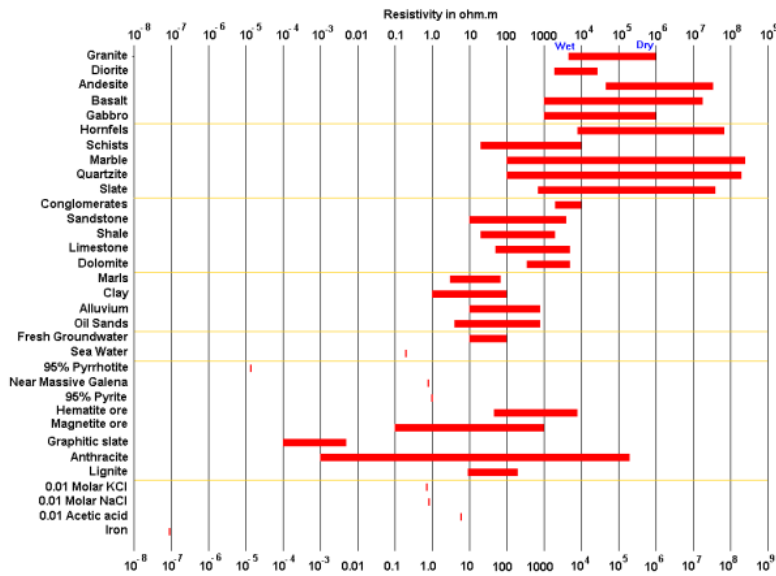
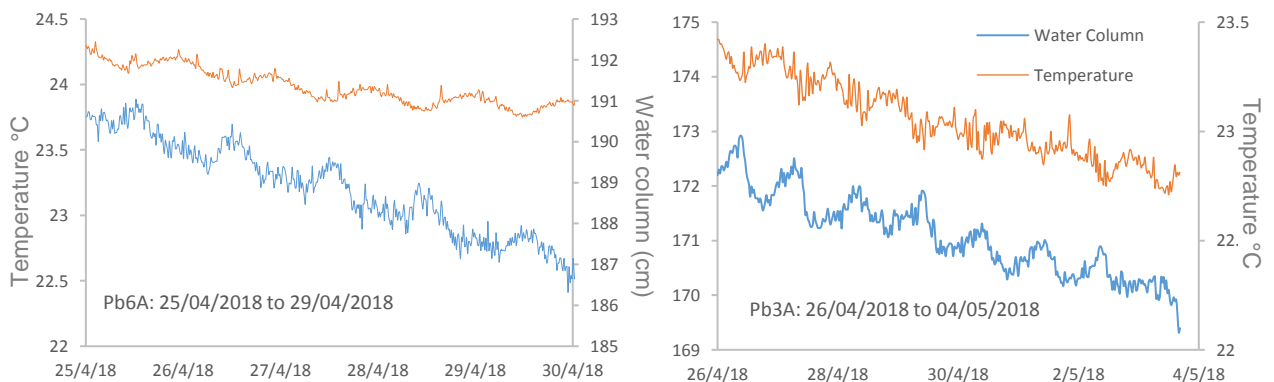
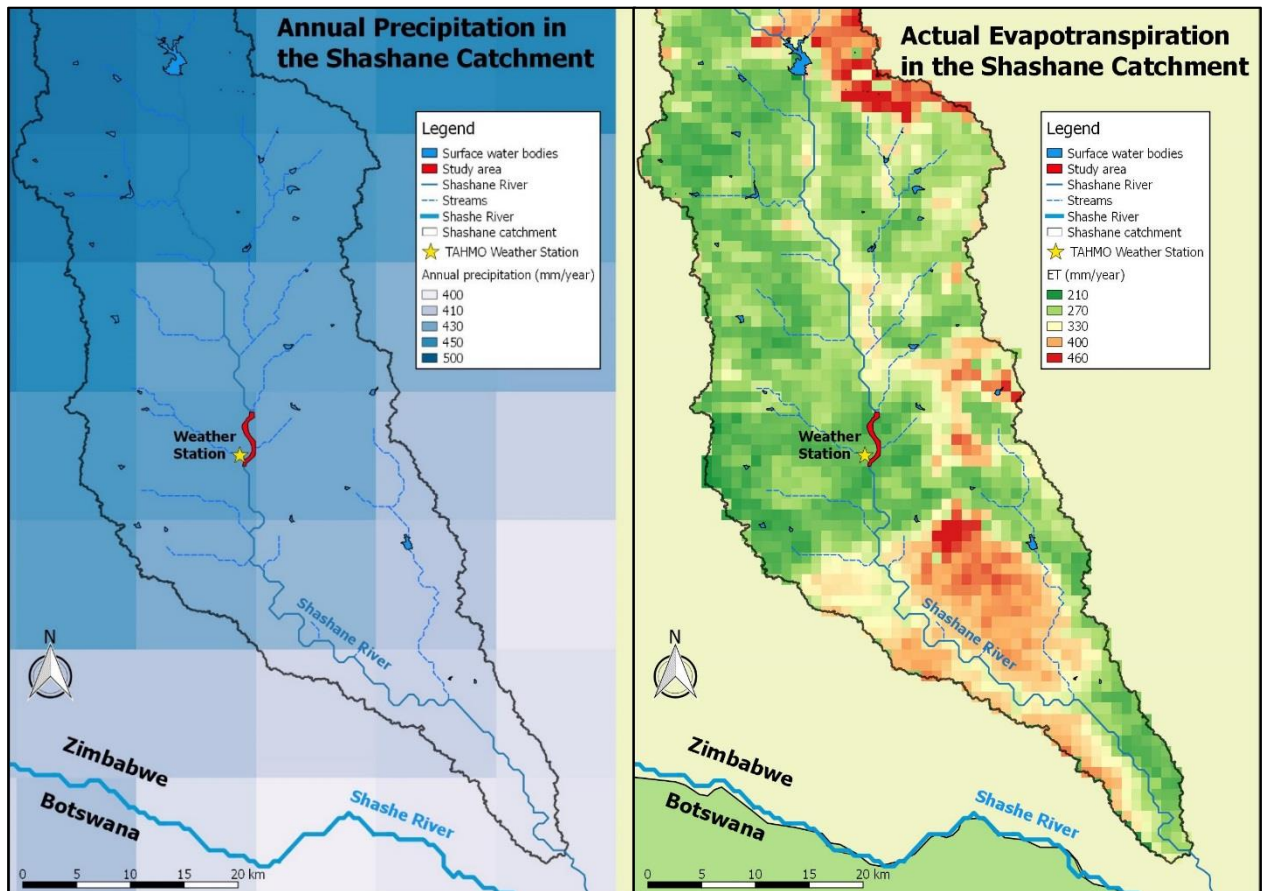


Figure 5. The resistivity of rocks, soils and minerals.

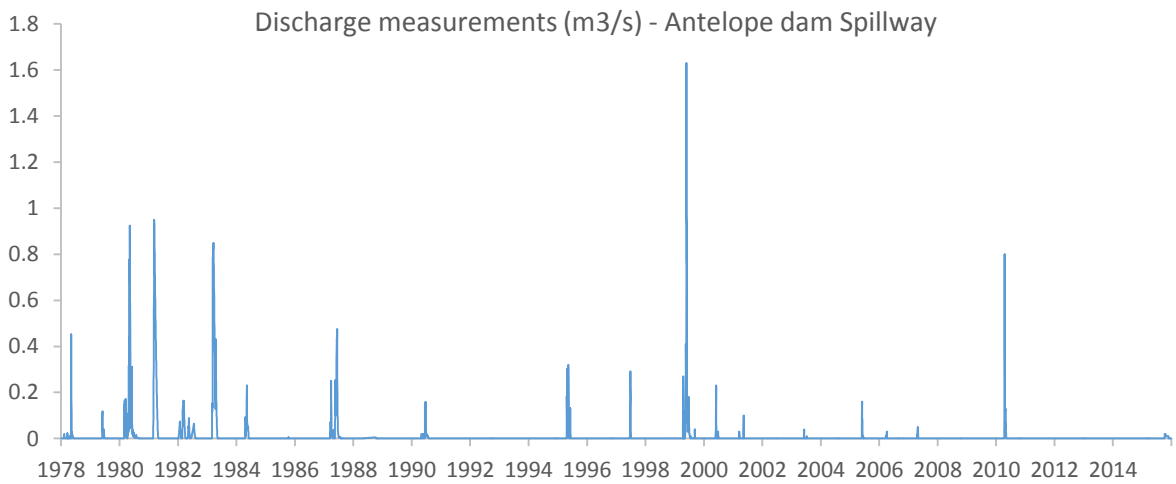
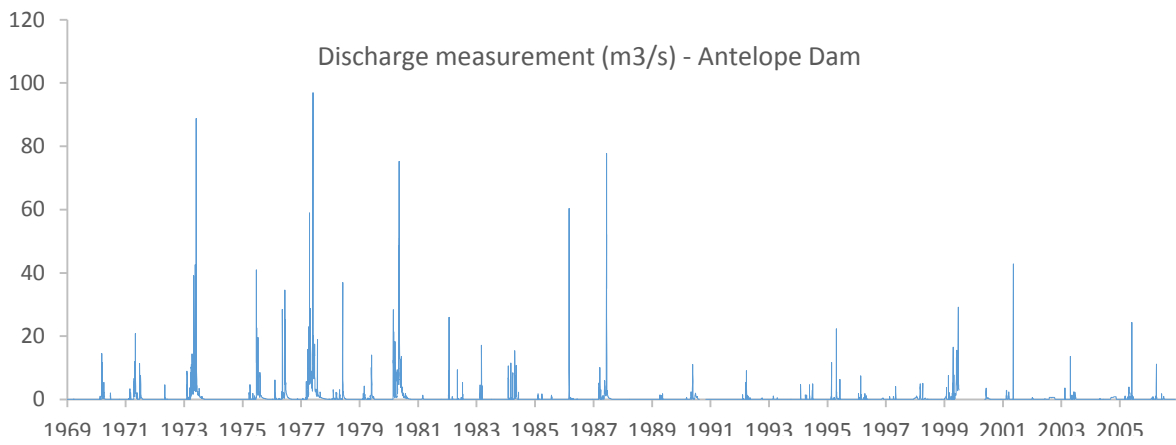
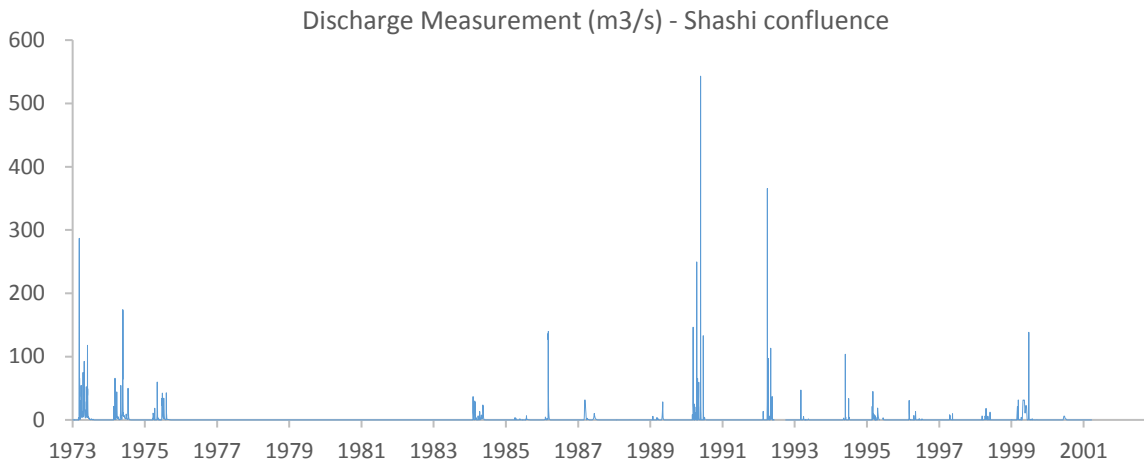
Typical formation factors (Nonner & Stigter, 2016)

LITHOLOGY	FORMATION FACTOR
Gravel	7.5
Coarse sand/gravel	6
Coarse sand	5
Medium sand	4.2
Fine sand	3.5
Clayey sand	<2.5

## Appendix D Hydrological data

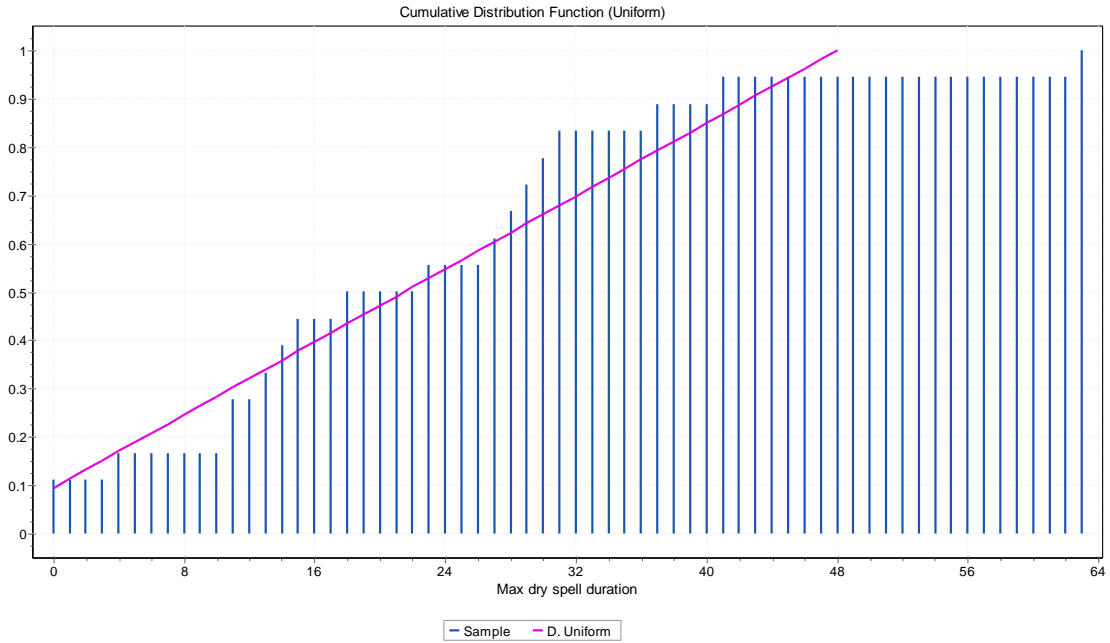


Groundwater level manual measurements during the fieldwork



**Statistical analysis of dry spells**





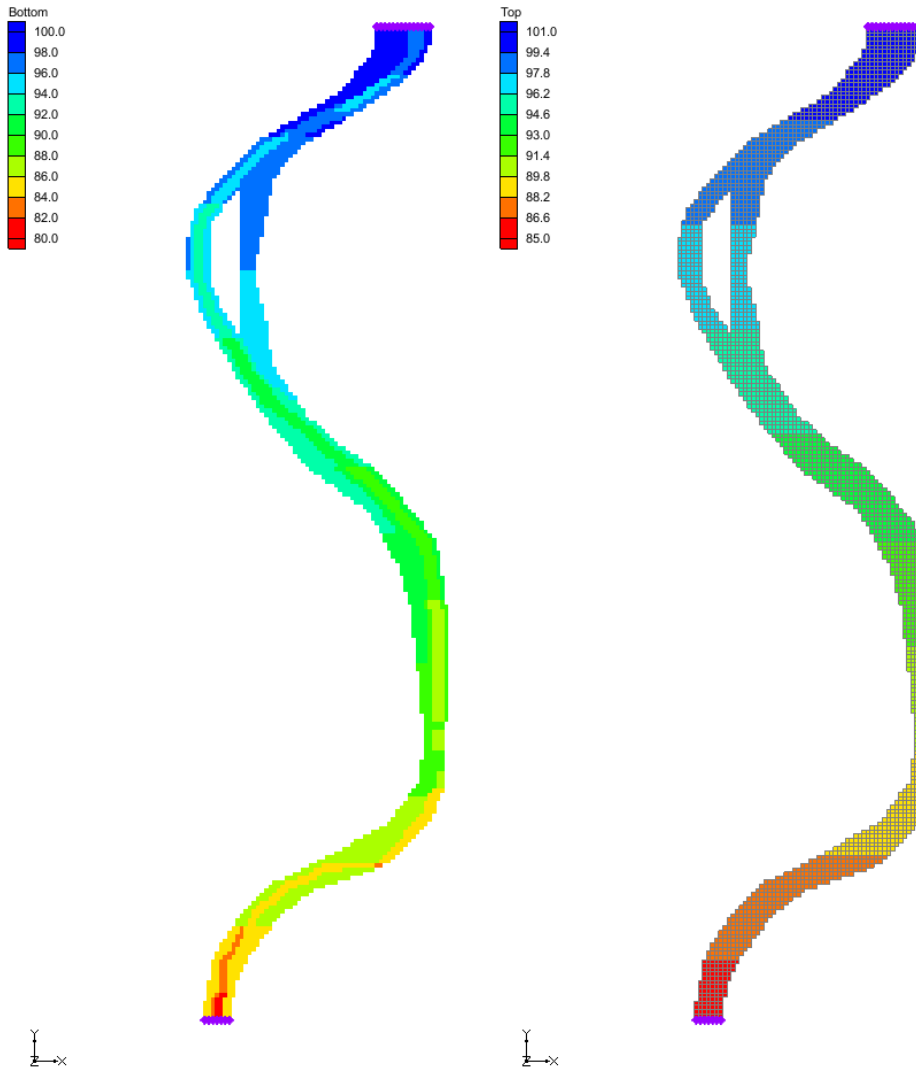
Rainy year	Max duration of dry spell (days)
1973/1974	37
1974/1975	0
1975/1976	11
1984/1985	11
1985/1986	27
1986/1987	0
1987/1988	41
1988/1989	63
1989/1990	31
1990/1991	14
1992/1993	28
1993/1994	13
1994/1995	30
1995/1996	29
1996/1997	23
1997/1998	18
1998/1999	4
1999/2000	15

Goodness of Fit - Details <a href="#">[hide]</a>					
<b>D. Uniform</b> [#1]					
Kolmogorov-Smirnov					
Sample Size	18				
Statistic	0.15409				
P-Value	0.73031				
Rank	1				
$\alpha$	0.2	0.1	0.05	0.02	0.01
Critical Value	0.2436	0.27851	0.30936	0.34569	0.37062
Reject?	No	No	No	No	No

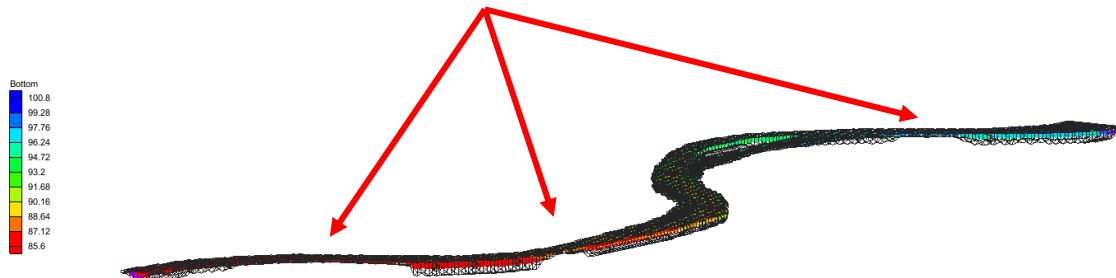
Descriptive Statistics			
Statistic	Value	Percentile	Value
Sample Size	18	Min	0
Range	63	5%	0
Mean	21.944	10%	0
Variance	237.05	25% (Q1)	11
Std. Deviation	15.397	50% (Median)	20.5
Coef. of Variation	0.70161	75% (Q3)	30
Std. Error	3.8491	90%	41
Skewness	0.76647	95%	63
Excess Kurtosis	0.60743	Max	63

# Appendix E Groundwater model

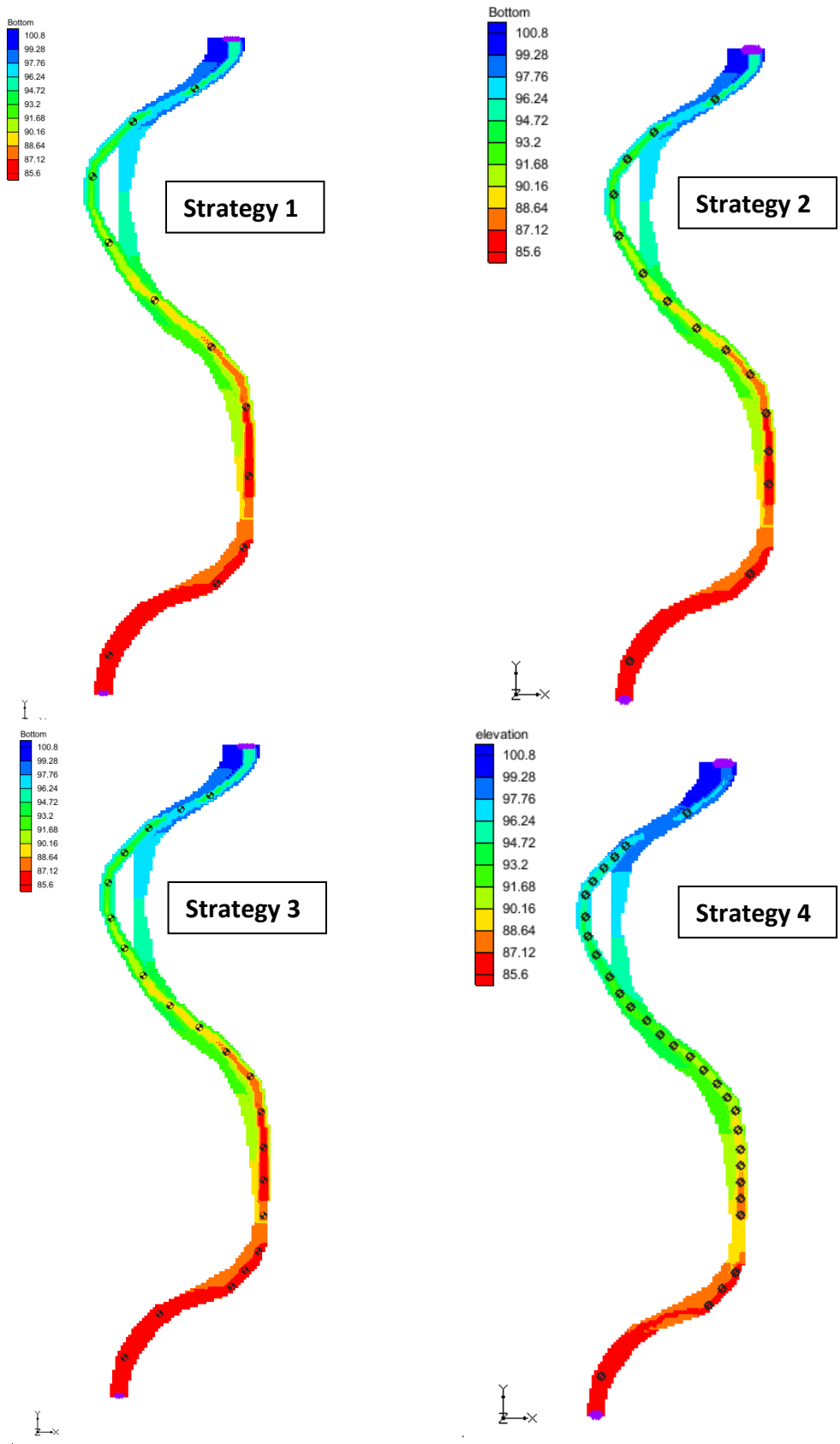
## Topographical model



Subsurface  
bedrock rises



# Spatial pumping strategies



# Appendix F Sensitivity Analysis

## Storage:

